# Waiuku Wastewater Treatment Plant
# Outfall modelling

Watercare

Report 44801314/01

November 2018

The expert in **WATER ENVIRONMENTS**

This report has been prepared under the DHI Business Management System certified by Bureau Veritas to comply with ISO 9001 (Quality Management)

ISO 9001
Management System Certification
BUREAU VERITAS
Certification Denmark A/S

# Waiuku Wastewater Treatment Plant
# Outfall modelling

## Numerical Modelling

*Waiuku Estuary*

| | |
|---|---|
| Prepared for | Watercare |
| Represented by | Jen Harbour |

| | |
|---|---|
| Project manager | John Oldman |

| | |
|---|---|
| Project number | 44801314 |
| Approval date | 27th November 2018 |
| Revision | Final |

DHI Water and Environment Ltd• B:HIVE, Smales Farm• Takapuna 0622 Auckland• New Zealand•
Telephone: +64 9 912 9638 • Telefax: • info.nz@dhigroup.com• www.dhigroup.com

# CONTENTS

# 1 Executive Summary

DHI have undertaken an assessment of the discharge of treated wastewater from the Waiuku wastewater treatment plant into the Waiuku Estuary.

Based on a previously calibrated hydrodynamic model of the Manukau Harbour, a refined model of the Waiuku/Mauku system has been used to assess the level of dilution that could be achieved for a future discharge from the existing wastewater treatment plant (WWTP) and outfall, which assumes a 26% increase in population.

The Waiuku/Mauku model has been calibrated against salinity data collected within the Waiuku Estuary as part of the ongoing monitoring of the existing Waiuku WWTP discharge.

A year-long simulation of the calibrated model was undertaken for 1999, which was deemed to be typical with regards to freshwater inflows to the Waiuku/Mauku system.

The dilutions achieved for the treated wastewater have been assessed for a conservative (non-decaying) tracer and viruses and bacteria. For viruses and bacteria, time varying inactivation rates were used which take into account daily and seasonal variation in solar radiation.

Predicted virus and bacteria concentrations have been provided to Streamlined Environmental Ltd. at seven selected sites within the Waiuku Estuary for the purposes of carrying out a quantitative microbial risk assessment.

Median dilutions for Enterococci and viruses achieved at the two sites 3 km north of the discharge point range from 9000-16000 for the future discharge scenario considered.

At an inter-tidal site 1500 m from the discharge point, median dilutions of 1800 and 1900 are achieved for viruses and Enterococci respectively.

At a subtidal site just to the north of the discharge point, median dilutions of 6100 and 7000 are achieved for viruses and Enterococci respectively.

Such dilutions are achieved because the discharge occurs on the first part of the outgoing tide (when ambient currents are relatively strong), the relative magnitude of the WWTP discharge compared to other freshwater inputs to the Waiuku Estuary and the degree of exchange that occurs between the Waiuku Estuary and the main body of the Manukau Harbour (which is driven by the inter-tidal nature of the Waiuku Estuary).

For sites to the south of the discharge point relatively high dilutions are achieved. This is because, to reach this part of the Waiuku Estuary, the treated wastewater plume is firstly transported away from the discharge site on the outgoing tide and then transported back towards these sites on the subsequent incoming tide.

This report provides an overview of the near-field assessment that has been carried out for the discharge, the calibration of the Waiuku Estuary model against salinity data, a summary of the data provided for the quantitative microbial risk assessment and an overview of the treated wastewater plume dynamics in the Waiuku Estuary.

# 2 Introduction

DHI were commissioned by Watercare Services Ltd (Watercare) to carry out an assessment of the discharge of treated wastewater from the Waiuku WWTP in the south of the Waiuku Estuary (Figure 2-1).

The existing discharge is in the southern end of the Waiuku Estuary (Figure 2-2). The existing consent allows for a maximum daily discharge from the Waiuku WWTP of 5500 $m^3$ plus an additional 33 $m^3$/day for every 1 mm of rainfall, if the weekly rainfall total has exceeded 40 mm. This equates to an additional 0.6% increase in daily discharge volume for every 1 mm of rain.


Figure 2-1. Waitangi and Mauku rivers showing the location of the existing WWTP.


Figure 2-2 Southern section of the Waiuku Estuary showing the location of the Waiuku wastewater treatment plant and outfall location on the eastern flank of the subtidal channel.

Table 2-1 shows a summary of the discharge scenarios considered in this study.

A high-level assessment of three potential future discharges showed very little difference between the scenarios in terms of achievable dilutions and reductions in salinity. This indicated that the Scenario 3 option, as the most conservative one that assumes the highest level of population growth, should be considered for the purposes of this resource consent application.

This report provides details of the assessment of both the Current Population scenario (Current) and Scenario 3 (Future Scenario).

Table 2-1 Discharge volume for current population and each growth projection scenario.

| **Inflow** | **Current Population** | **Scenario 1** | **Scenario 2** | **Scenario 3** |
|---|---|---|---|---|
| Population Equivalent | 9,578 | 11,110 | 11,589 | 12,068 |
| Population Increase | - | 16% | 21% | 26% |
| Flow volume ($m^3$/yr) | 749,418 | 869,325 | 906,796 | 944,267 |
| Mean daily volume ($m^3$/yr) | 2053 | 2382 | 2484 | 2587 |
| Average flow rate during 3-hour discharge window ($m^3$/s) | 0.10 | 0.11 | 0.12 | 0.12 |

An existing calibrated hydrodynamic model developed for Watercare for the Clarks Beach WWTP discharge resource consent (DHI, 2014 and DHI, 2016) has been used for this work. The model has been refined for the upper parts of the Waiuku Estuary so that the mixing of treated wastewater from the WWTP and freshwater from the Waiuku River are accurately simulated.

For the Clarks Beach work, the dynamics of the proposed discharge at the Clarks Beach WWTP within the main body of the Manukau Harbour and the lower part of the Waiuku Estuary was quantified for typical El Niño (1991) and La Niña years (1999). This was done as the effects of winds on circulation in the wider Manukau are significant.

For assessing the Waiuku WWTP discharge simulations were carried out just for 1999. This is because the southern part of the Waiuku Estuary is less influenced by winds (compared to the wider Manukau) and 1999 is very typical with respect to rainfall, and hence, freshwater inflows to the Waiuku/Mauku system.

Representative decay processes for viruses and bacteria have been simulated to provide estimates of the Waiuku treated wastewater plume footprint and to quantify the level of dilution achieved within the Waiuku Estuary.

For this study, all data is presented using the New Zealand Transverse Mercator projection (NZTM) and the vertical datum is Auckland Vertical Datum.

# 3 Data Overview

This section of the report provides a summary of the data used for modelling including data for the model setup, derivation of treatment plant flow data (from monitoring data and rainfall data) and representation of time-varying inactivation processes for viruses and bacteria.

## 3.1 Bathymetry

Bathymetry data was obtained from MIKE C-MAP (DHI, 2017), from digitised aerial images and from 1 m resolution 2013 LiDAR data (extending into inter-tidal zone) from Land Information New Zealand. Details of the coverage of the various datasets are provided in DHI (2014).

## 3.2 Rain

An analysis of Auckland Airport rain data from 1999-2017 showed that 1999 is very representative of the long-term data in terms of total rainfall, number of rain days and number of days of more than 10 mm rainfall (Table 3-1).

Table 3-1 Summary of rainfall data (1999-2017) compared to 1999.

| **Inflow** | **1999-2017 averages** | **1999** |
|---|---|---|
| Total Rainfall (mm) | 1089 | 1039 |
| Rain Days | 181 | 171 |
| Days > 10 mm | 33 | 33 |

The rain data for 1999 is shown in Figure 3-1. The figure also shows periods when the 7-day rainfall exceeds 40 mm. During such times, it has been assumed that an additional discharge of treated wastewater over and above the average daily value (as per the existing consent conditions) would occur.

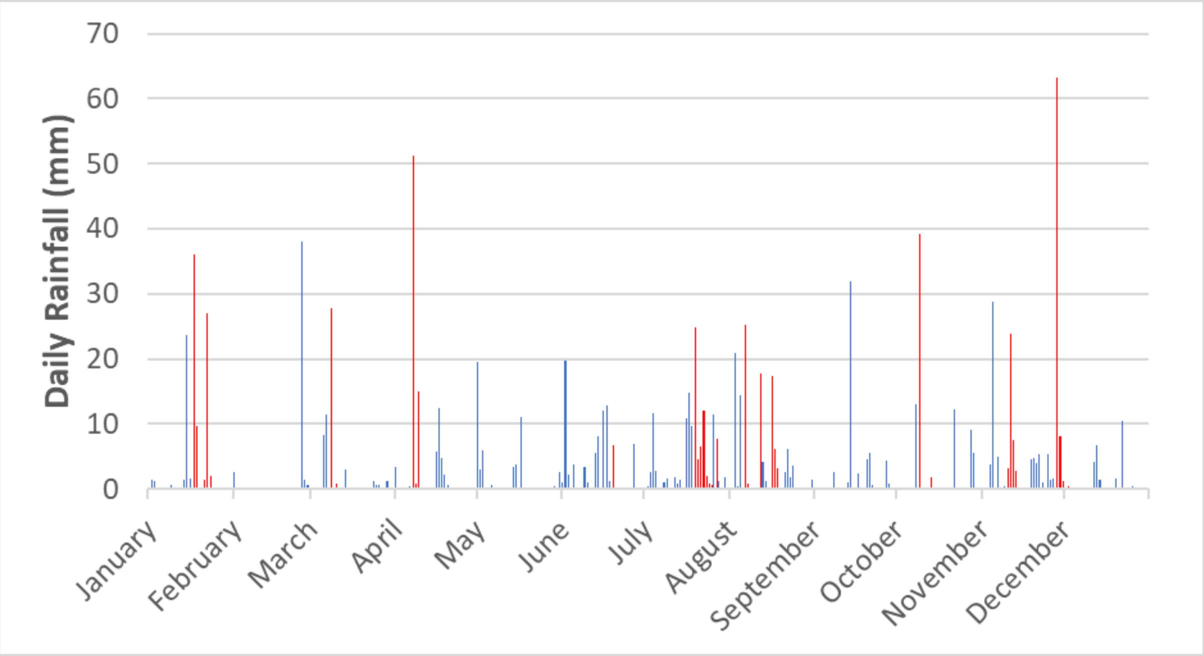


Figure 3-1 Rain for 1999. Values in red indicate when the 7-day rainfall total exceeds 40 mm and additional treated wastewater (over and above the daily mean value) is likely to be discharged from the Waiuku WWTP.

## 3.3 Freshwater Inflows

The two main freshwater inflows to the Waiuku Estuary are the Waitangi and Mauku Rivers (Figure 2-1). Gauging data from Auckland Council has been used to derive river inflows based on daily rainfall for both these freshwater inflows.

Based on the available flow data it has been assumed that the baseflow for the Waitangi River is 0.25 $m^3/s$.

To derive the relationship between rainfall and Waitangi inflows, the baseflow (0.25 $m^3/s$) was subtracted from the available flow data. The regression between the percentile daily rainfall and percentile gauged flow over and above the assumed baseflow value for the Waitangi site is shown in Figure 3-2. The regression coefficient (0.0608) is used to convert the observed daily rainfall from the Auckland Airport data to a non-baseflow value for the Waitangi River.

Analysis of Auckland Council data identified that the ungauged part of the Waiuku catchment adds another 28% to the gauged Waitangi inflow and the Mauku freshwater inflow is 40% higher than the Waitangi gauged inflows (DHI, 2016).

These estimates are used to derive the daily inflows for 1999 for both the Waiuku and Mauku estuaries.

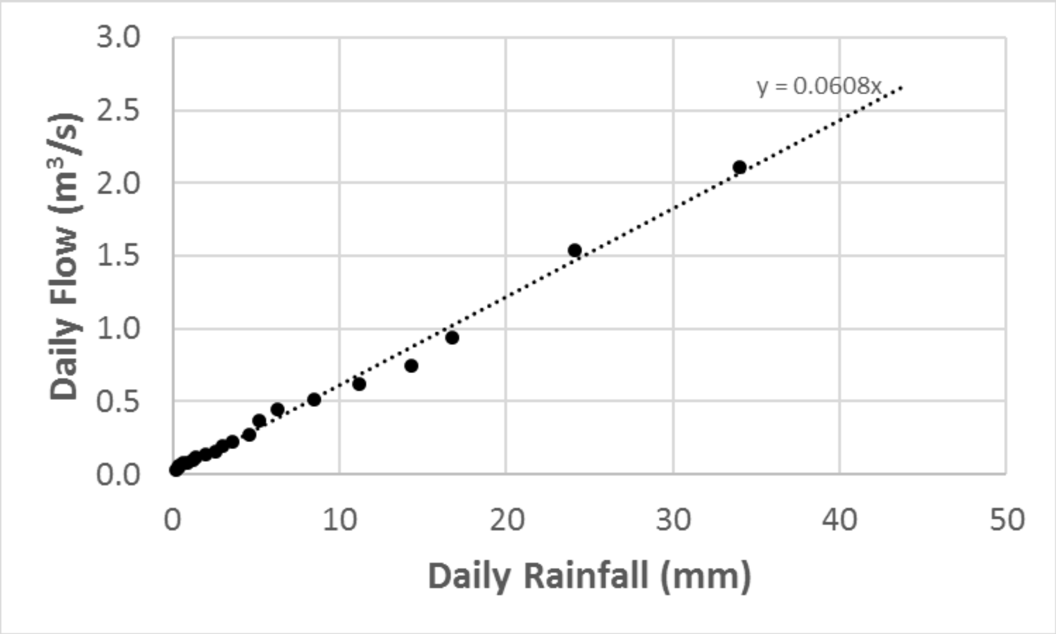


Figure 3-2 Percentile estimates (5th through to 95th) for daily rainfall (mm) and mean daily river flow ($m^3/s$) for the Waitangi River.

## 3.4 Salinity Data

Salinity data is collected as part of the ongoing monitoring for the existing WWTP discharge at five sites within the Waiuku Estuary (Figure 3-3). Data is collected on the outgoing tide prior to low water. A summary of the monitoring data is shown in Figure 3-4.

Just after peak ebb currents have occurred (~2:00 hours prior to low water), salinities range from 31.0 – 32.0 PSU. As the tide falls further (~1:45 before low water) salinities at the southern sites drop to around 30.0 PSU. During wet weather sampling, there is an overall drop in salinities with salinity at the southern site (A) dropping to around 27.0 PSU while the salinity at the northern site (F) drops to less than 31.0 PSU.

Based on the earlier calibration of the harbour wide model (DHI, 2016) the background salinity for the wider Manukau (i.e. the boundary background salinity for the Waiuku/Mauku model) was set to 34.2 PSU.


Figure 3-3 Water quality monitoring sites.

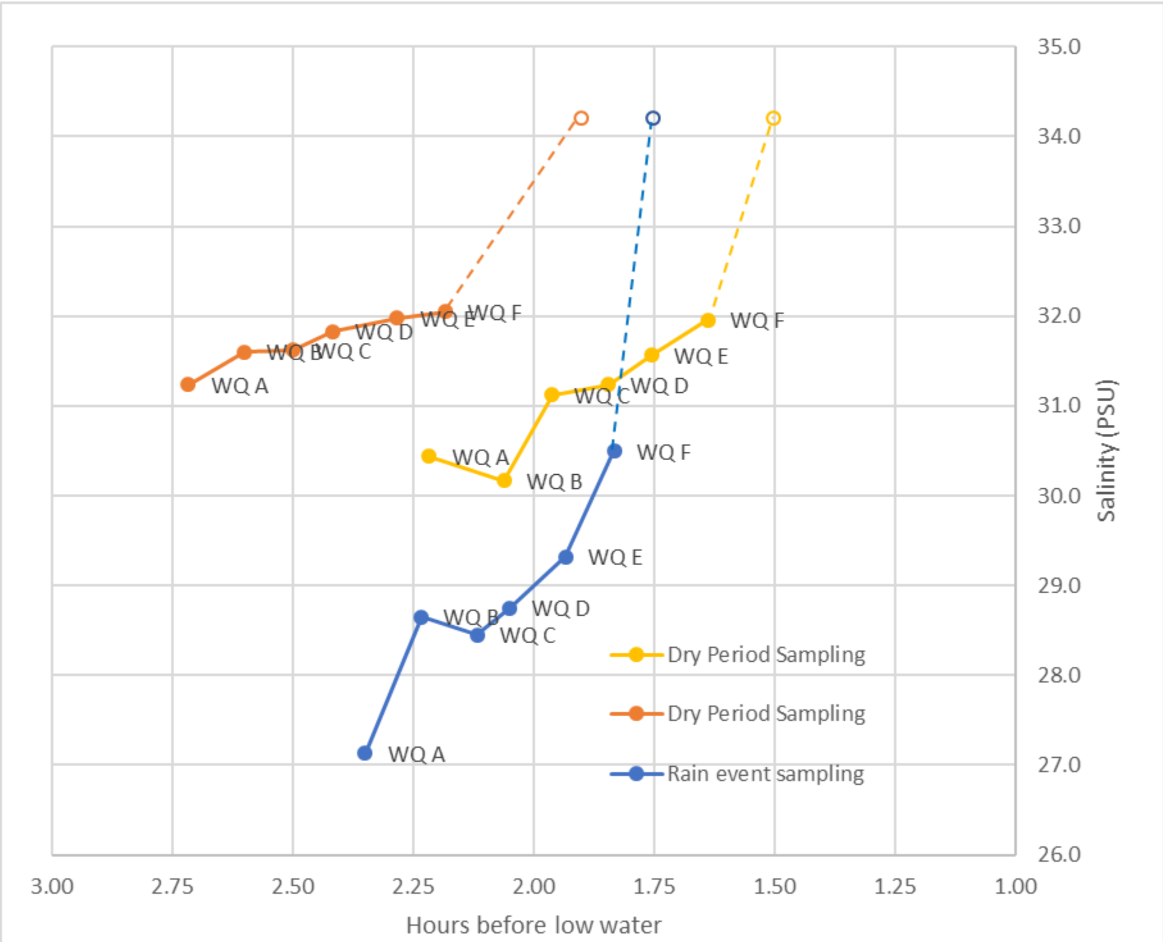


Figure 3-4 Summary of monitoring data collected within the Waiuku Estuary. The dashed line shows the extension of the monitoring data line assuming a background salinity of 34.2 PSU in the wider Manukau Harbour.

## 3.5 Wind and Solar Radiation

Hourly observations of wind data and solar radiation from Auckland Airport were obtained from NIWA's climate database (CliFlo).

A comparison of the wind rose from the long-term record and the winds from 1999 (Figure 3-5) show that the distribution of winds for 1999 is very close to the long term average wind distribution with a predominance of south-west winds.

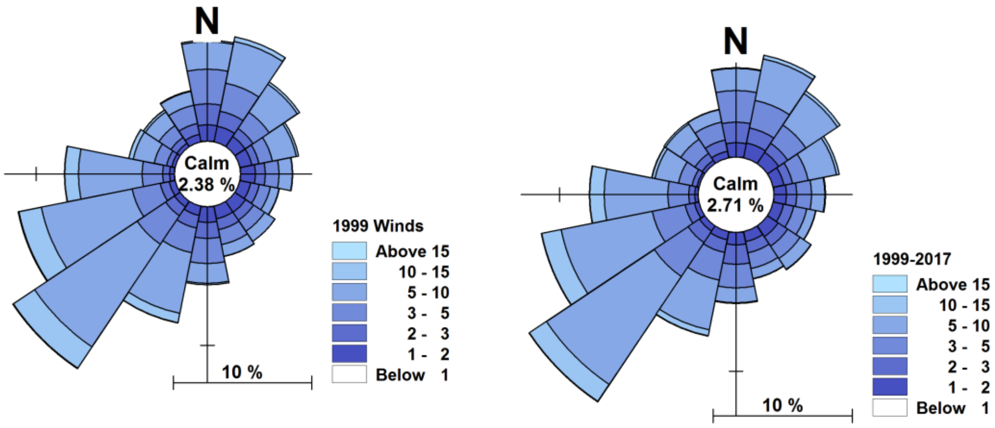


Figure 3-5 Wind rose for wind data from 1999 (left) and from the long-term wind record (right).

## 3.6 Discharge Data

Treatment plant flow data from July 2013 – July 2018 (Figure 3-6) has been analysed to quantify the current discharge rate and its seasonality.

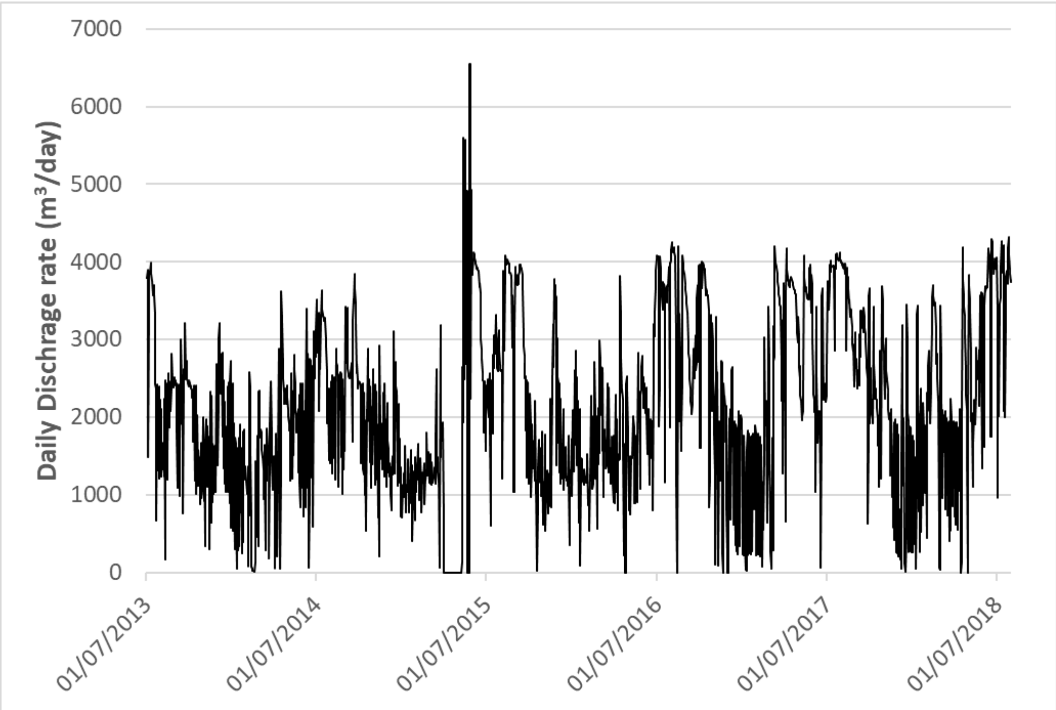


Figure 3-6 Treatment plant discharge data for July 2013 – July 2018.

The average daily discharge for the period July 2013 – July 2018 is 2215 $m^3$/day with 75th, 90th and 95th percentile values of 3030, 3830 and 3970 $m^3$/day respectively.

The average daily discharge rate for each calendar month is shown in Figure 3-7.

This data is used to derive scenario discharge data for the 1999 model simulation.

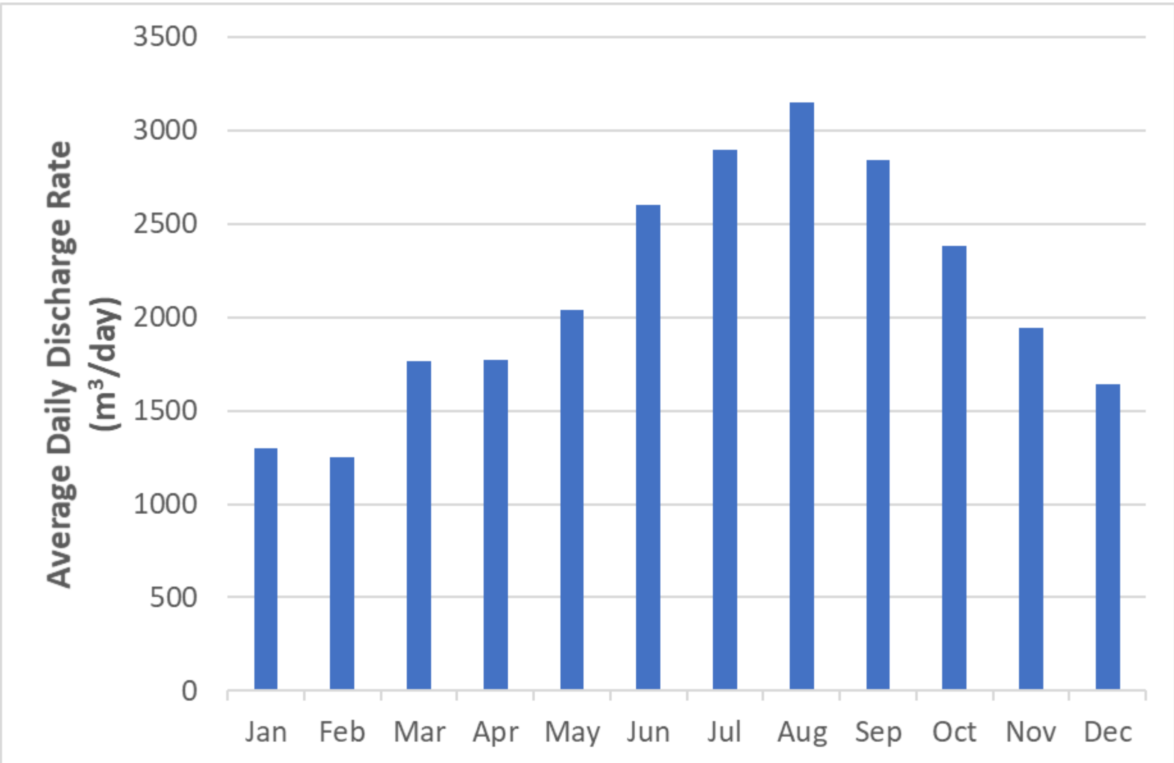


Figure 3-7 Average daily discharge rate from treatment plant discharge data July 2013 – July 2018.

# 4 Model Set Up

The wastewater dilution model is underpinned by a 2D hydrodynamic model, MIKE 21 FM which simulates tidal and wind driven currents within the Waiuku and Mauku estuaries. The model is based on the whole harbour model (Figure 4-1) developed for the Clarks Beach WWTP discharge options study (DHI, 2014 and DHI, 2016). The whole harbour model has been extensively calibrated against harbour wide currents, water level variations and salinity observations as well as site specific data collected for the Clarks Beach options study.

For this study, just the Waiuku and Mauku part of the whole harbour model mesh has been extracted and refined as necessary near the Waiuku WWTP discharge (Figure 4-2). Water levels from the whole harbour model have been extracted from the previous annual simulations and used as boundary conditions for the Waiuku/Mauku model.

Much of the Waiuku/Mauku system is inter tidal with data from the Waiuku/Mauku mesh indicating that 80-85% of the area of the Waiuku/Mauku system is not inundated at low water.

Other boundary conditions for the Waiuku/Mauku model include wind data from the Auckland Airport automated weather station, Waiuku freshwater inflows from the Waiuku and Mauku catchments and the tidally staged discharge from the Waiuku WWTP.

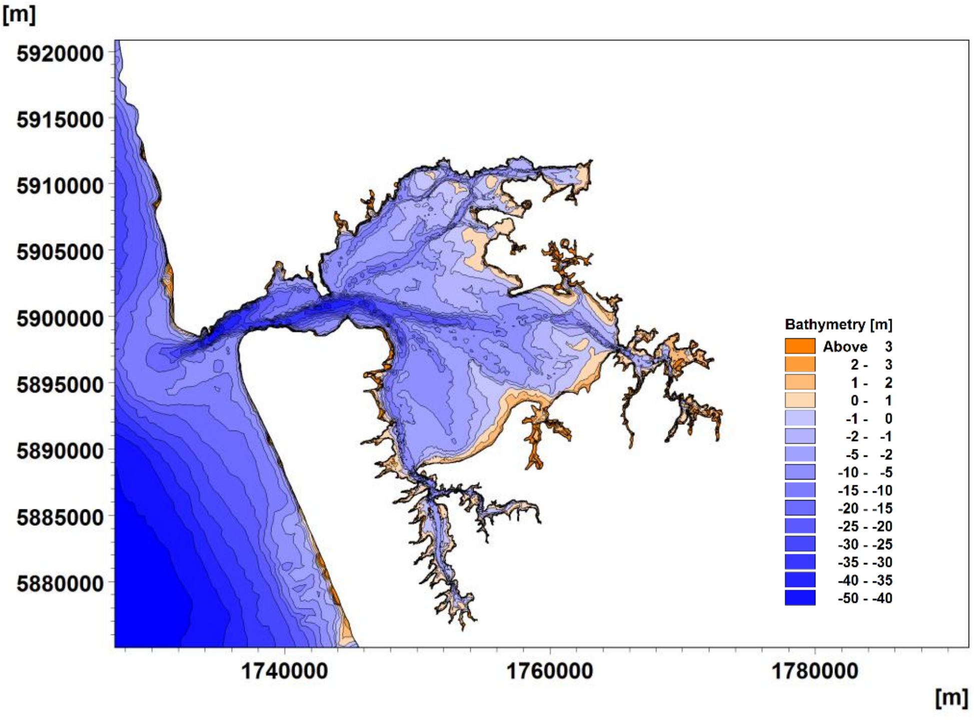


Figure 4-1 Harbour wide bathymetry used for the Clarks Beach WWTP options study (DHI, 2016).

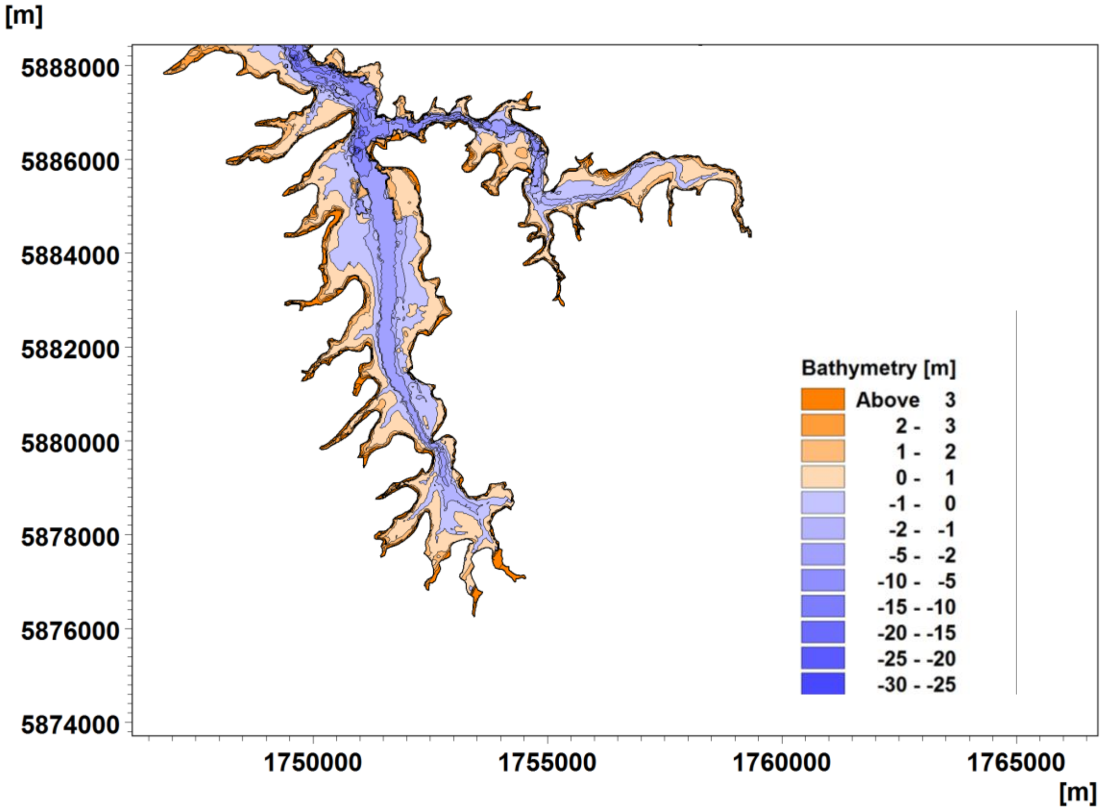


Figure 4-2 Model bathymetry in the Waiuku and Mauku estuaries.

## 4.1 Waiuku entrance water level Boundaries

Water level variations at the entrance to the Waiuku Estuary (Figure 4-3) were extracted from the whole harbour model from the Clarks Beach WWTP options study (DHI, 2014 and DHI, 2016) and used as boundary conditions for the Waiuku/Mauku model

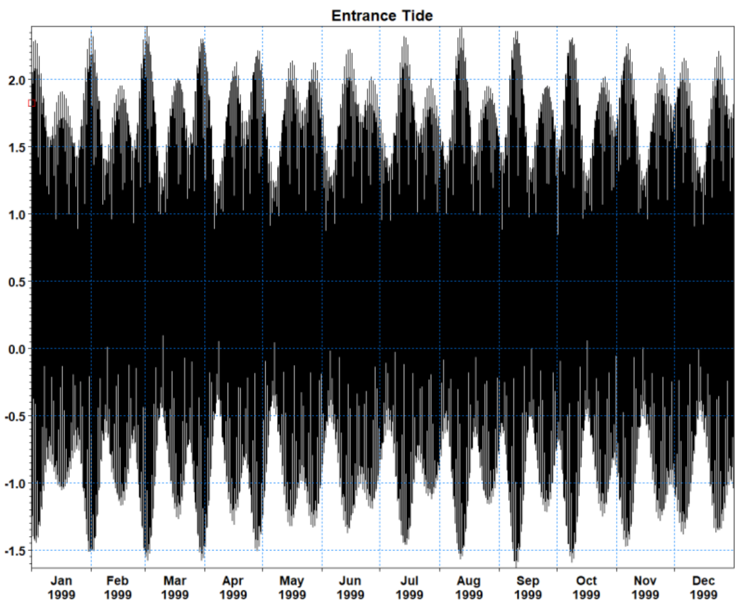


Figure 4-3 Water level variations at the entrance to the Waiuku Estuary for 1999.

## 4.2 Representation of Treated Wastewater

Treatment plant discharge data (Section 3.6) has been used to derive the discharge data for the 1999 annual simulation.

The starting point for defining the discharge rate is the total annual volume (Table 2-1) which, based on the 3-hour discharge window, gives a mean discharge rate ($m^3/s$).

The mean discharge rate was then adjusted according to the observed seasonality of existing discharge (Figure 3-7) - giving highest discharge rates in winter and lowest discharge rates in summer.

An additional 0.6% of discharge for every 1 mm rainfall was added whenever the 7-day rainfall total exceeded 40 mm.

Figure 4-4 shows the schematic existing discharge for January and July 1999 along with the schematic Waitangi River flows and the predicted tides at the outfall site.

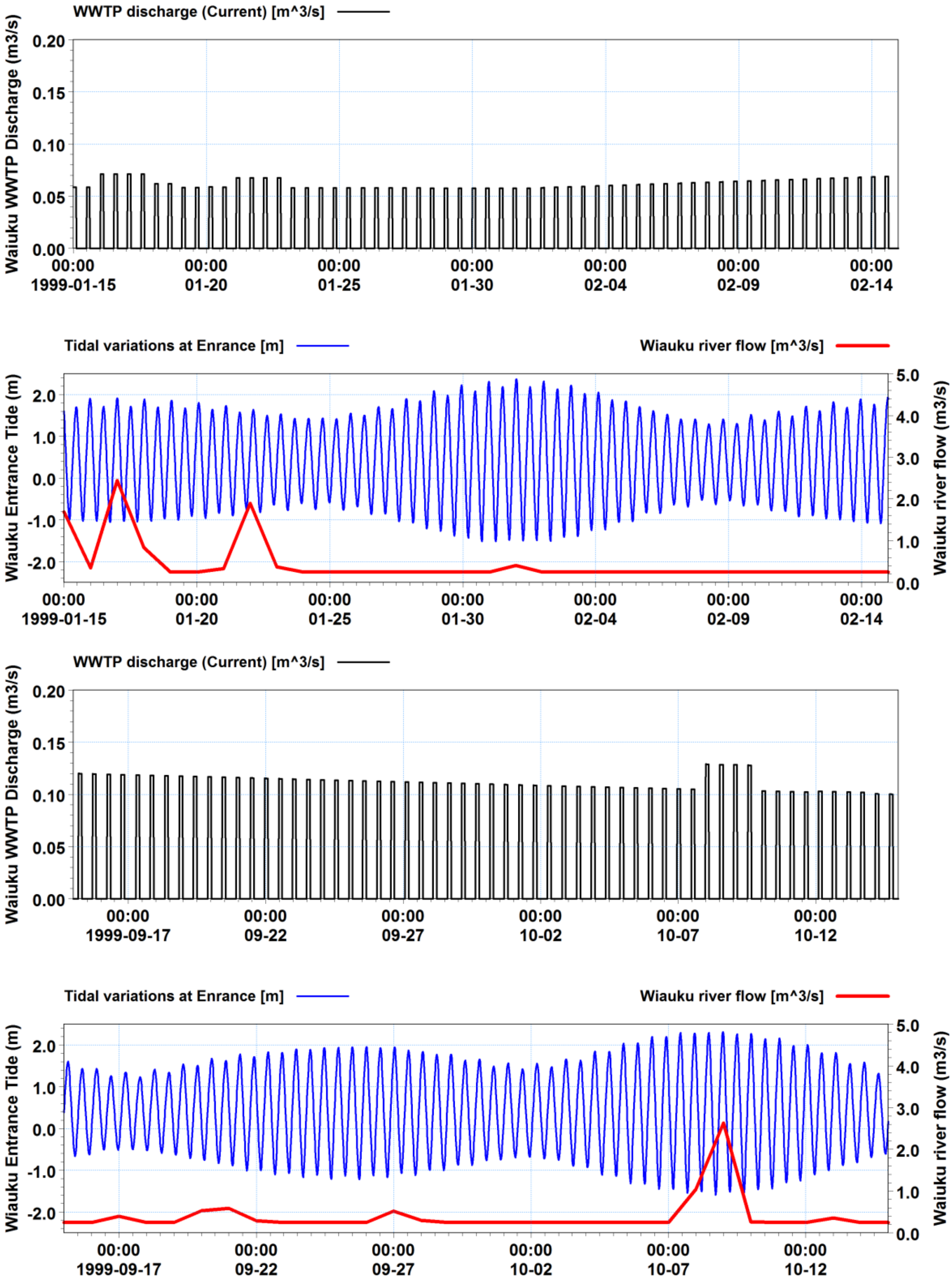


Figure 4-4 Typical schematic discharges for summer (top panel) and winter (bottom panel) for the existing discharge scenario for 1999. Also shown are the tidal variations at the entrance to the Waiuku Estuary (blue) and the assumed Waiuku River flow (black).

To simulate the behaviour of the wastewater plume, the advection-dispersion (AD) module was used. The AD module simulates the spread of dissolved and suspended substances subject to the transport process described by the HD module. The wastewater plume was defined as a decaying tracer with decay processes represented in the following way.

Viruses were modelled assuming worst case dark (night time) inactivation coefficients for summer and winter of 0.044 $h^{-1}$ and 0.015 $h^{-1}$ respectively, while the daytime coefficients were assumed to be 0.33 $h^{-1}$ and 0.045 $h^{-1}$ for summer and winter respectively. These inactivation coefficients were derived from data presented in Sinton et. al (1994) and Noble et. al (1999).

For Enterococci, the dark inactivation coefficients for summer and winter were assumed to be 0.020 $h^{-1}$ and 0.013 $h^{-1}$ respectively, while the daytime coefficients were assumed to be 0.36 $h^{-1}$ and 0.19 $h^{-1}$ for summer and winter respectively. These inactivation coefficients were derived from data presented in Noble et. al (1999).

The seasonal and daily variation for inactivation rates for both viruses and Enterococci were derived based on the above dark and light inactivation rates. The seasonal variation in the maximum dark and light rates were derived using a sigmoidal variation based on the number of days to and from winter solstice as follows;

$$k_{DayNumber} = k_{winter} + (k_{summer} + k_{winter})/(1 + exp(6-12*DayNumber/182))$$

Where $k_{summer}$ or $k_{winter}$ are the dark (or light) inactivation rates (as above) and $k_{DayNumber}$ is the daily maximum dark (or light) inactivation rate for the day of year being considered – where *DayNumber* is defined as the time to or from the winter solstice;

$$DayNumber = \text{abs}(Day\ of\ the\ Year - 182)$$

Lastly, the light inactivation rate was modulated on an hourly basis based on the observed solar radiation from Auckland Airport. The actual inactivation rate was assumed to be the predicted maximum daily inactivation rate (from above formula) multiplied by the ratio of the observed hourly solar radiation to the maximum clear sky solar radiation for the day being considered.

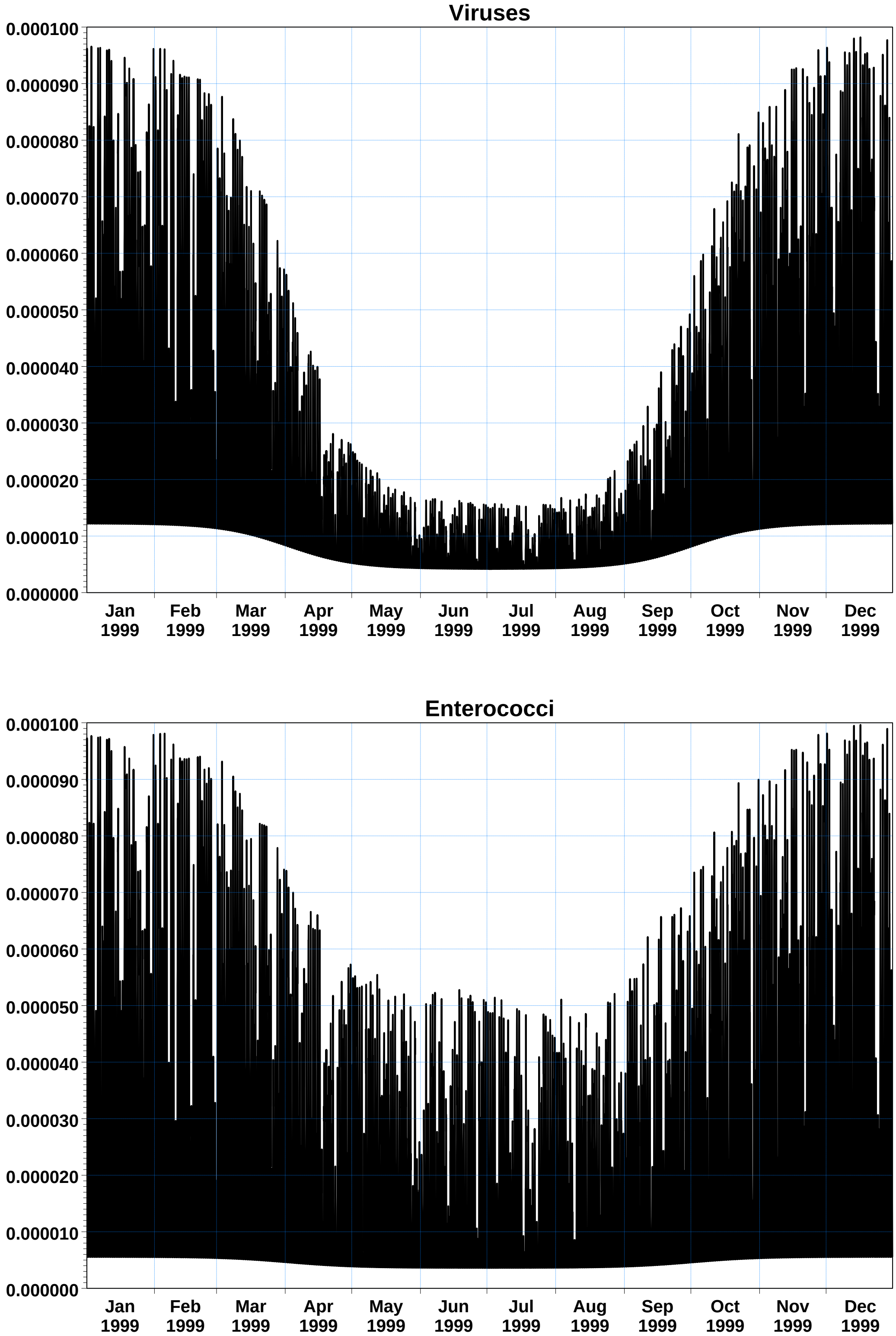


Figure 4-5 Time-varying decay rates ($hr^{-1}$) for viruses (top panel) and bacteria (bottom panel) for the 1999 simulation.

# 5 Salinity Calibration

The calibration of the hydrodynamic model included a comparison of model performance against limited observed salinities in the immediate vicinity of the outfall.

Figures 5-1 to 5-6  show the time series of observed and predicted salinities for January-February 2017. This period only includes three sampling dates but includes sampling after an extended dry period and sampling after moderate and heavy rain.

The regression plot for all of the data (i.e. across all sites) is shown in Figure 5-7 and the data in Figure 5-1 shows the metrics of the errors associated with the calibration and the goodness-of-fit measures based on $r^2$ (the coefficient of determination), the coefficient of efficiency or Nash-Sutcliffe coefficient (Nash and Sutcliffe, 1970), and the index of agreement (Willmott et al., 1985).

This calibration shows that the mixing of freshwater within the Waiuku system is, given the limited number of observations, reasonably well simulated across a relative wide spatial extent (Figure 3-3).

Table 5-1 Error and goodness-of-fit metrics for the salinity calibration.

| Parameter | Value | Unit |
|---|---|---|
| Mean Error | -0.0798 | PSU |
| Mean Absolute Error | 0.9389 | PSU |
| Root Mean Square Error | 1.0616 | PSU |
| Standard deviation of Residuals | 1.0586 | PSU |
| Coefficient of Determination | 0.4784 | [-] |
| Coefficient of Efficiency | 0.2144 | [-] |
| Index of Agreement | 0.8252 | [-] |

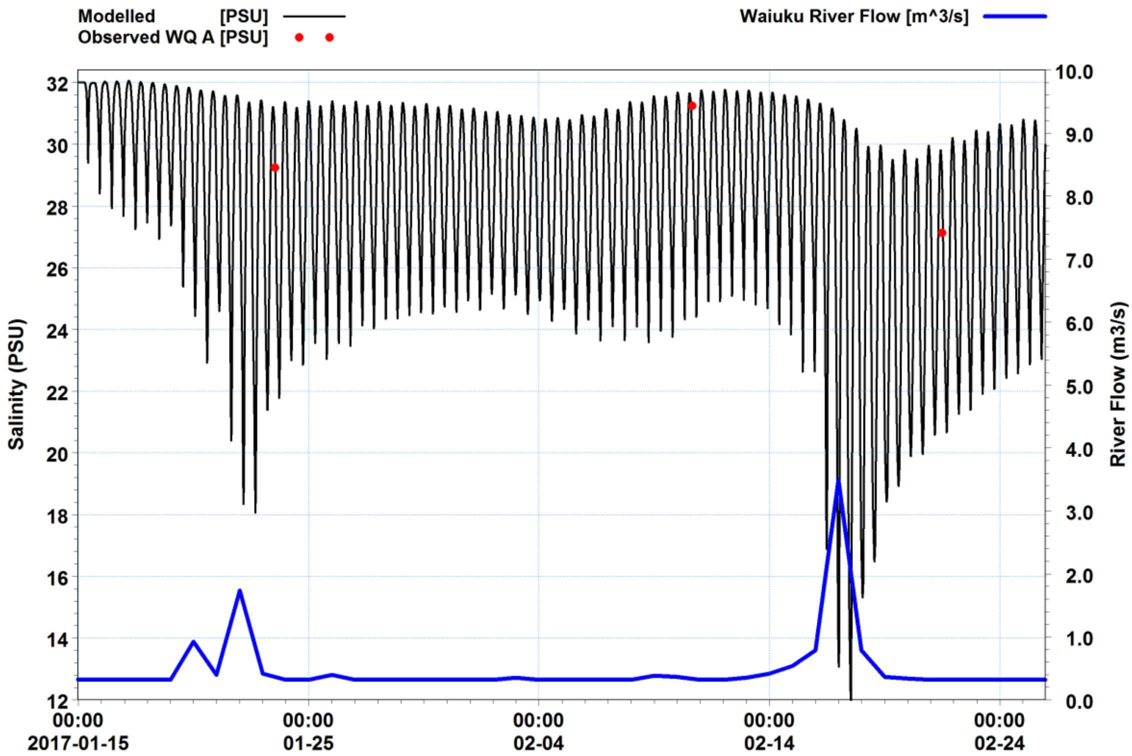


Figure 5-1 Observed (symbol) and predicted (black line) salinities at Waiuku monitoring site A (Figure 3-3) for January-February 2017. Estimated river flows for the Waitangi Stream (blue line) indicate timing of sampling relative to rainfall events.

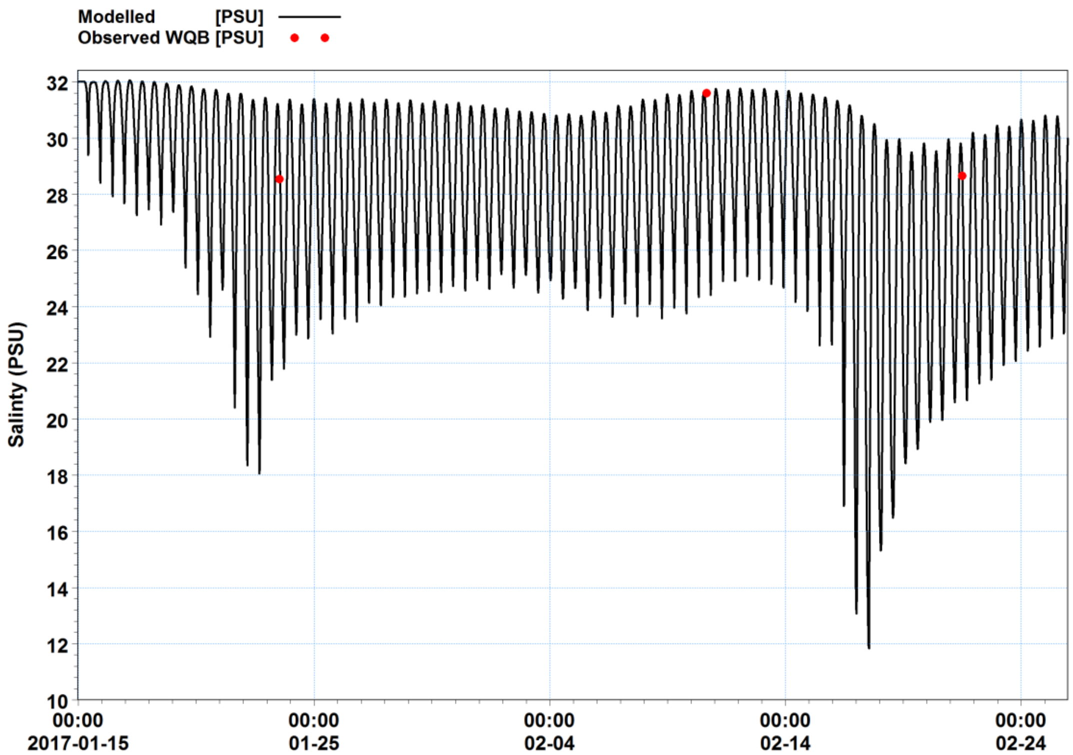

Figure 5-2 Observed (symbol) and predicted (black line) salinities at Waiuku monitoring site B (Figure 3-3) for January-February 2017.

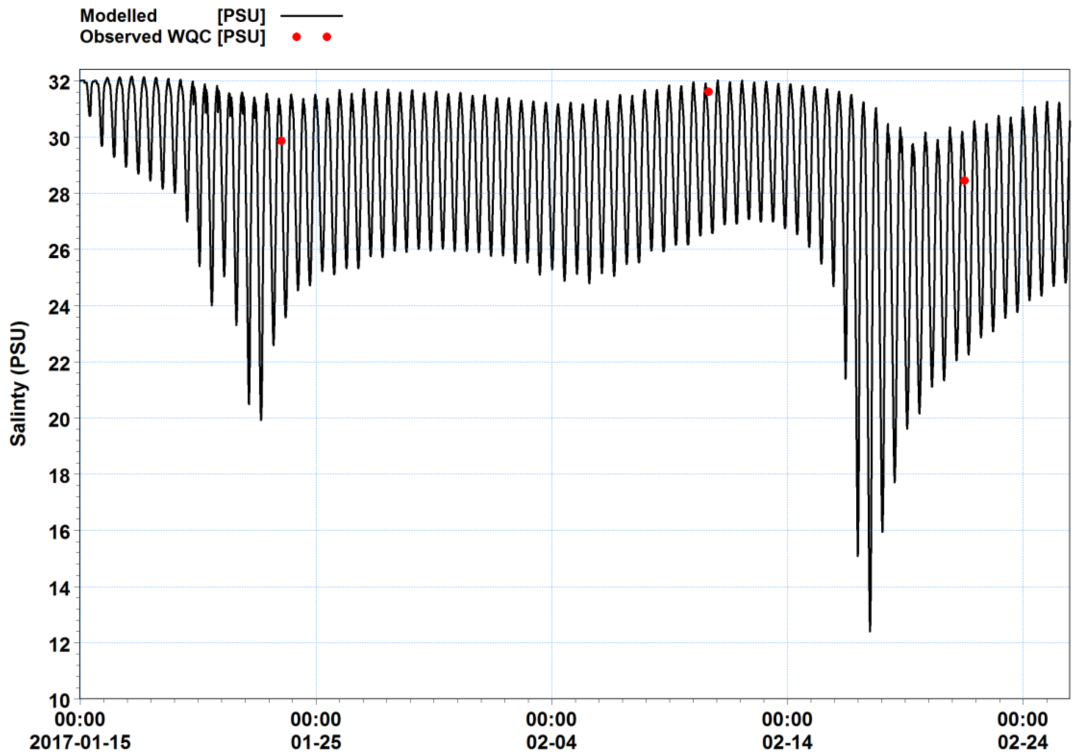


Figure 5-3 Observed (symbol) and predicted (black line) salinities at Waiuku monitoring site C (Figure 3-3) for January-February 2017.

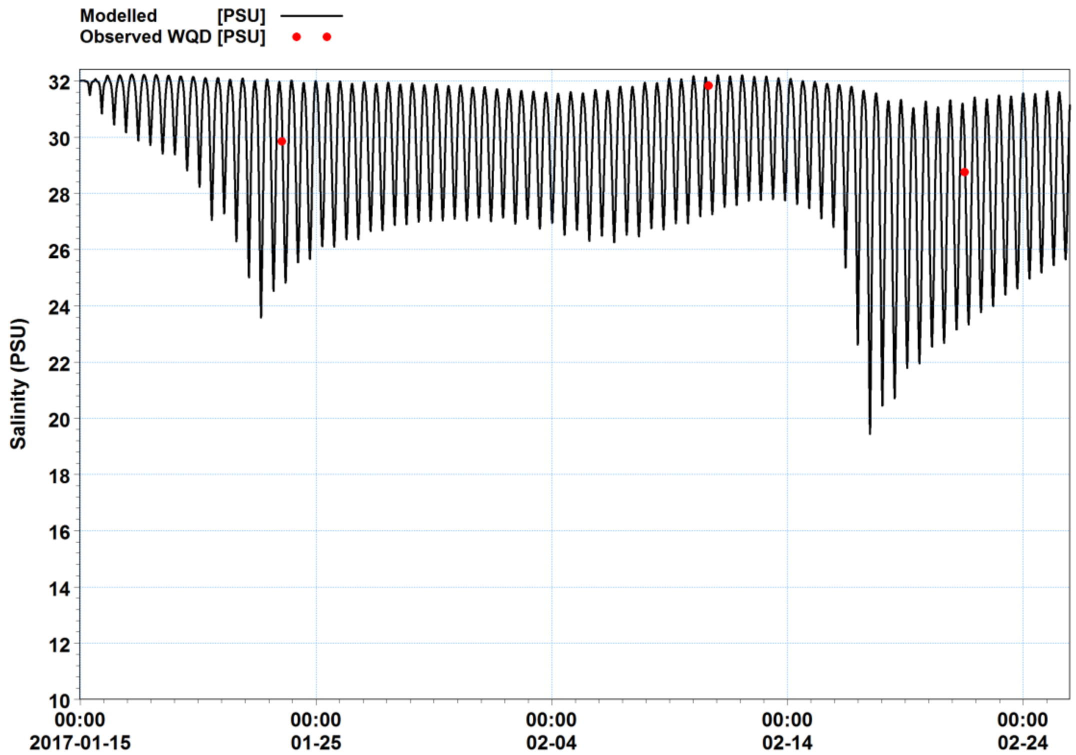


Figure 5-4 Observed (symbol) and predicted (black line) salinities at Waiuku monitoring site D (Figure 3-3) for January-February 2017.

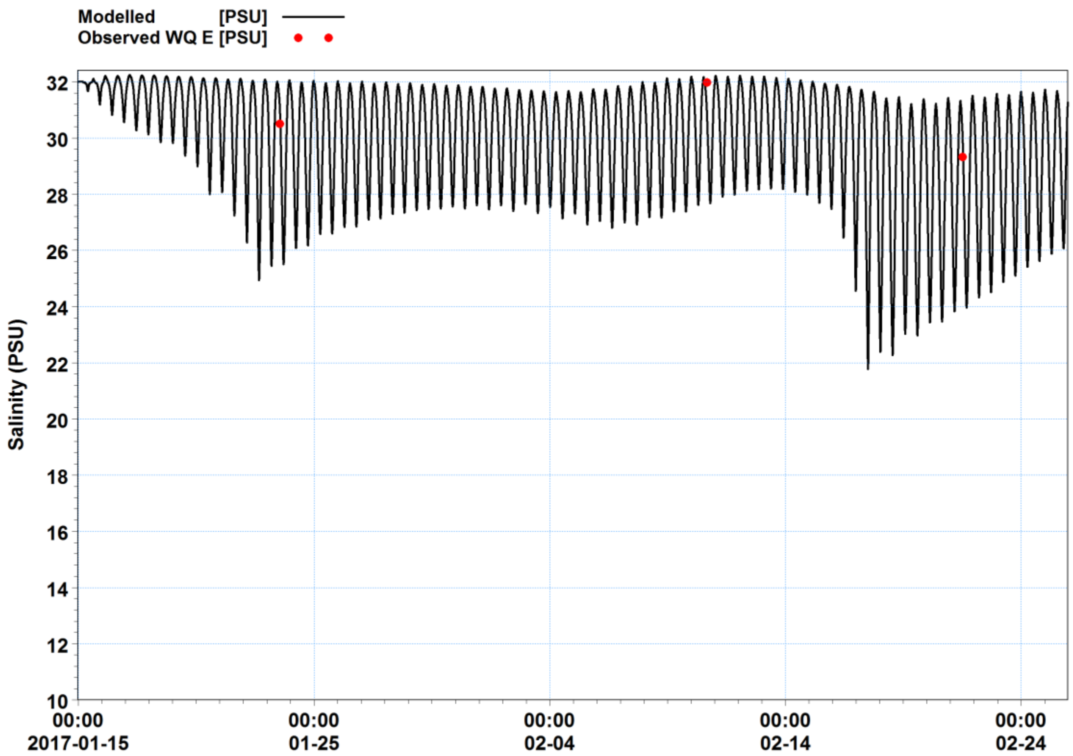


Figure 5-5 Observed (symbol) and predicted (black line) salinities at Waiuku monitoring site E (Figure 3-3) for January-February 2017.

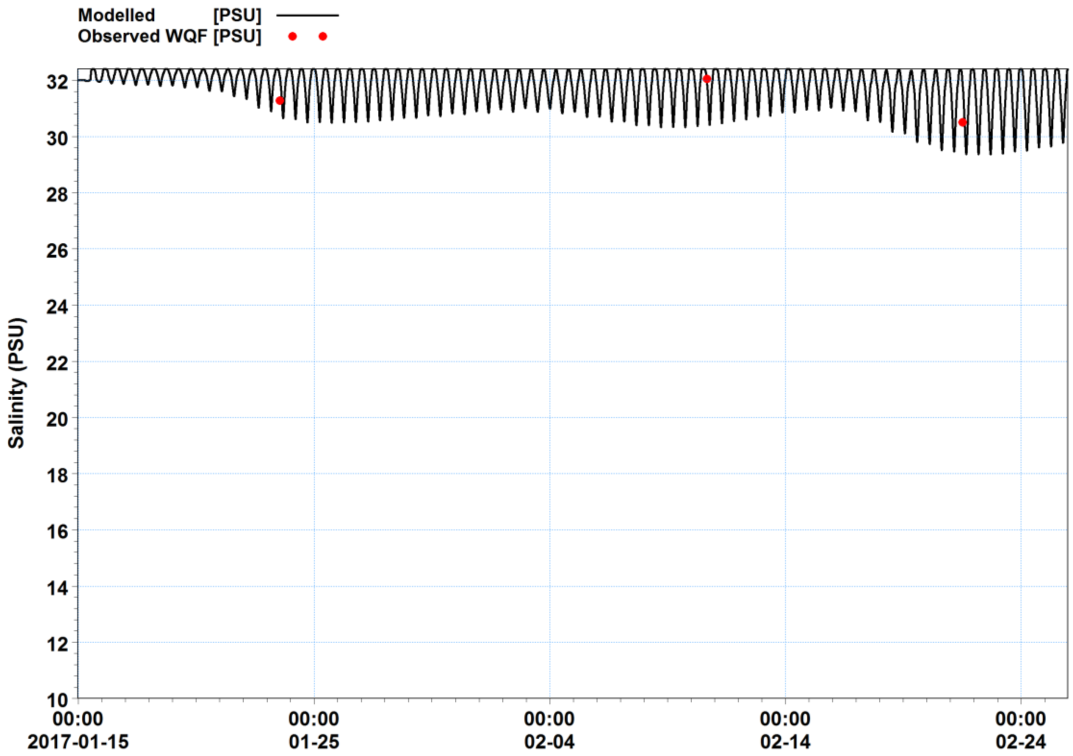


Figure 5-6 Observed (symbol) and predicted (black line) salinities at Waiuku monitoring site F (Figure 3-3) for January-February 2017.

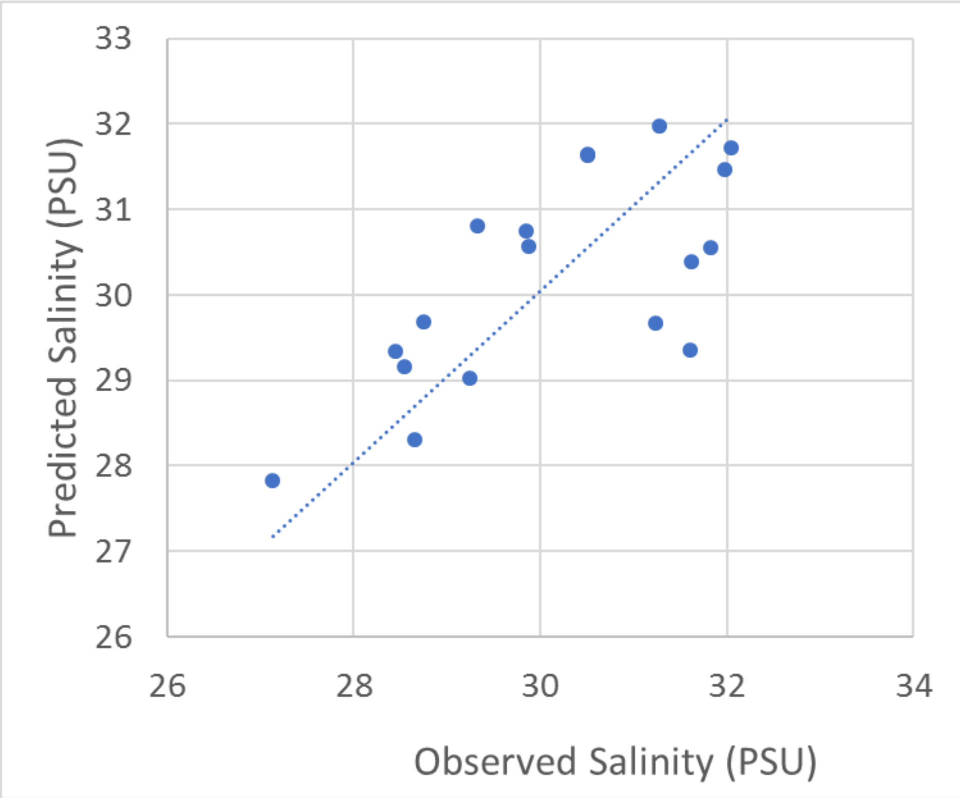


Figure 5-7 Regression plot for observed and predicted salinities for January-February 2017.

# 6 Near Field Assessment

CORMIX (Doneker and Jirka, 2007) provides estimates of the near-field behaviour of a discharge for given steady state ambient current, water depths and overflow rate.

Schematic water depth and ambient currents from the earlier MIKE 21 FM model (DHI, 2016) were extracted for all of 1999 (Figure 6-1). This figure also shows the schematic conditions (indicated as red dots) chosen for assessing the near-field behaviour of the Waiuku WWTP discharge.

Note that CORMIX has a limitation on the ratio of the water depth to outfall diameter so schematic conditions for water depths < 1.2 m cannot be simulated. For such conditions (which occur towards the end of the discharge window) the plume is likely to be fully mixed.

Results from the CORMIX simulations for each of the schematic conditions considered are summarised in

Table 6.1 for a discharge rate of 0.25 $m^3/s$. The discharge rate is the maximum rate that is likely to occur for the scenarios being considered during a wet winter period.

Table 6.2 provides a summary of results for a discharge rate of 0.11 $m^3/s$. This discharge rate is representative of an average discharge rate (Table 2-1).

Because the discharge is timed to occur during the first part of the ebb tide, ambient currents are always increasing in strength with time and, as such, the schematic CORMIX results will provide conservative estimates of the level of dilution achieved and the degree of vertical mixing in the water column.

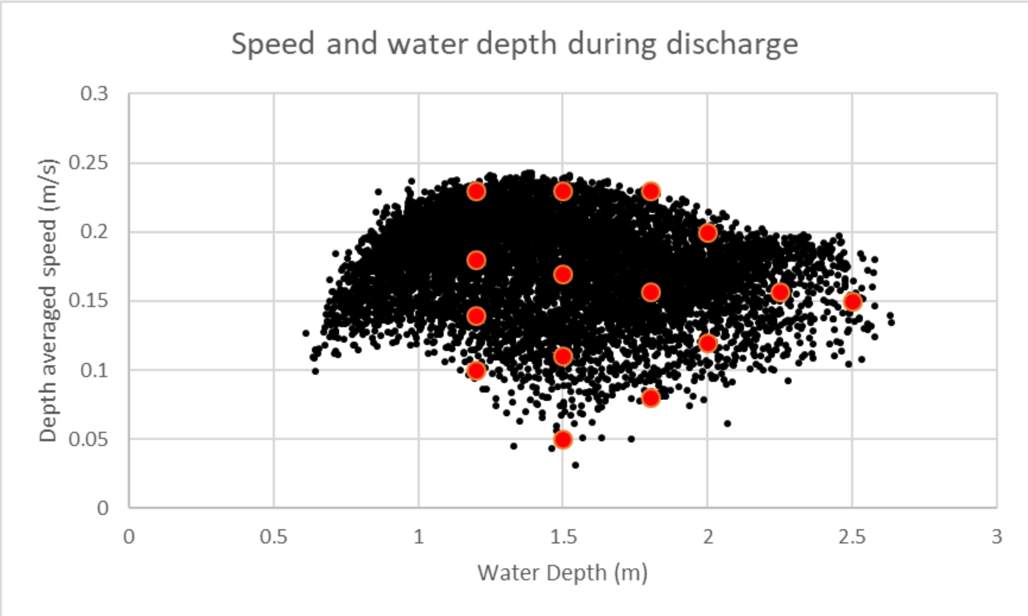


Figure 6-1 Scatter plot of predicted water depths and ambient currents at the outfall location from the 1999 annual simulation for the Clarks Beach study (DHI, 2016). Red dots indicate schematic conditions selected for near-field assessment.

The results show that, for much of the time, the plume rapidly becomes close to fully mixed in the water column. Highlighted rows in Table 6.1 and Table 6.2 are the schematic conditions when this is not the case. Based on the time-series of predicted water depths and currents from the 1999 simulation, such conditions will occur for less than 15% of time.

The size of the near-field region is relatively small (< 25 m) and the level of dilution achieved 50 m from the outfall ranges from 5 through to 20.

Given the conservative nature of the CORMIX predictions, the results of the CORMIX modelling indicate that it is appropriate to assume that within a few tens of meters of the outfall the Waiuku WWTP discharge will become fully mixed in the water column and that a 2D depth-averaged far-field model will adequately reproduce the dynamics of the treated wastewater plume for the range of discharges being considered.

Table 6.1 Ambient conditions modelled for current discharge rate (0.25 $m^3/s$).

| Scenario ID | Water Depth (m) | Ambient Current (m/s) | Plume Thickness (% of Water column) | Distance to edge of Near Field (m) | Dilution at 50m |
|---|---|---|---|---|---|
| A | 1.20 | 0.10 | 89% | 19 | 5 |
| B | 1.20 | 0.14 | 82% | 8 | 5 |
| C | 1.20 | 0.18 | 71% | 5 | 6 |
| D | 1.20 | 0.23 | 53% | 4 | 7 |
| E | 1.50 | 0.05 | 96% | 22 | 21 |
| F | 1.50 | 0.11 | 93% | 21 | 13 |
| 7 | 1.50 | 0.17 | 92% | 22 | 10 |
| G | 1.50 | 0.23 | 91% | 19 | 8 |
| H | 1.80 | 0.08 | 95% | 15 | 18 |
| I | 1.80 | 0.16 | 93% | 22 | 12 |
| J | 1.80 | 0.23 | 91% | 20 | 10 |
| K | 2.00 | 0.12 | 94% | 21 | 15 |
| L | 2.00 | 0.20 | 92% | 21 | 12 |
| M | 2.25 | 0.16 | 94% | 23 | 15 |
| N | 2.50 | 0.15 | 94% | 23 | 17 |

Table 6.2 Ambient conditions modelled for current discharge rate (0.11 $m^3/s$).

| Scenario ID | Water Depth (m) | Ambient Current (m/s) | Plume Thickness (% of Water column) | Distance to edge of Near Field (m) | Dilution at 50m |
|---|---|---|---|---|---|
| A | 1.20 | 0.10 | 94% | 14 | 13 |
| B | 1.20 | 0.14 | 93% | 15 | 11 |
| C | 1.20 | 0.18 | 92% | 14 | 10 |
| D | 1.20 | 0.23 | 90% | 12 | 10 |
| E | 1.50 | 0.05 | 97% | 11 | 20 |
| F | 1.50 | 0.11 | 95% | 10 | 14 |
| 7 | 1.50 | 0.17 | 93% | 11 | 12 |
| G | 1.50 | 0.23 | 69% | 1 | 6 |
| H | 1.80 | 0.08 | 96% | 9 | 19 |
| I | 1.80 | 0.16 | 94% | 12 | 15 |
| J | 1.80 | 0.23 | 73% | 2 | 7 |
| K | 2.00 | 0.12 | 96% | 11 | 17 |
| L | 2.00 | 0.20 | 75% | 2 | 8 |
| M | 2.25 | 0.16 | 88% | 3 | 6 |
| N | 2.50 | 0.15 | 89% | 4 | 6 |

# 7 Simulation Results

## 7.1 Hydrodynamics

The WWTP outfall is located on the eastern flank of a small sub-tidal channel some 200 m offshore of the WWTP (Figure 7-1).

The average discharge through this channel during the WTWP discharge window (three hours starting 15 minutes after High Water) ranges between 28-68 $m^3/s$. These values indicate that, when the plume becomes fully mixed across the sub-tidal channel and through the water column dilutions of the order of 220-500 are likely.

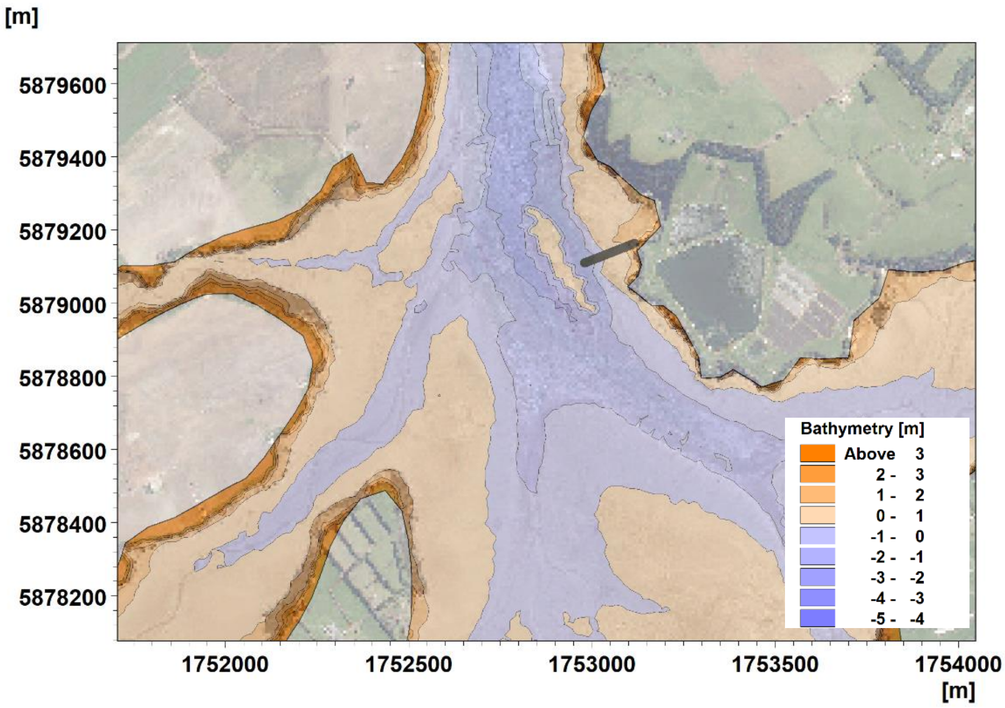


Figure 7-1 Detailed bathymetry in the area immediately offshore of the WWTP.

Estimates of the flushing capacity of the southern sector of the Waiuku Estuary have been calculated by releasing a conservative tracer on the first 3 hours of a spring, mean or neap tide.

The time series plots of the total mass exported from the southern sector of the Waiuku Estuary (Figure 7-2) indicate that 50% of the conservative tracer is flushed from the system within 3-6 days and 90% of the conservative tracer is flushed from the system within 16-21 days.

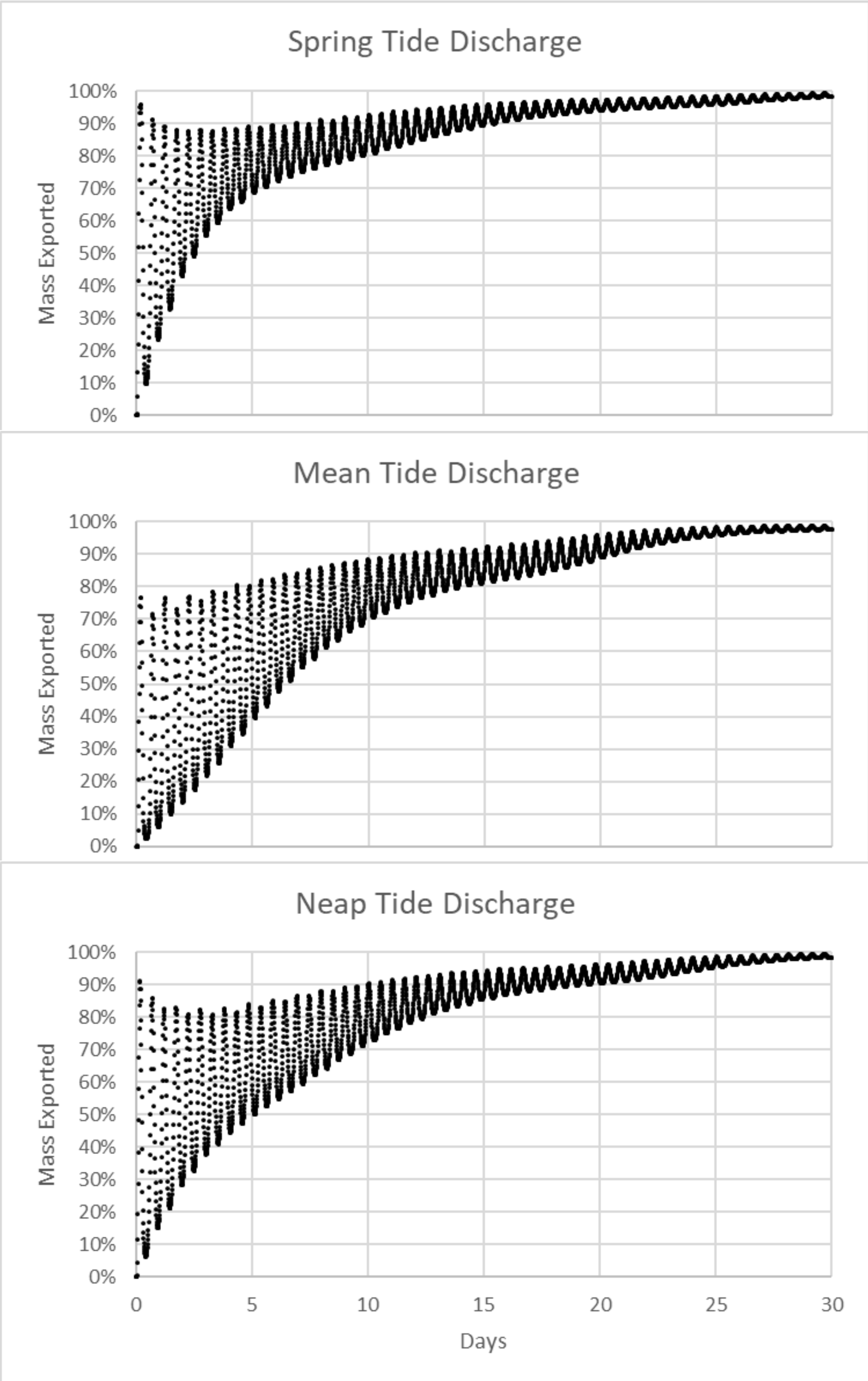


Figure 7-2 Time series of total mass exported from the southern sector of the Waiuku Estuary following the release of a conservative tracer on a spring (top panel), mean (middle panel) and neap tide (bottom panel)

## 7.2 Viruses and Bacteria

Time series of virus and bacteria concentrations were extracted from the year-long 1999 simulation at the locations presented in Figure 7-3 and Table 7-1

Time series plots of predicted concentrations at the SF_WQ_Site5 (closest to the outfall) for the Enterococci are shown in Figure 7-4 and viruses in Figure 7-5. Additional time-series plots of the predicted concentrations for all other sites are presented in Appendix B.

The variability of the concentration of Enterococci and viruses predicted at the sites considered is mainly caused by the seasonal changes in rainfall (effecting freshwater inputs including the WWTP discharge) and sunlight inactivation. In summer, the lower WWTP discharge rates (Figure 4-4) combines with the enhanced sunlight inactivation (Figure 4-5) leading to lowest predicted concentrations in bacteria and viruses. In winter, the highest WWTP discharge occur combined with the lowest amount of inactivation leading to highest predicted concentrations in bacteria and viruses.

An analysis of the dilution percentiles at the selected sites for the current discharge scenario are presented in Table 7-2 and Table 7-3.

The tabulated percentile dilutions for Future Scenario are given in Table 7-4 and Table 7-5.

$50^{th}$ (median) and $99^{th}$ percentile exceedance plots for the bacteria and virus concentrations are provided in Figures 7-6 to 7-9 for Future Scenario. Because only subtle changes are predicted compared to the Current scenario, percentile exceedance plots for the Current Scenario are not presented.

The water quality model results show that the median dilution achieved at the two northern sites ranges from 9000-16000 under the Future Scenario (Table 7-4 and Table 7-5) with lowest levels of dilution achieved at shallower eastern site (SF_WQ_Site2).

The lowest levels of dilution are achieved at the Red Cockle Bed site with median dilutions of 1800 and 1900 for viruses and Enterococci respectively under the Future Scenario (Table 7-4 and Table 7-5). This is because the plume tends to be transported into the eastern subtidal areas to the north of the discharge point as shown by the zone of lower percentile dilutions in Figure 7-8. This is a result of the predominant westerly winds (Figure 3-5) transported the treated wastewater plume into this zone.

Median dilutions achieved at the Needles site are 6100 and 7000 for viruses and Enterococci respectively under the Future Scenario (Table 7-4 and Table 7-5). These higher levels of dilution are due to the combined effect of the constriction near this site (resulting in relatively strong tidal flows), the fact the site is always inundated (and therefore is deeper than other sites considered) and the more dominant transport of the treated wastewater plume towards the eastern inter-tidal areas.

Median dilutions achieved at the southern sites range from 20000 to 49000 (Table 7-4 and Table 7-5). This high level of dilution comes about since, to reach these sites, the treated wastewater plume firstly is transported away from the discharge site on the outgoing tide and then it is transported back towards these sites on the subsequent incoming tide. This results in significant levels of dilution.

In addition to the seasonal variation, there is a strong modulation relating to the tide range with highest concentrations generally occurring during spring tides when the treated wastewater plume is advected away from the discharge site at its maximum rate (due to stronger tidal currents) and it is transported into areas of the Waiuku system which are not inundated during mean or neap tides (because of the reduced tidal range during neap and mean tides compared to spring tides).

Other variations in concentrations occur due to the combination of the time-varying inactivation and the effects of winds on the dynamics of the treated wastewater plume.

For example, dips in in predicted concentrations at SF_WQ_Site5 (Figure 7-4 and Figure 7-5) occur in early July and August which corresponds to a period of neap tides and moderate north-easterly winds.

Highest concentrations at SF_WQ_Site5 occur mid to late July which corresponds to an extended period of cloud cover (which results in the lowest inactivation rates Figure 4-5) and spring tides.

## 7.3 Conservative Tracer

Time series of conservative tracer concentrations were extracted from the year-long 1999 simulation at the locations presented in Figure 7-3 and Table 7-1.

An analysis of the dilution percentiles at the selected sites for the current discharge scenario and Future Scenario are presented in Table 7-6 and Table 7-7 respectively. This data provides an indication of the dilution that is achieved at the selected sites in the absence of any decay, uptake of contaminants or other chemical processes.

Table 7-1 Sites used for the QMRA and percentage of time site is inundated.

| Site | NZTM Easting (m) | NZTM Northing (m) | Percentage of time inundated |
|---|---|---|---|
| SF_WQ_Site2 | 1752409 | 5882565 | 58 |
| SF_WQ_Site3 | 1751265 | 5882403 | 75 |
| SF_WQ_Site4 - Red Cockle Beds | 1752501 | 5880312 | 100 |
| Needles Reserve - Oysters | 1752602 | 5879717 | 68 |
| SF_WQ_Site5 | 1753991 | 5878579 | 53 |
| Tahuna Marae - Oysters | 1751686 | 5878094 | 36 |
| Sandspit Safewsim site | 1753300 | 5877948 | 47 |

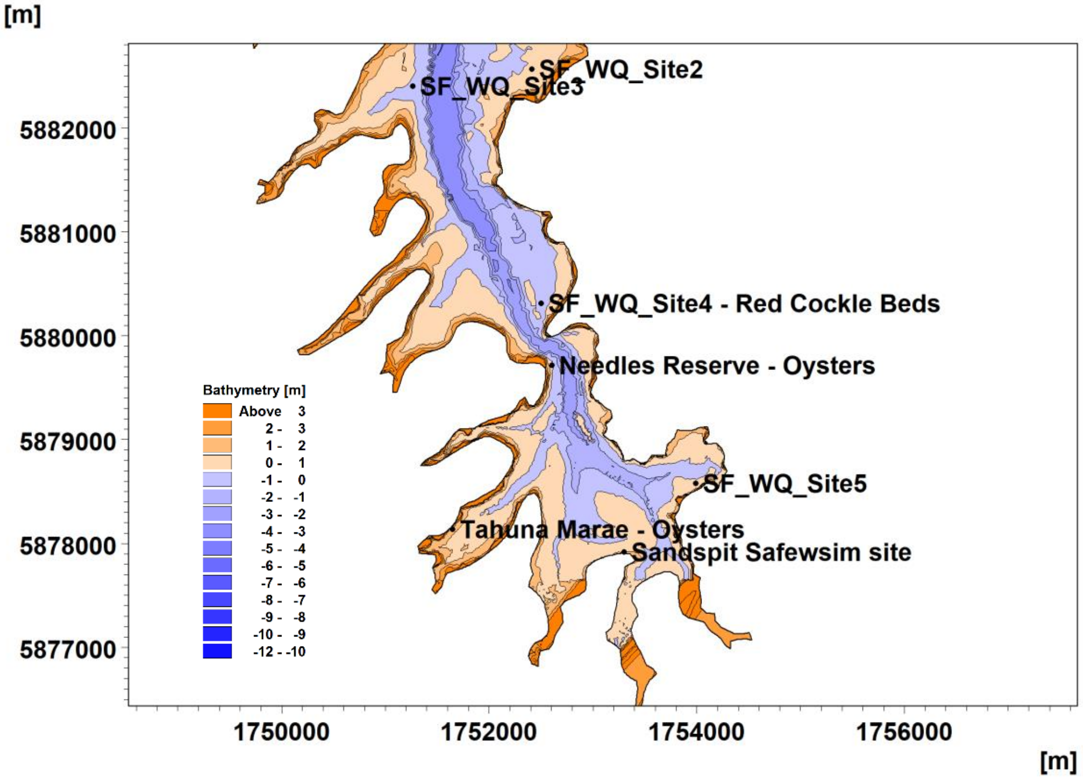


Figure 7-3 Location of selected sites for time series extraction of virus and bacteria concentrations.

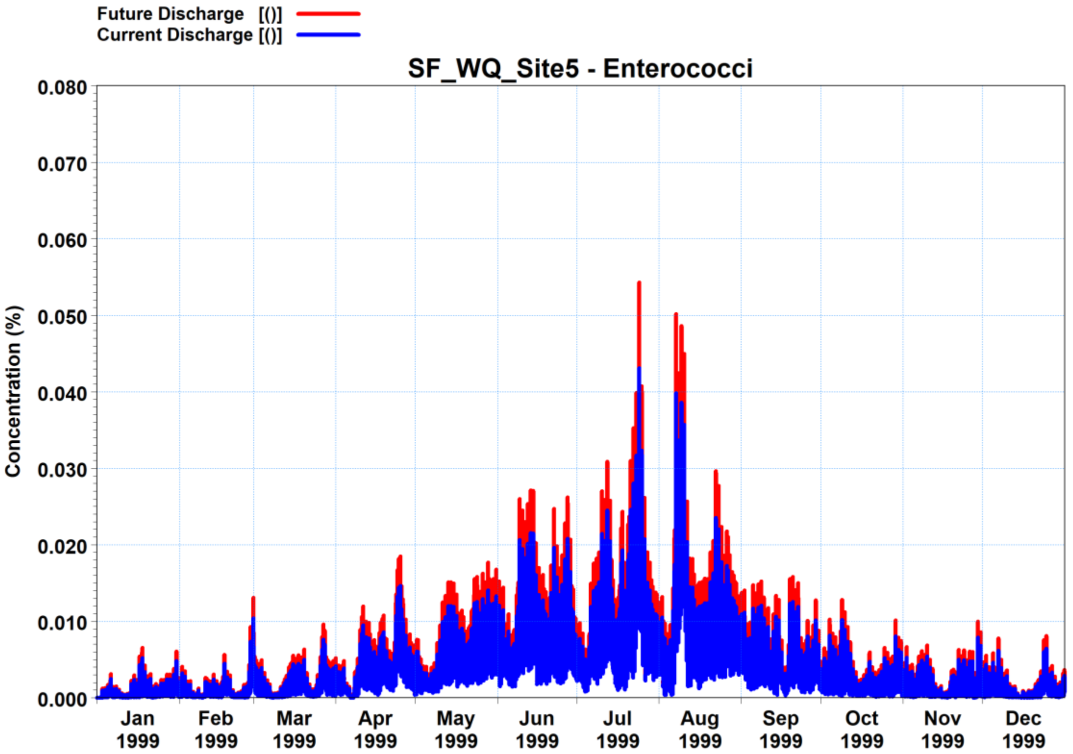


Figure 7-4 Time-series of predicted Enterococci concentrations at SF WQ Site 5 (nearest the outfall).

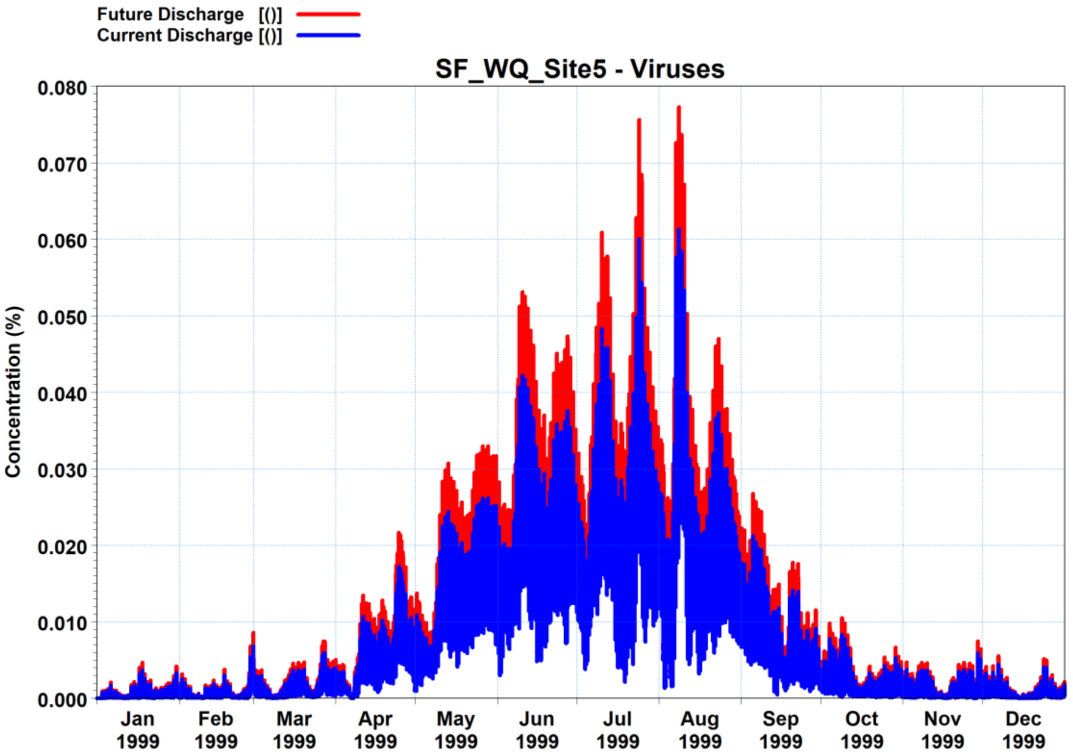


Figure 7-5 Time-series of predicted virus concentrations at SF WQ Site 5 (nearest the outfall).

Table 7-2 Bacteria - percentile dilutions at the QMRA sites for current discharge scenario. Values are rounded down to the nearest 10, 100 or 1000 depending on the magnitude of the dilution.

| Percentile | SF_WQ_Site2 | SF_WQ_Site3 | SF_WQ_Site4 - Red Cockle Beds | Needles Reserve - Oysters | SF_WQ_Site5 | Tahuna Marae - Oysters | Sandspit Safewsim site |
|---|---|---|---|---|---|---|---|
| 25th | 29000 | 74000 | 7400 | 20000 | 160000 | 120000 | 250000 |
| 50th | 12000 | 21000 | 2400 | 8800 | 48000 | 33000 | 62000 |
| 75th | 5900 | 7300 | 1300 | 4200 | 19000 | 13000 | 23000 |
| 90th | 3600 | 3600 | 830 | 2500 | 11000 | 6800 | 12000 |
| 95th | 2900 | 2600 | 680 | 1900 | 8500 | 5000 | 8800 |
| 99th | 2100 | 1700 | 540 | 1300 | 5100 | 3000 | 5000 |

Table 7-3 Virus - percentile dilutions at the QMRA sites for current discharge scenario. Values are rounded down to the nearest 10, 100 or 1000 depending on the magnitude of the dilution.

| Percentile | SF_WQ_Site2 | SF_WQ_Site3 | SF_WQ_Site4 - Red Cockle Beds | Needles Reserve - Oysters | SF_WQ_Site5 | Tahuna Marae - Oysters | Sandspit Safewsim site |
|---|---|---|---|---|---|---|---|
| 25th | 34000 | 71000 | 6500 | 23000 | 240000 | 160000 | 380000 |
| 50th | 11000 | 17000 | 2200 | 7700 | 40000 | 25000 | 48000 |
| 75th | 3600 | 5500 | 1100 | 2800 | 7400 | 6100 | 7700 |
| 90th | 2300 | 2200 | 700 | 1500 | 4600 | 3200 | 4700 |
| 95th | 1900 | 1600 | 580 | 1200 | 3700 | 2500 | 3700 |
| 99th | 1500 | 1100 | 450 | 940 | 2600 | 1800 | 2500 |

Table 7-4 Bacteria - percentile dilutions at the QMRA sites for Future Scenario. Values are rounded down to the nearest 10, 100 or 1000 depending on the magnitude of the dilution.

| Percentile | SF_WQ_Site2 | SF_WQ_Site3 | SF_WQ_Site4 - Red Cockle Beds | Needles Reserve - Oysters | SF_WQ_Site5 | Tahuna Marae - Oysters | Sandspit Safewsim site |
|---|---|---|---|---|---|---|---|
| 25th | 23000 | 59000 | 5900 | 16000 | 130000 | 100000 | 190000 |
| 50th | 9900 | 16000 | 1900 | 7000 | 38000 | 26000 | 49000 |
| 75th | 4700 | 5800 | 1000 | 3300 | 15000 | 10000 | 18000 |
| 90th | 2800 | 2800 | 660 | 1900 | 9000 | 5400 | 9900 |
| 95th | 2300 | 2000 | 540 | 1500 | 6700 | 4000 | 7000 |
| 99th | 1600 | 1300 | 430 | 1000 | 4000 | 2400 | 4000 |

Table 7-5 Virus - percentile dilutions at the QMRA sites for Future Scenario. Values are rounded down to the nearest 10, 100 or 1000 depending on the magnitude of the dilution.

| Percentile | SF_WQ_Site2 | SF_WQ_Site3 | SF_WQ_Site4 - Red Cockle Beds | Needles Reserve - Oysters | SF_WQ_Site5 | Tahuna Marae - Oysters | Sandspit Safewsim site |
|---|---|---|---|---|---|---|---|
| 25th | 27000 | 56000 | 5100 | 18000 | 190000 | 130000 | 300000 |
| 50th | 9000 | 13000 | 1800 | 6100 | 32000 | 20000 | 38000 |
| 75th | 2900 | 4300 | 920 | 2200 | 5900 | 4900 | 6100 |
| 90th | 1800 | 1700 | 550 | 1200 | 3600 | 2600 | 3800 |
| 95th | 1500 | 1300 | 460 | 1000 | 2900 | 2000 | 2900 |
| 99th | 1200 | 920 | 360 | 750 | 2100 | 1400 | 2000 |

Table 7-6 Conservative tracer - percentile dilutions at the QMRA sites for current discharge scenario. Values are rounded down to the nearest 10 or 100 depending on the magnitude of the dilution.

| Percentile | SF_WQ_Site2 | SF_WQ_Site3 | SF_WQ_Site4 - Red Cockle Beds | Needles Reserve - Oysters | SF_WQ_Site5 | Tahuna Marae - Oysters | Sandspit Safewsim site |
|---|---|---|---|---|---|---|---|
| 25th | 980 | 1800 | 670 | 920 | 640 | 530 | 550 |
| 50th | 720 | 930 | 410 | 550 | 490 | 390 | 410 |
| 75th | 530 | 520 | 290 | 370 | 370 | 310 | 320 |
| 90th | 430 | 360 | 220 | 280 | 310 | 270 | 280 |
| 95th | 390 | 310 | 200 | 250 | 280 | 250 | 250 |
| 99th | 320 | 240 | 160 | 200 | 240 | 220 | 220 |

Table 7-7 Conservative tracer - percentile dilutions at the QMRA sites for Future Scenario. Values are rounded down to the nearest 10 or 100 depending on the magnitude of the dilution.

| Percentile | SF_WQ_Site2 | SF_WQ_Site3 | SF_WQ_Site4 - Red Cockle Beds | Needles Reserve - Oysters | SF_WQ_Site5 | Tahuna Marae - Oysters | Sandspit Safewsim site |
|---|---|---|---|---|---|---|---|
| 25th | 780 | 1400 | 530 | 730 | 510 | 420 | 430 |
| 50th | 570 | 740 | 330 | 440 | 380 | 310 | 320 |
| 75th | 420 | 410 | 230 | 290 | 300 | 250 | 250 |
| 90th | 340 | 290 | 180 | 220 | 250 | 210 | 220 |
| 95th | 300 | 240 | 160 | 190 | 220 | 200 | 200 |
| 99th | 250 | 190 | 130 | 160 | 190 | 170 | 180 |

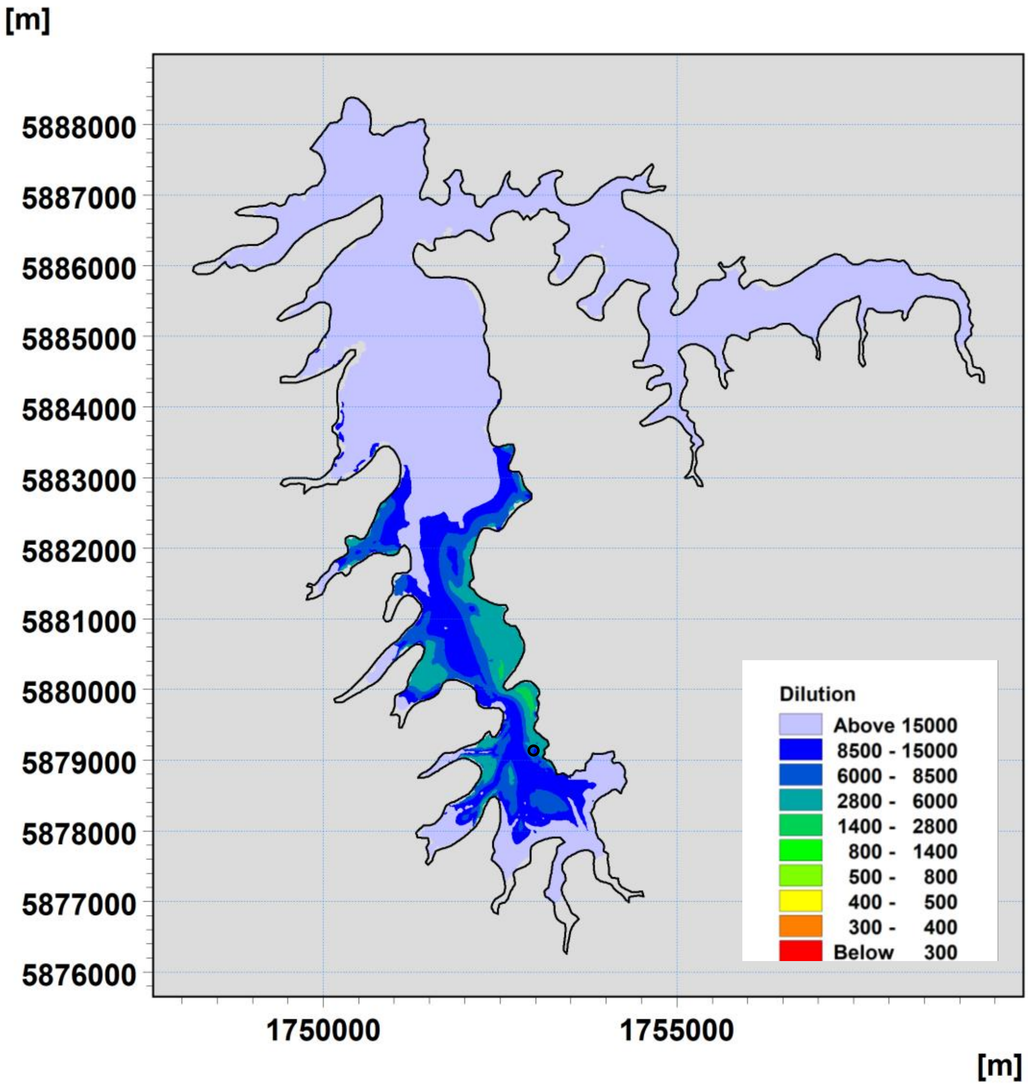


Figure 7-6 50th percentile virus dilution, Future Scenario. Black circle shows location of the WWTP discharge point.

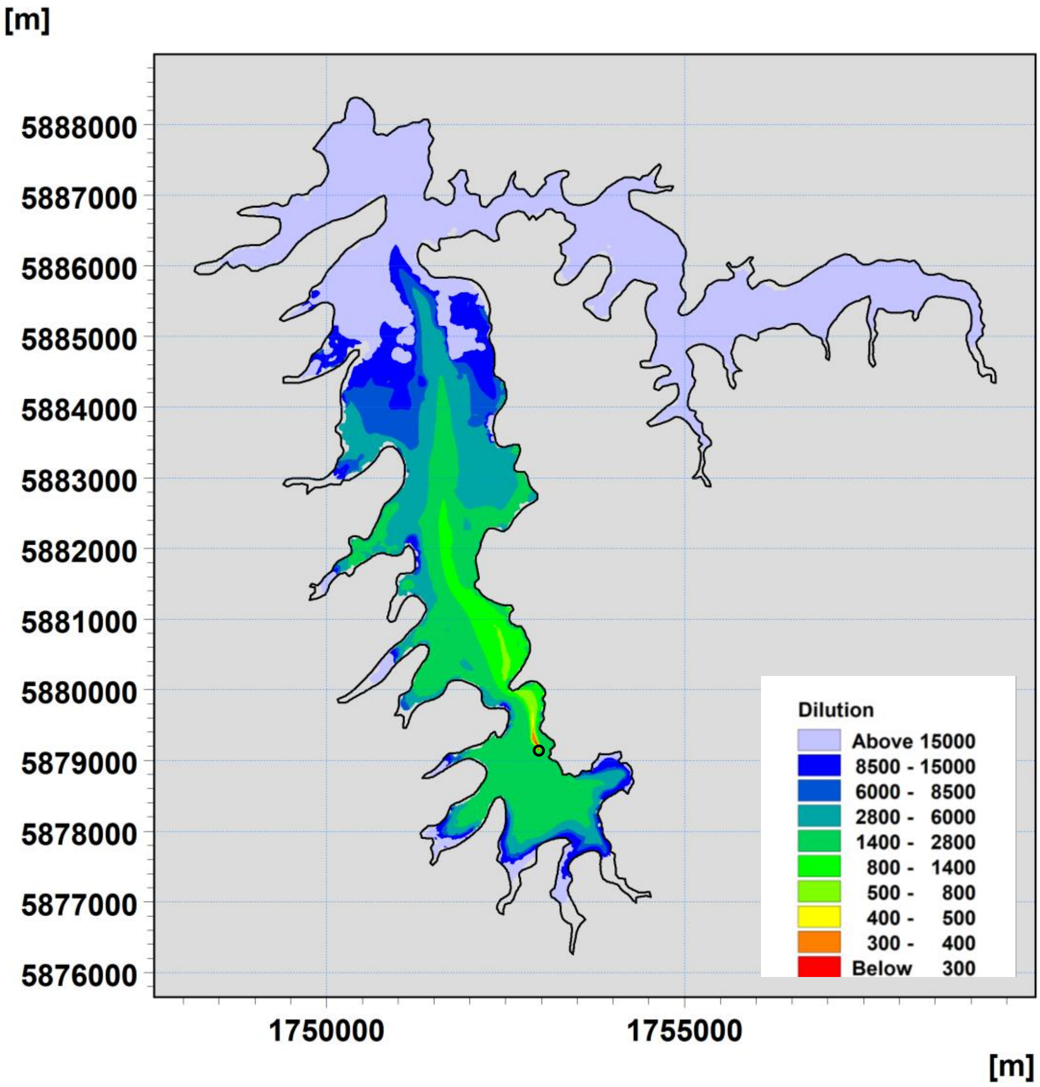


Figure 7-7 90th percentile virus dilution, Future Scenario. Black circle shows location of the WWTP discharge point.

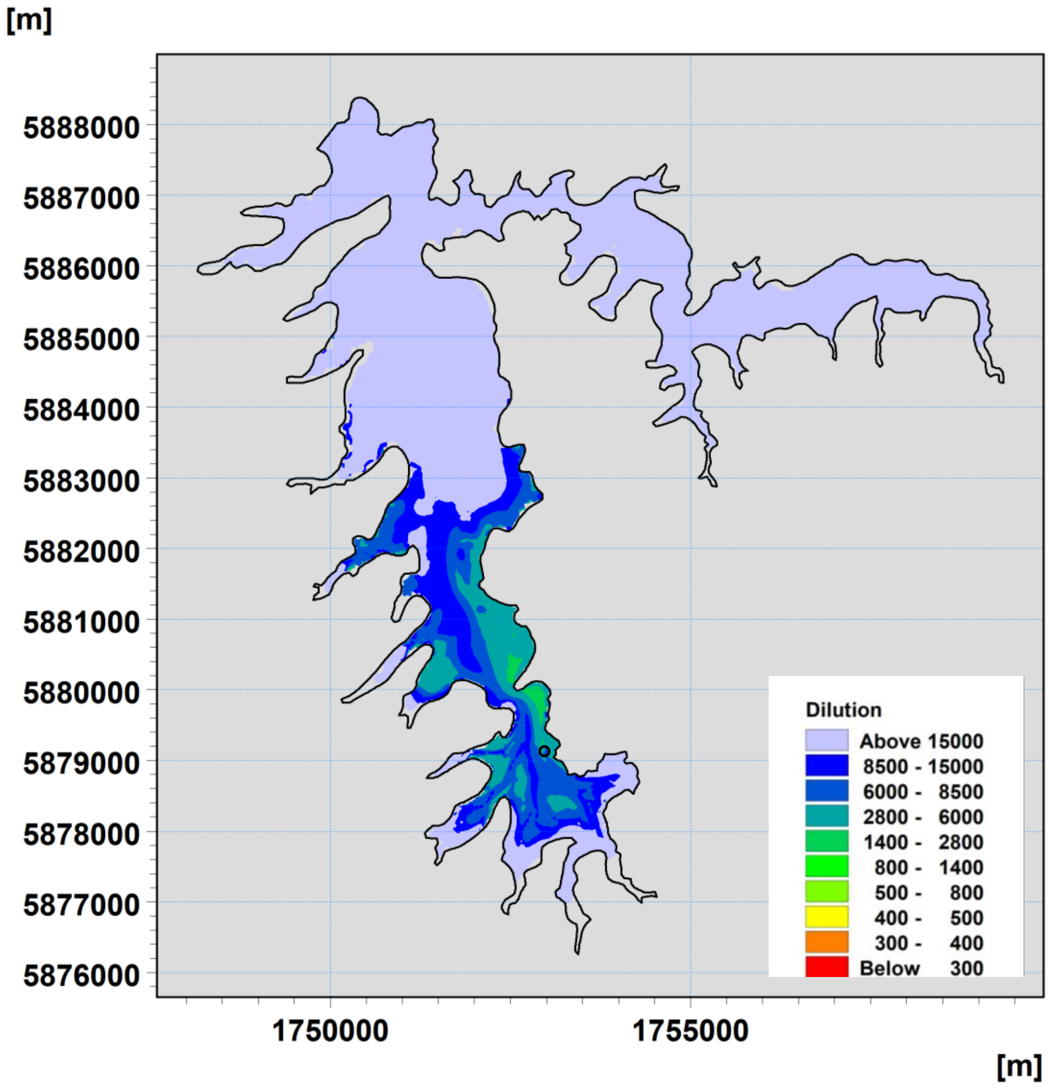


Figure 7-8 50th percentile bacteria dilution, Future Scenario. Black circle shows location of the WWTP discharge point.

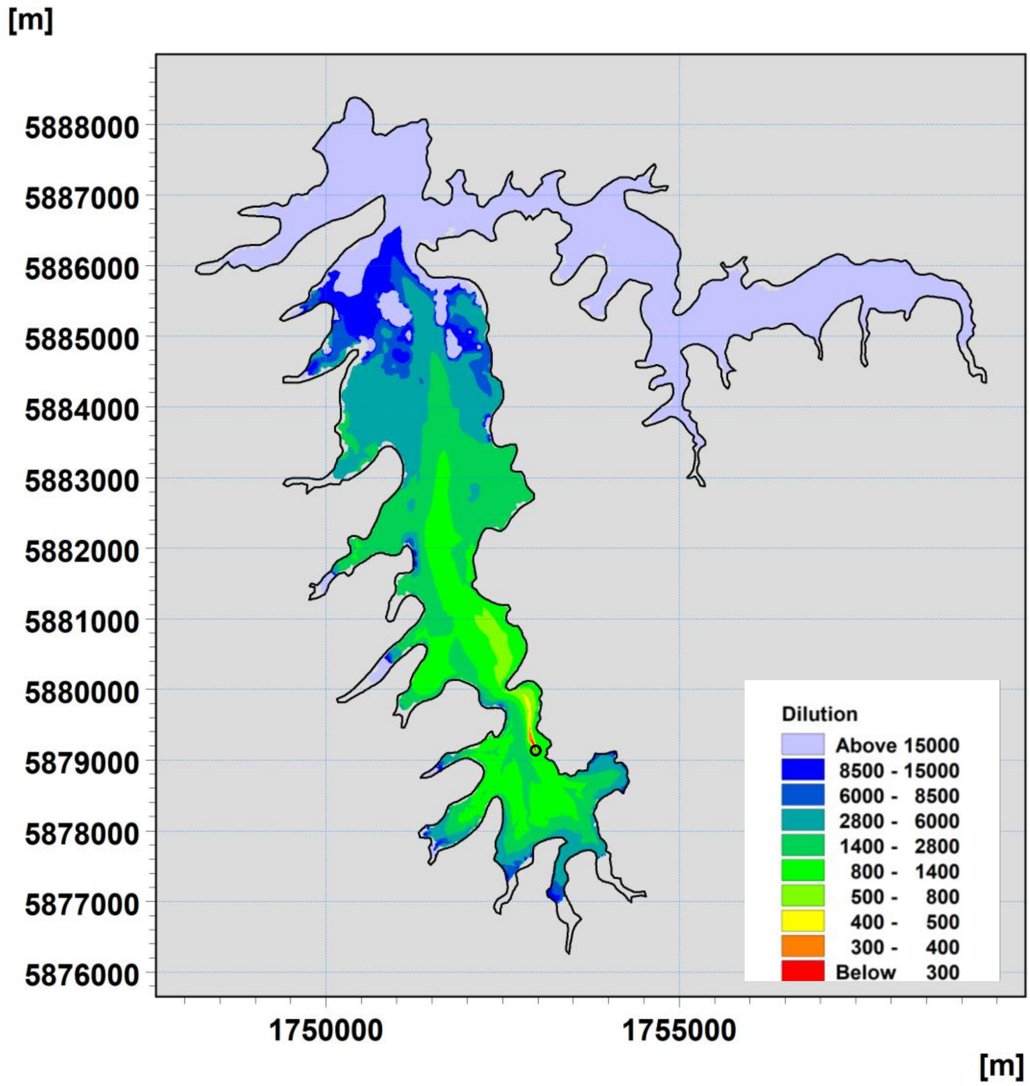


Figure 7-9 90th percentile bacteria dilution, Future Scenario. Black circle shows location of the WWTP discharge point.

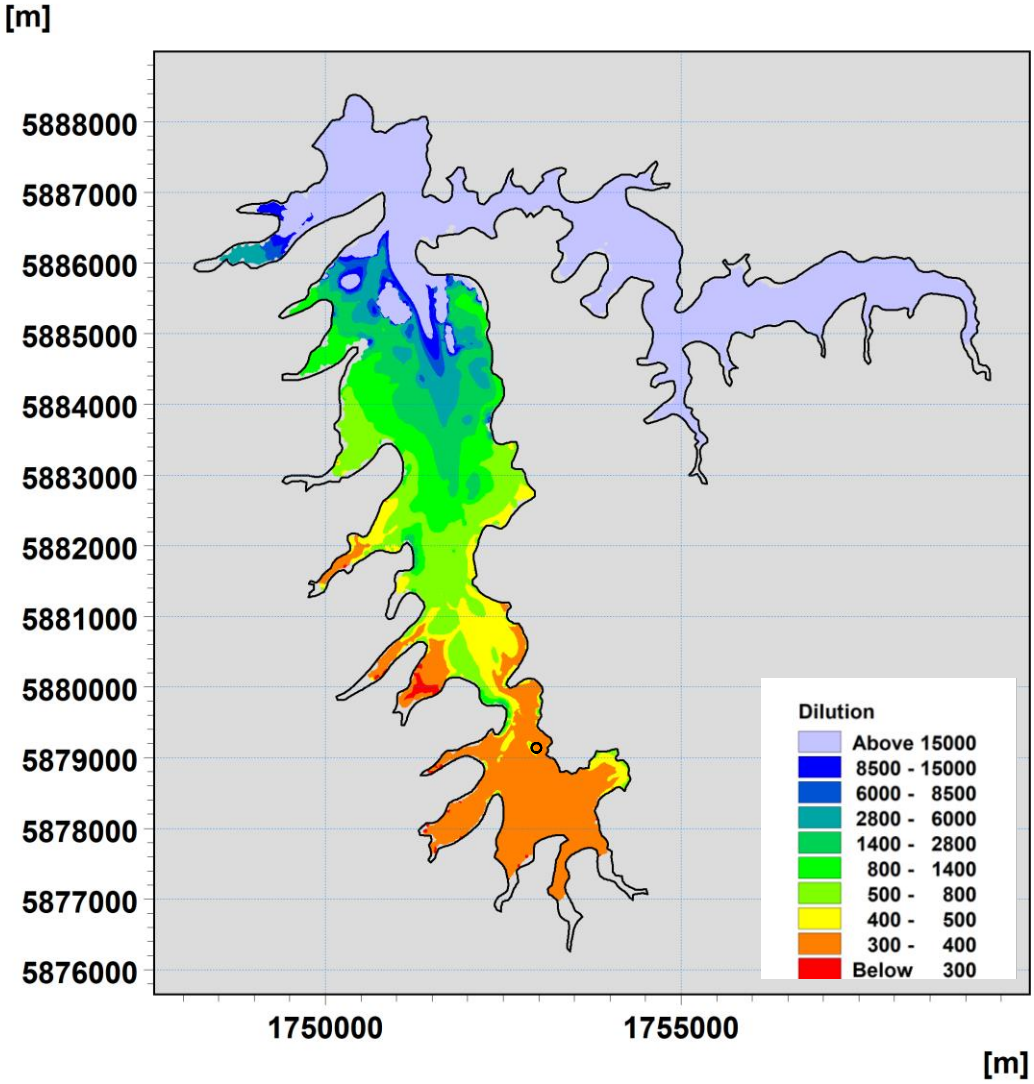


Figure 7-10 50th percentile conservative tracer dilution, Future Scenario. Black circle shows location of the WWTP discharge point.

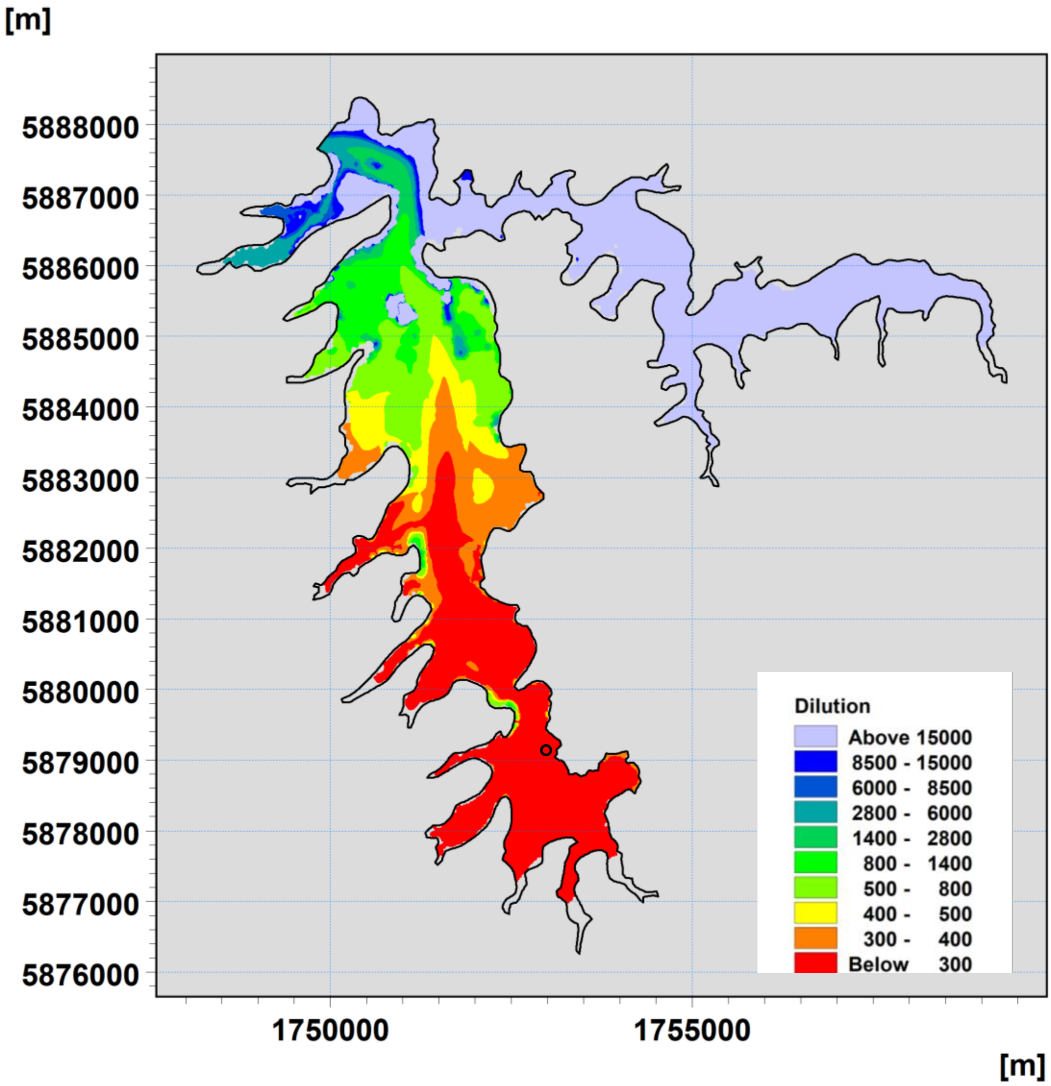


Figure 7-11 90th percentile conservative tracer dilution, Future Scenario. Black circle shows location of the WWTP discharge point.

# 8 Summary

This report provides details of an assessment of both a Current and Future scenario discharge regime for the existing Waiuku WWTP.

A high-level assessment of the three potential future discharges (based on different levels of population growth) showed very little difference between the scenarios in terms of achievable dilutions and reductions in salinity. This indicated that the Future Scenario option (which is based on a population increase of 26%) could be assessed in detail for the short-term consent application.

The assessment of the Current and preferred Future discharge scenarios is based on the results from a previously calibrated hydrodynamic model (DHI, 2016) which has been refined and further validated against available salinity data in the southern sector of the Waiuku Estuary. This validation shows that the model provides good estimates of the mixing of freshwater in the Waiuku Estuary.

Results from near-field modelling indicate that the Waiuku WWTP discharge has a relatively small near-field region (< 25 m), and, for the discharge rates being considered, the treated wastewater plume will rapidly become fully mixed. This is in part because the discharge occurs on the first half of the outgoing tide when ambient currents are relatively strong and increase over time during the discharge window.

Results from an annual simulation for a typical year (1999) have been used to provide an overview of the level of dilution achieved in the Waiuku Estuary for a conservative (non-decaying) tracer and viruses and bacteria. For viruses and bacteria, time varying inactivation rates were used which consider daily and seasonal variation in solar radiation.

Time-series of predicted virus and bacteria concentrations have been provided at five selected sites within the Waiuku Estuary for the purposes of carrying out a quantitative microbial risk assessment.

Median dilutions for Enterococci and viruses achieved at the two sites 3 km north of the discharge point range from 9000-16000 for the future discharge scenario considered.

At an inter-tidal site 1500 m from the discharge point, median dilutions of 1800 and 1900 are achieved for viruses and Enterococci and respectively.

At a subtidal site just to the north of the discharge point, median dilutions of 6100 and 7000 are achieved for viruses and Enterococci and respectively.

Such dilutions are achieved because the discharge occurs on the first part of the outgoing tide (when ambient currents are relatively strong), the relative magnitude of the WWTP discharge and other freshwater inputs to the Waiuku Estuary and the degree of exchange that occurs between the Waiuku Estuary and the main body of the Manukau Harbour (due to the inter-tidal nature of the Waiuku Estuary).

For sites to the south of the discharge point 99$^{th}$ percentile dilutions of greater than 1400 and median dilutions of greater than 20000 are achieved. This is because, to reach this part of the Waiuku Estuary, the treated wastewater plume is firstly transported away from the discharge site on the outgoing tide and then transported back towards these sites on the subsequent incoming tide.

# 9 References

Doneker, R.L. and G.H. Jirka, 20076.CORMIX User Manual: A Hydrodynamic Mixing Zone Model and Decision Support System for Pollutant Discharges into Surface Waters", EPA-823-K-07-001

DHI 2014. *Clarks Beach WWTP Options Study, Hydrodynamic Modelling*. Report prepared for Watercare Services Ltd.

DHI 2016. *Clarks Beach WWTP Options Study Hydrodynamic Modelling.* Report prepared for Watercare Services Ltd.

DHI 2017. *MIKE C-MAP, Extraction of World Wide Bathymetry Data and Tidal Information*. User Guide.

Nash, J.E., Sutcliffe, J. 1970. River flow forecasting through conceptual models, Part I A discussions of principles, J. Hydrol., 10, 282-290.

Noble, R.T., Lee, I.M. and Schiff, K.C. 1999. *Inactivation of indicator micro-organisms from various sources of faecal contamination in seawater and freshwater*. Journal of Applied Microbiology 2004, 96, 464–472

Sinton, L.W., Davies-Colley, R.J., and Bell, R.G. 1994. *Inactivation of Enterococci and fecal coliforms from sewage and meatworks effluents in seawater chambers*. Applied and Environmental Microbiology 2040–2048.

Willmott, C.J., Ackleson, S.G., Davis, R.E., Feddema, J.J, Klink, K.M., Leg-ates, D.R., O'Donnell, J., Rowe, C.M., 1985. Statistics for the evaluation and comparison of models, J. Geophys. Res., 90, 8995-9005.

# Appendix A – CORMIX near-field results

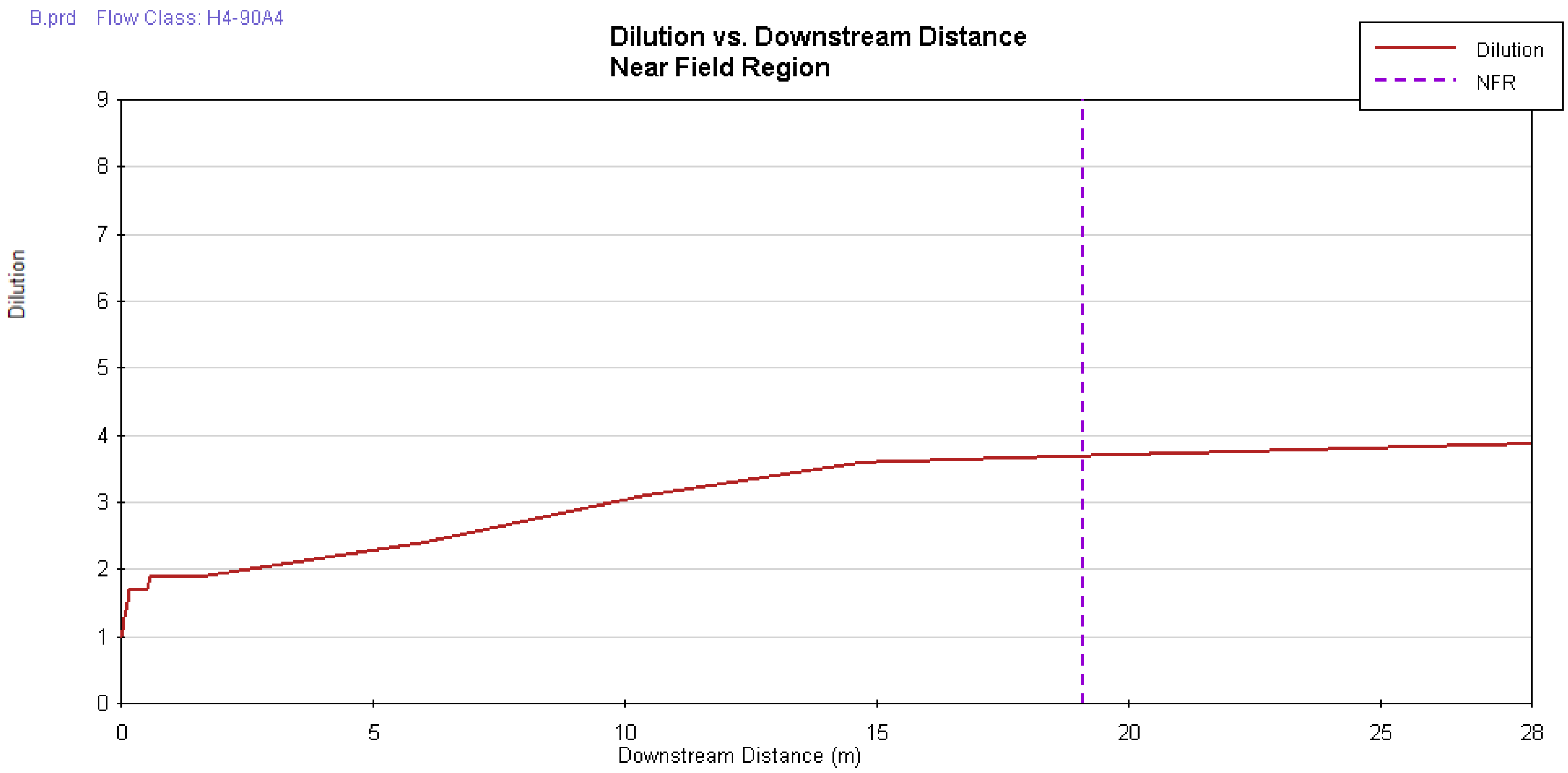


Figure A-1 CORMIX results in the near-field for Scenario A (Table 6.1).

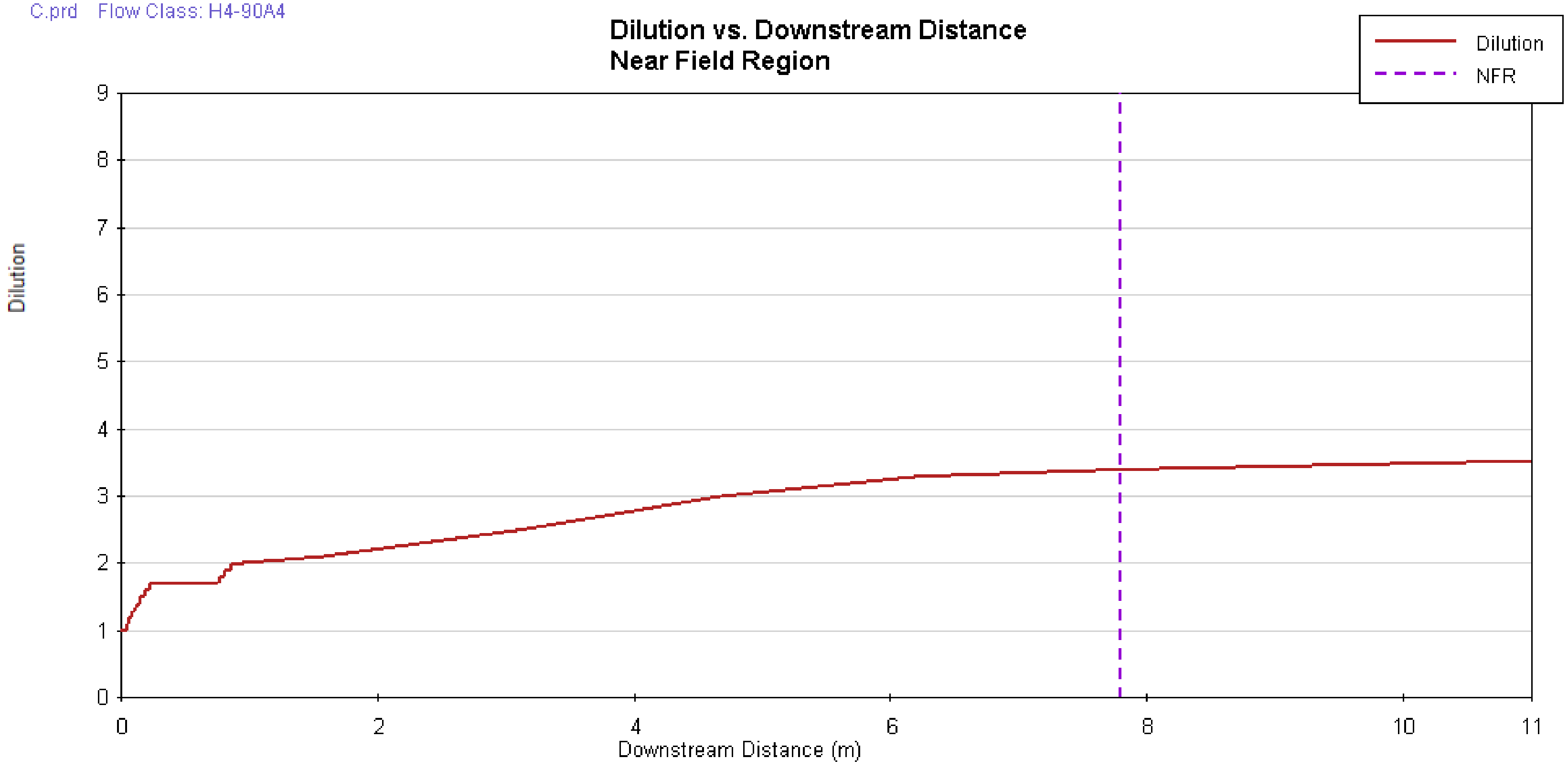


Figure A-2 CORMIX results in the near-field for Scenario B (Table 6.1).

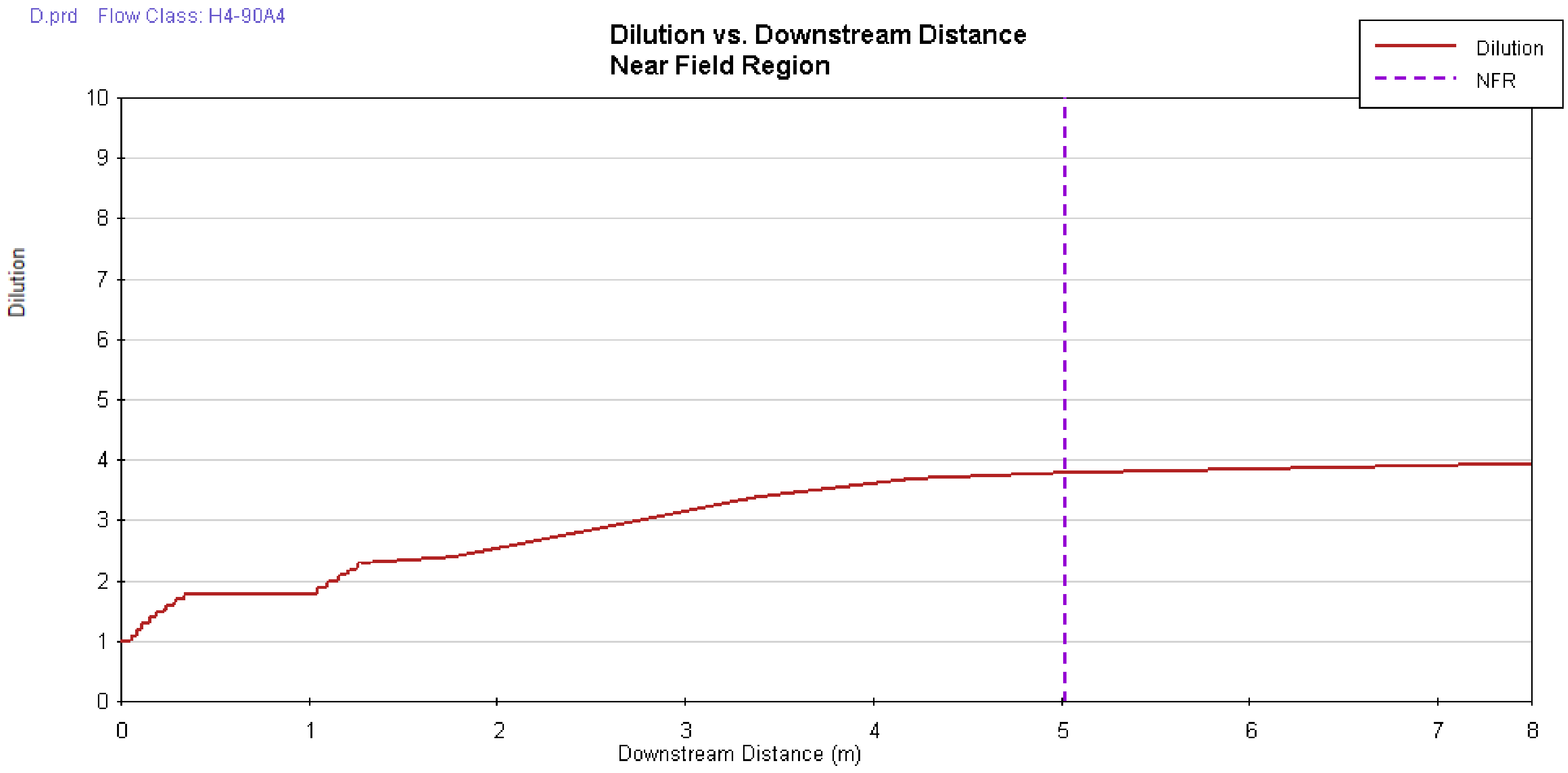


Figure A-3 CORMIX results in the near-field for Scenario C (Table 6.1).

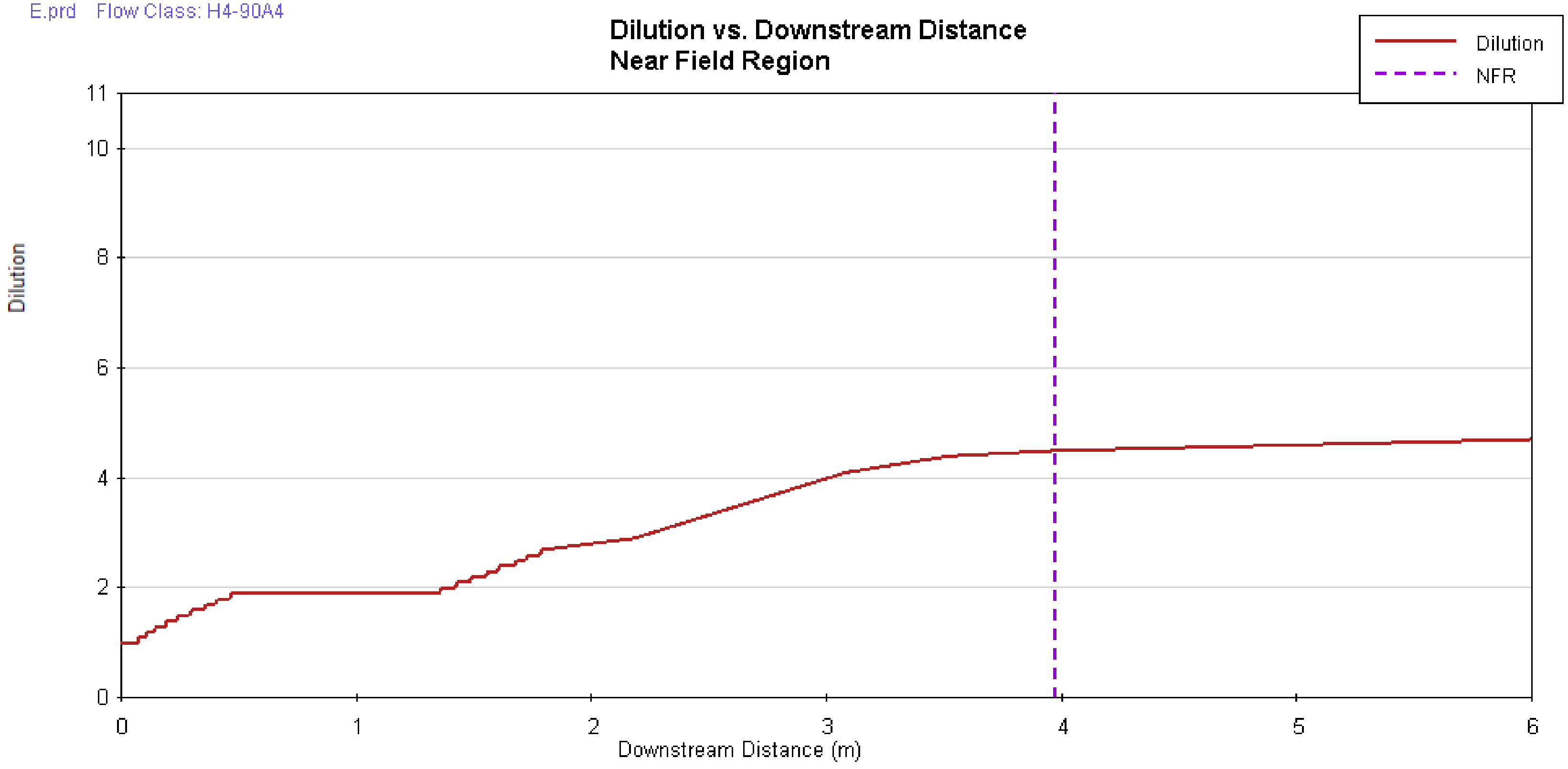


Figure A-4 CORMIX results in the near-field for Scenario D (Table 6.1).

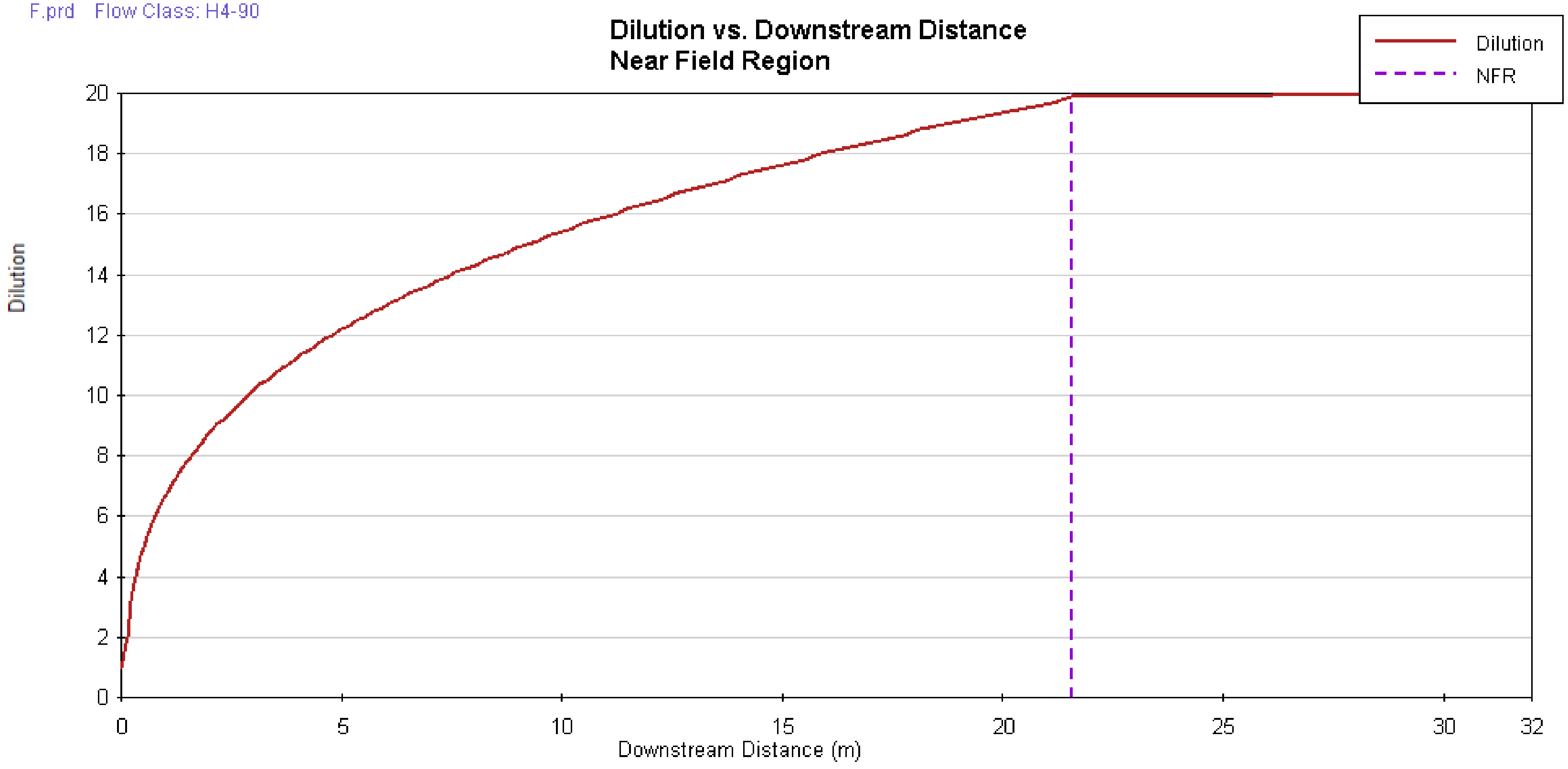


Figure A-5 CORMIX results in the near-field for Scenario E (Table 6.1).

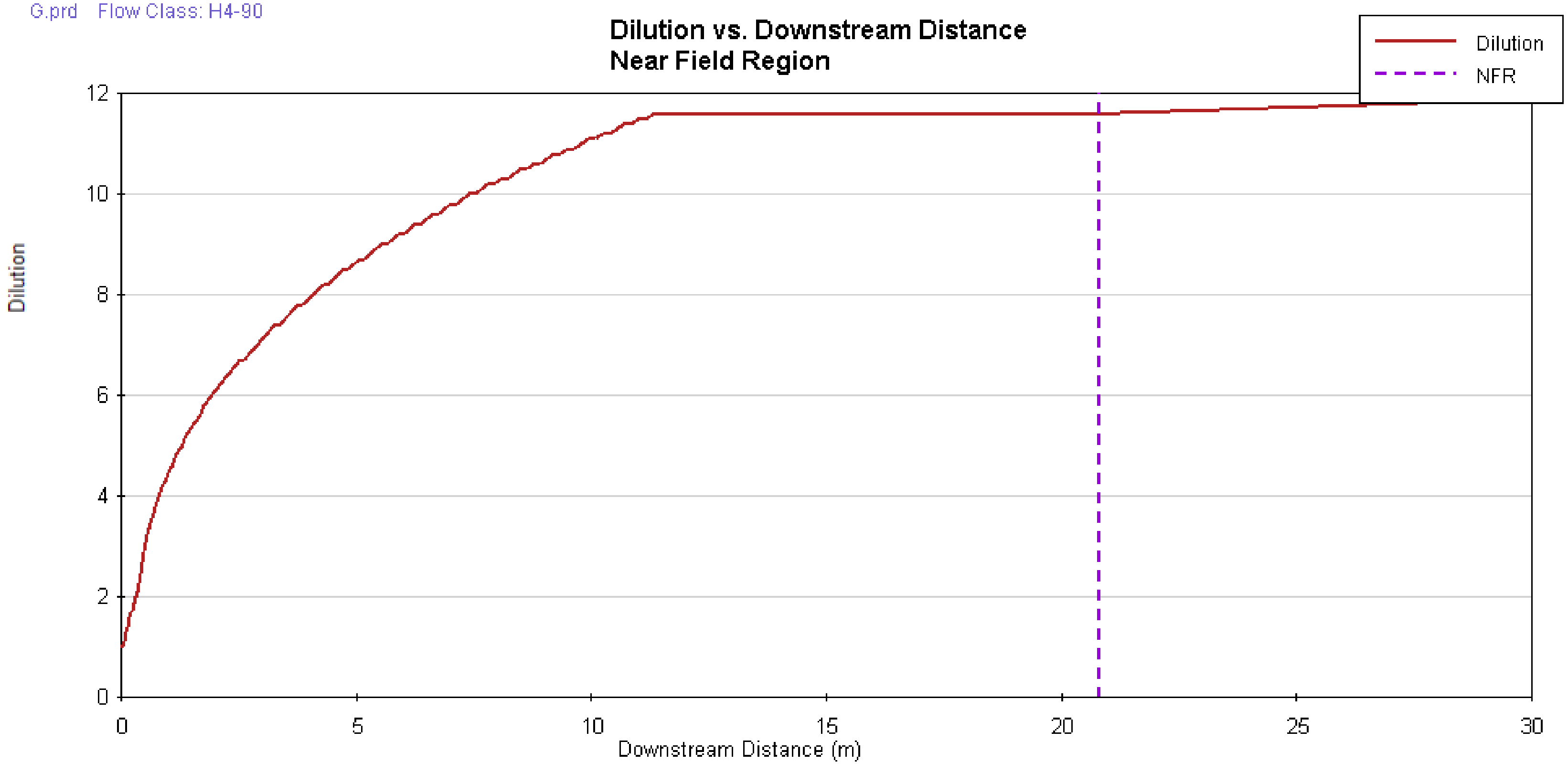


Figure A-6 CORMIX results in the near-field for Scenario F (Table 6.1).

.

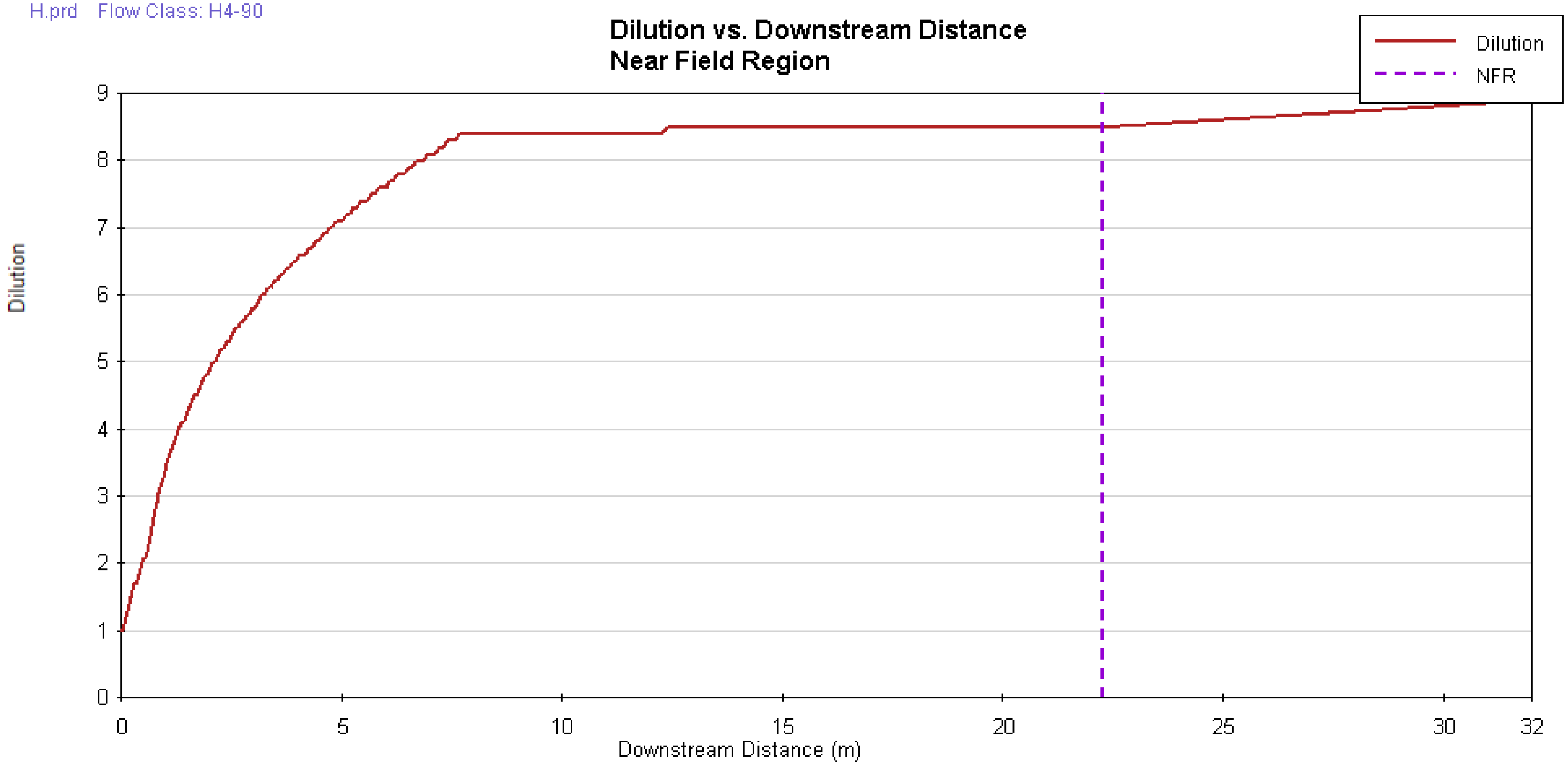


Figure A-7 CORMIX results in the near-field for Scenario G (Table 6.1).

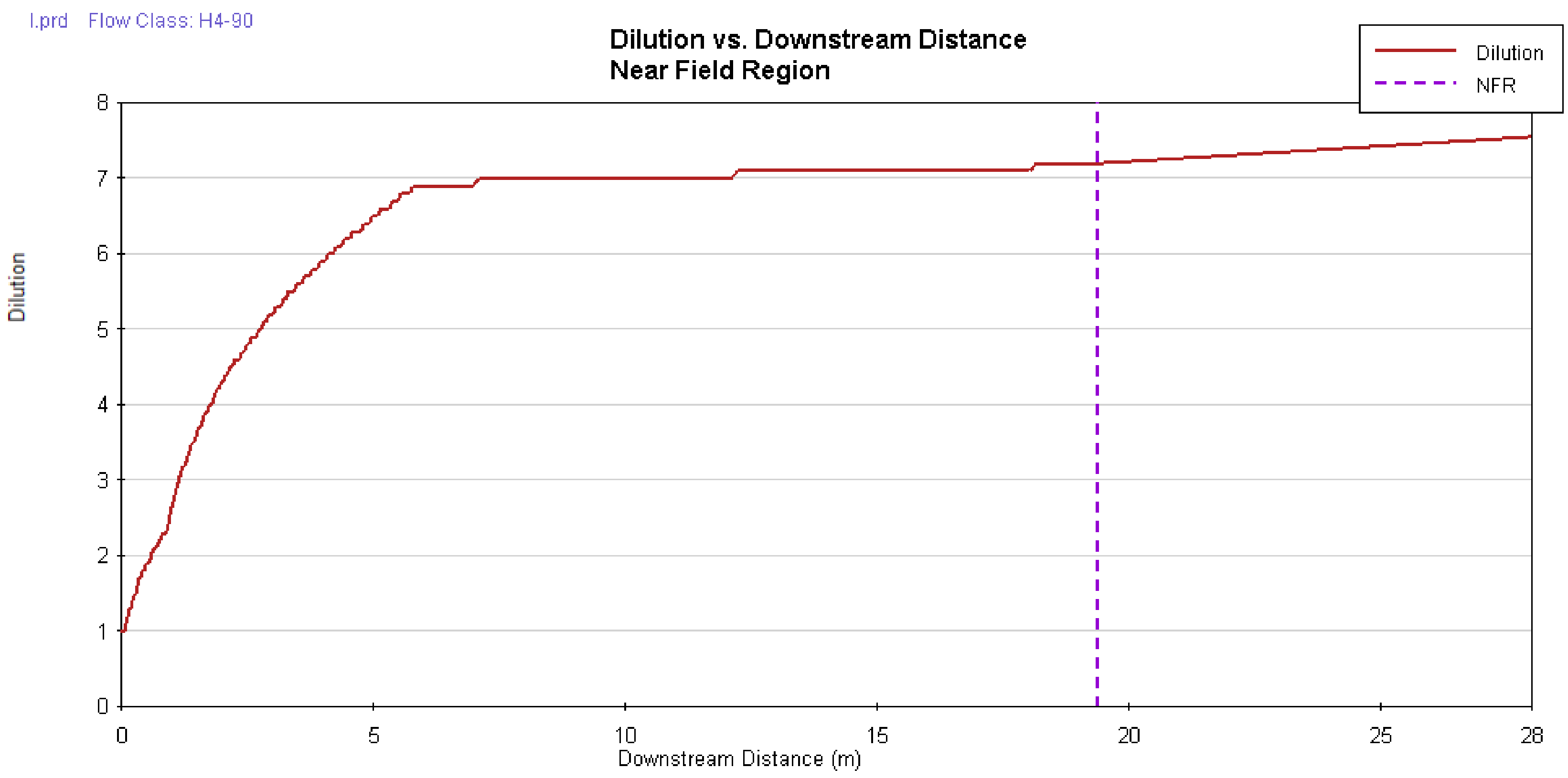


Figure A-8 CORMIX results in the near-field for Scenario H (Table 6.1).

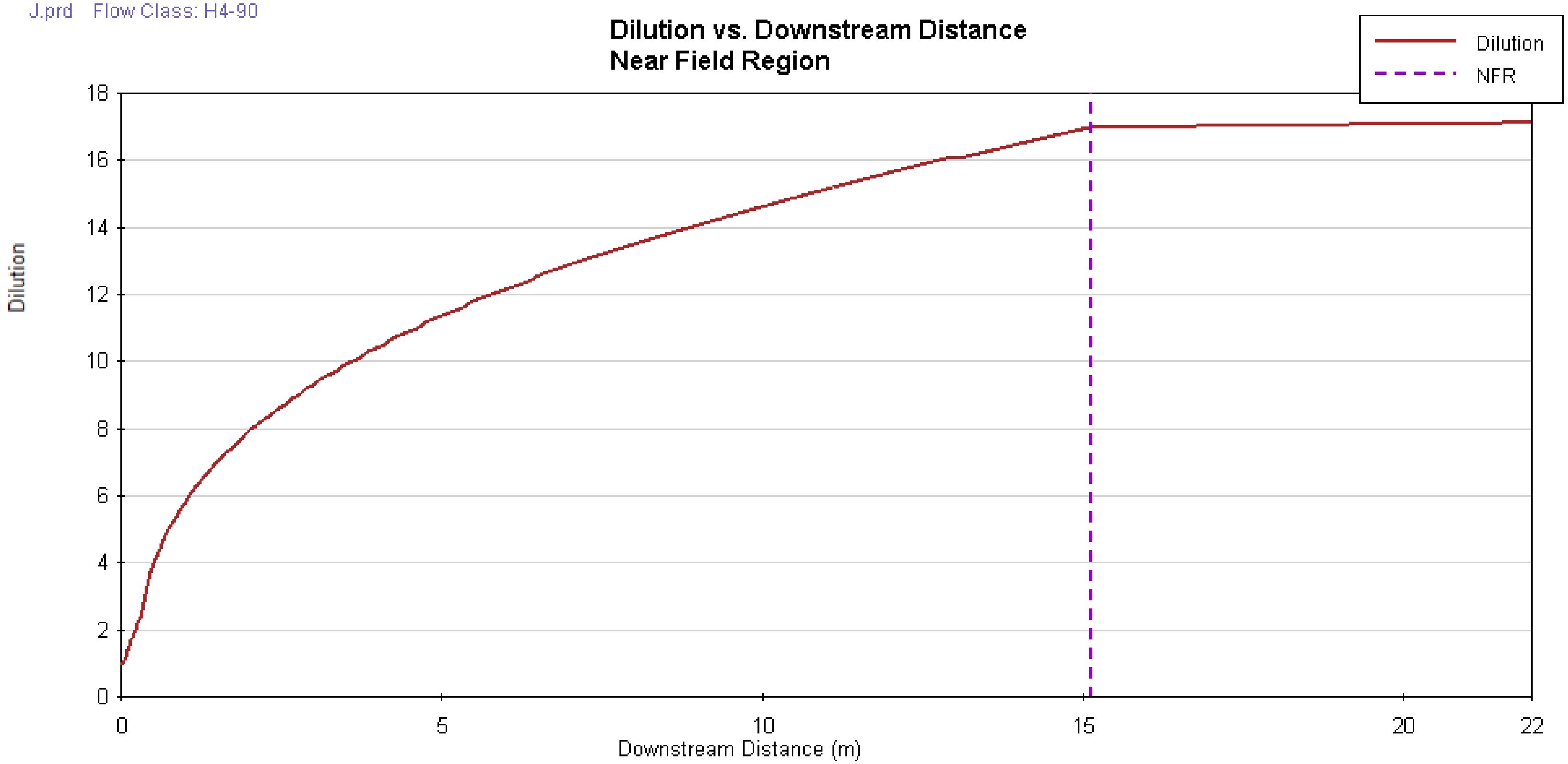


Figure A-9 CORMIX results in the near-field for Scenario I (Table 6.1).

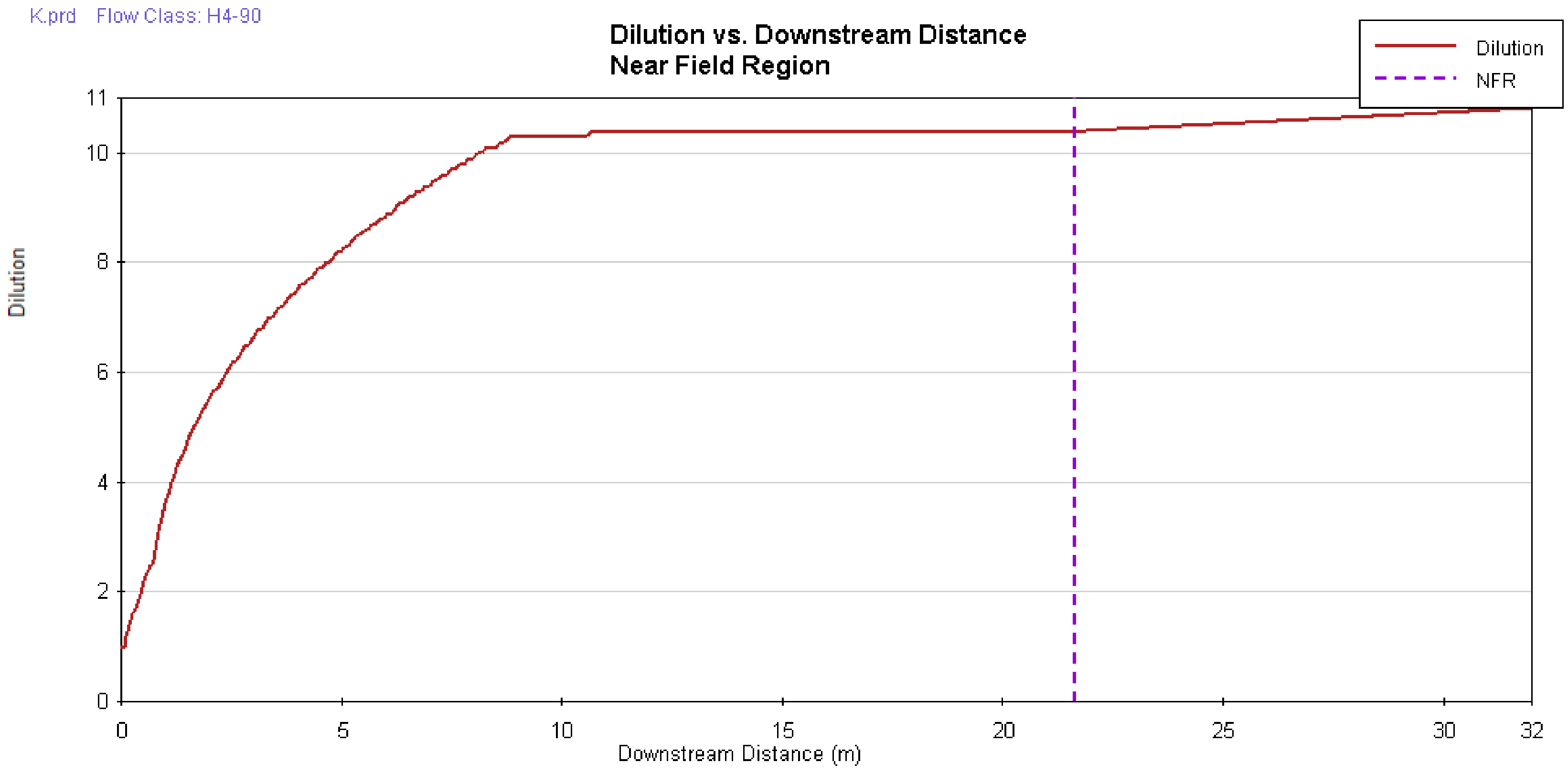


Figure A-10 CORMIX results in the near-field for Scenario J (Table 6.1).

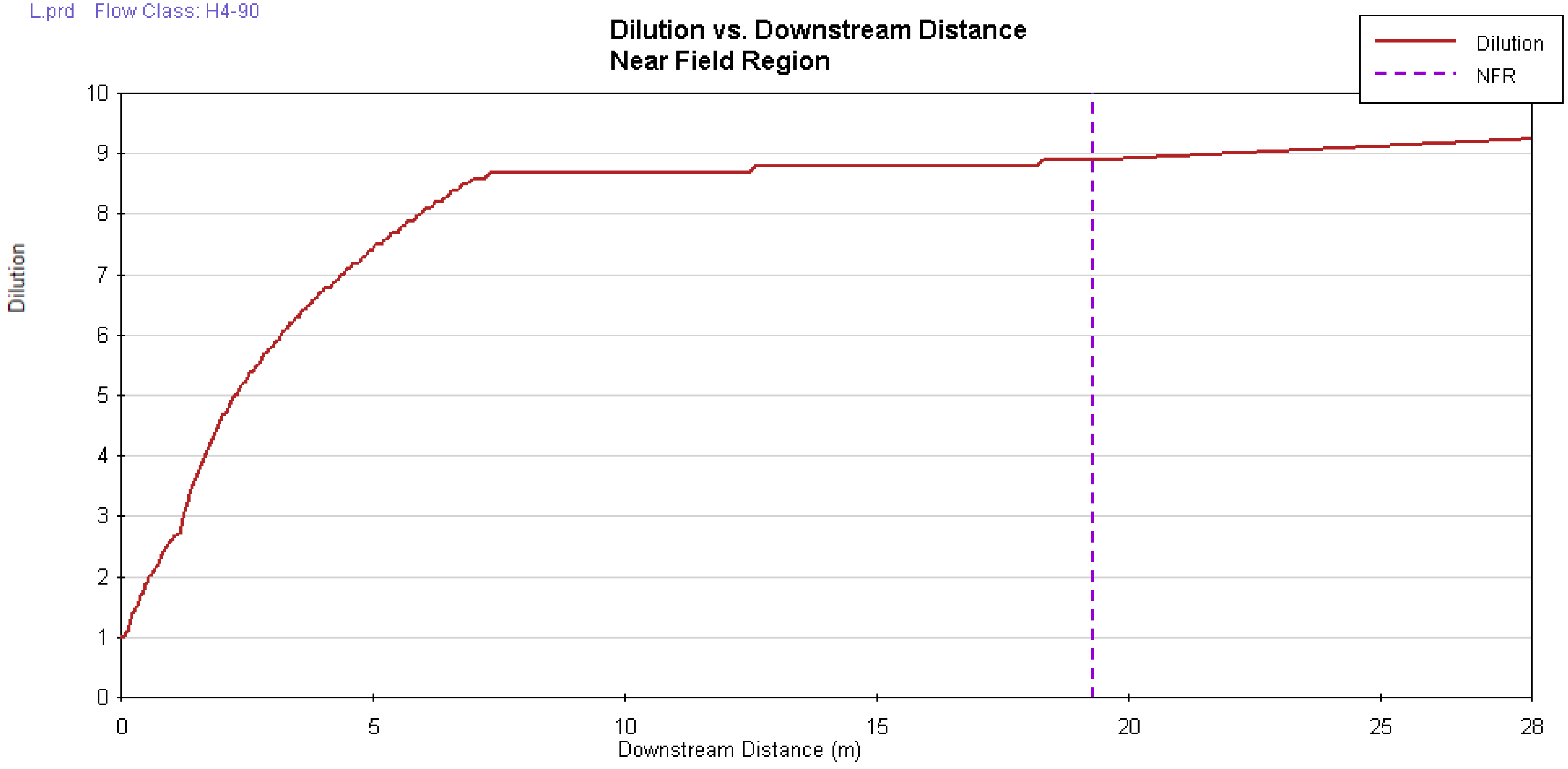


Figure A-11 CORMIX results in the near-field for Scenario K (Table 6.1).

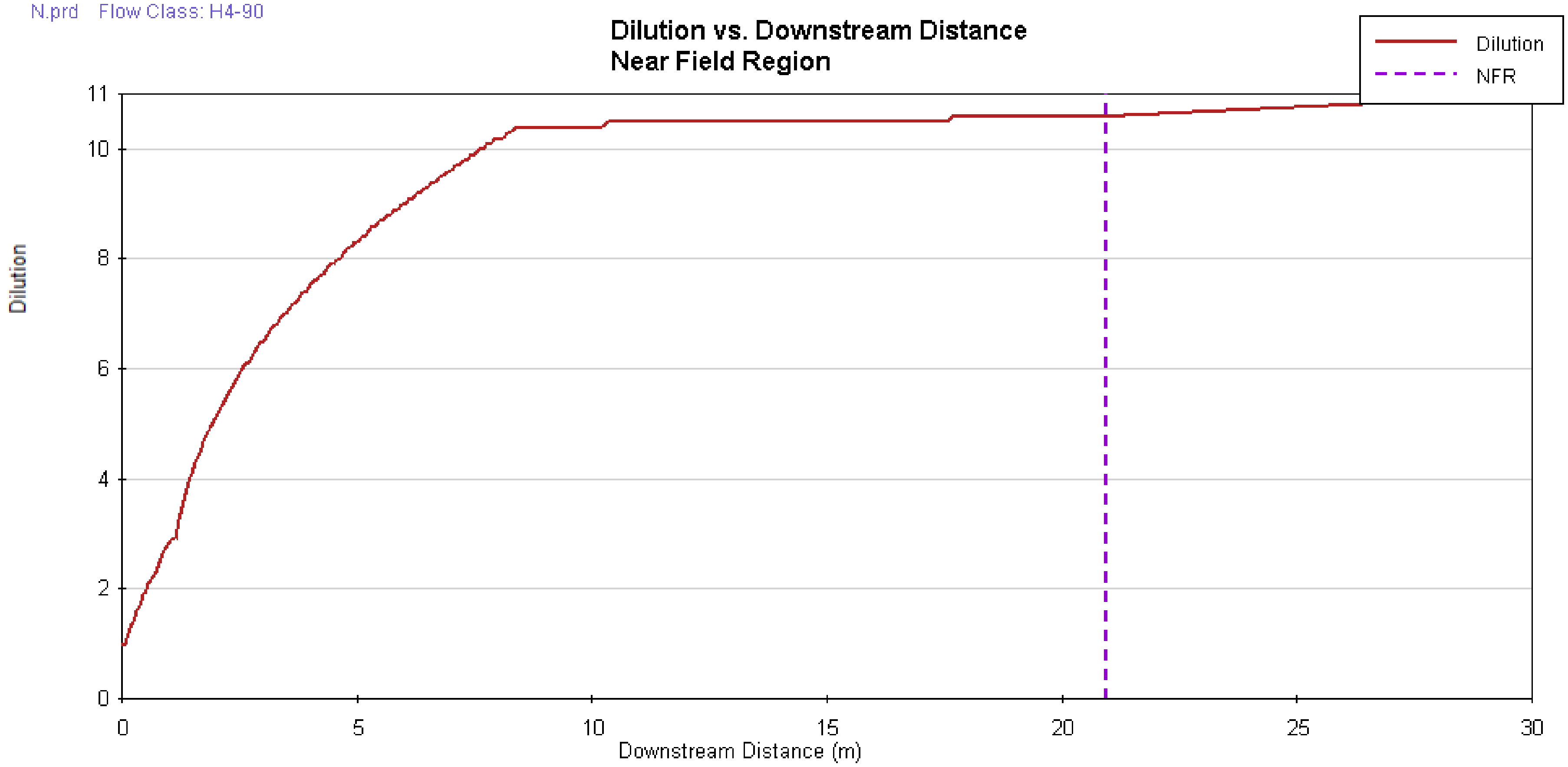


Figure A-0-12 CORMIX results in the near-field for Scenario L (

Table 6.1Table 6.1).

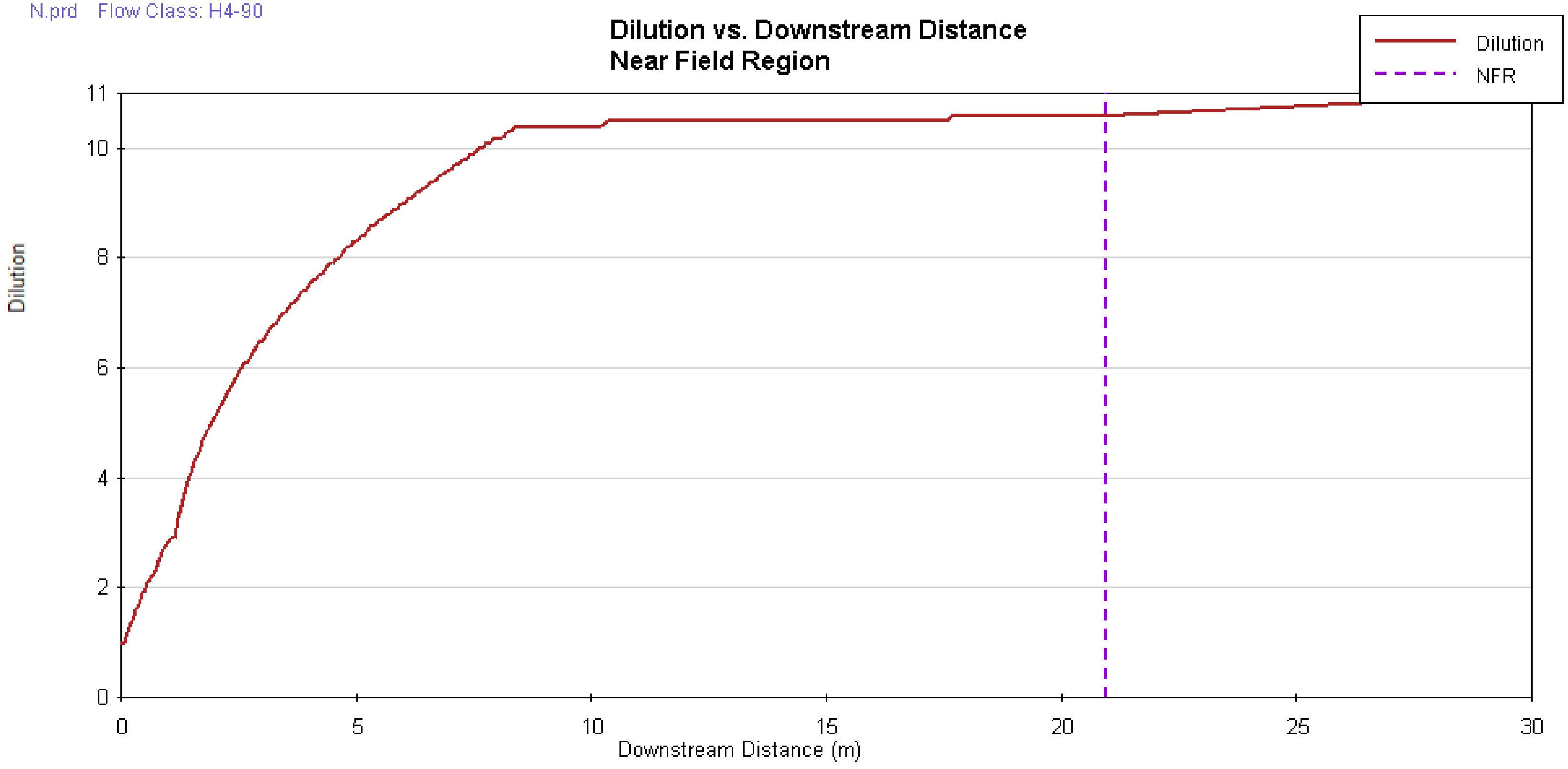


Figure A-13 CORMIX results in the near-field for Scenario M (Table 6.1).

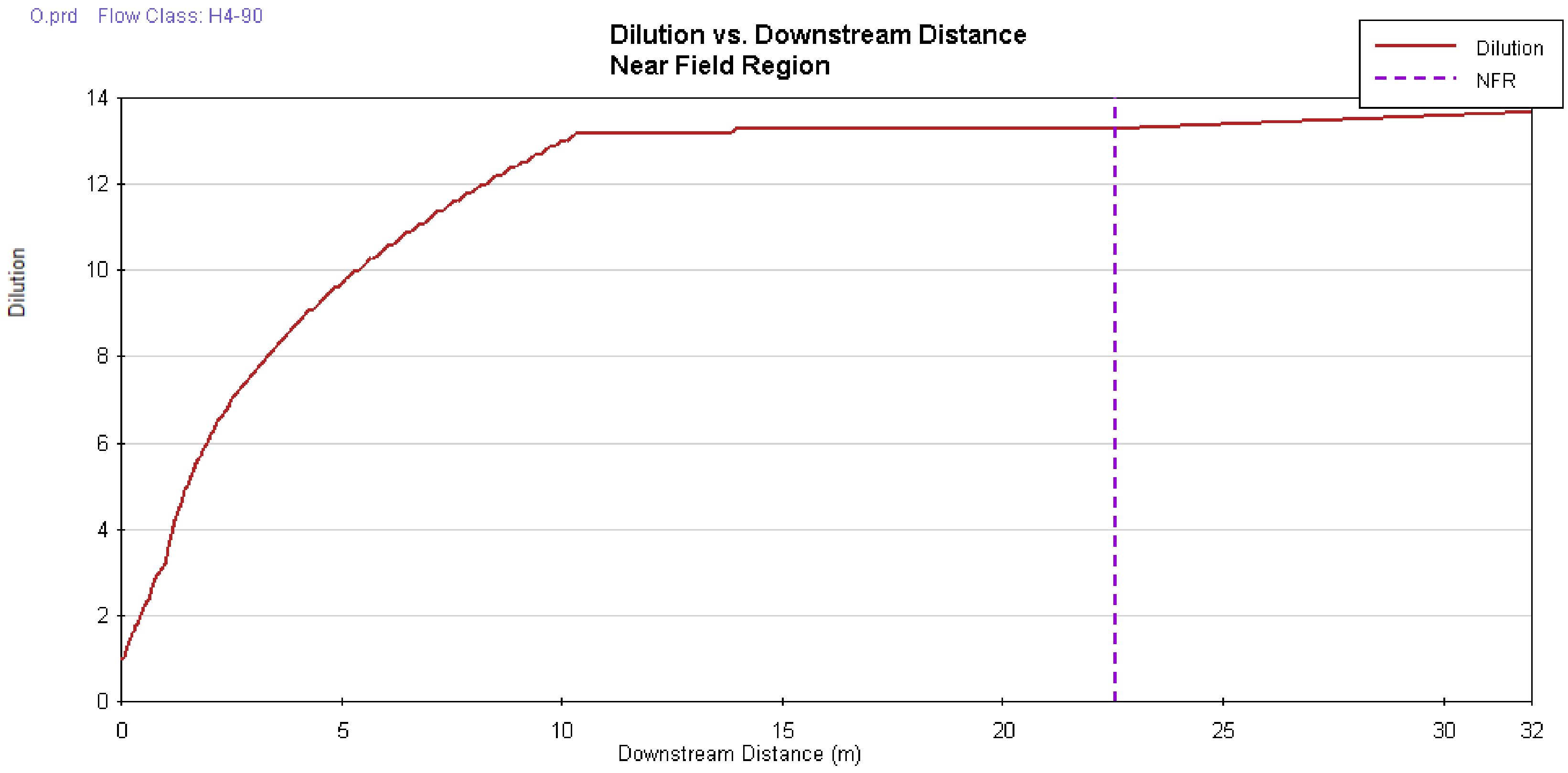


Figure A-14 CORMIX results in the near-field for Scenario N (Table 6.1).

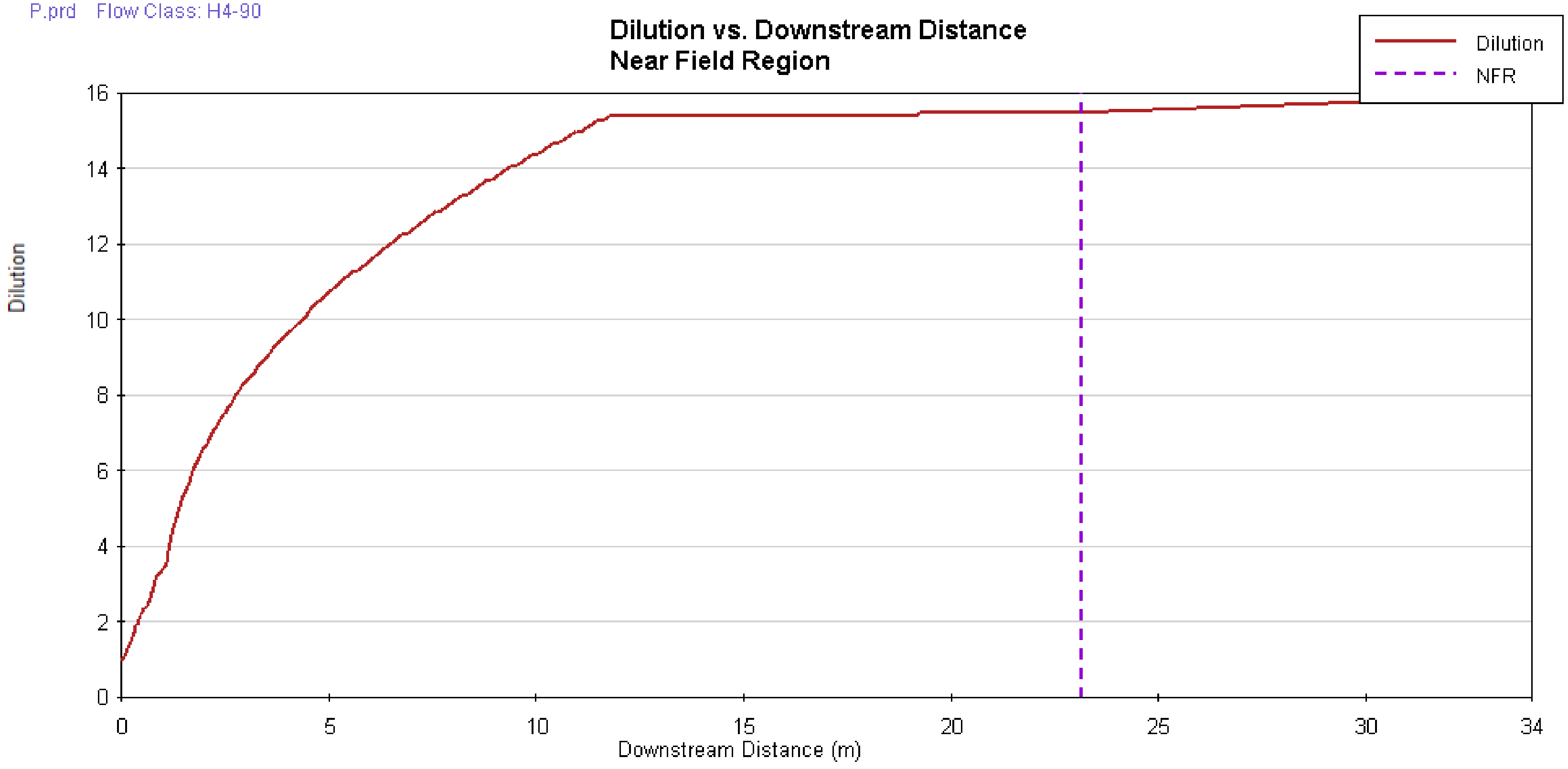


Figure A-15 CORMIX results in the near-field for Scenario O (Table 6.1).

# Appendix B - Time-series plots QMRA sites

Time series plots from Future Scenario for the seven QMRA sites for Enterococci and viruses.

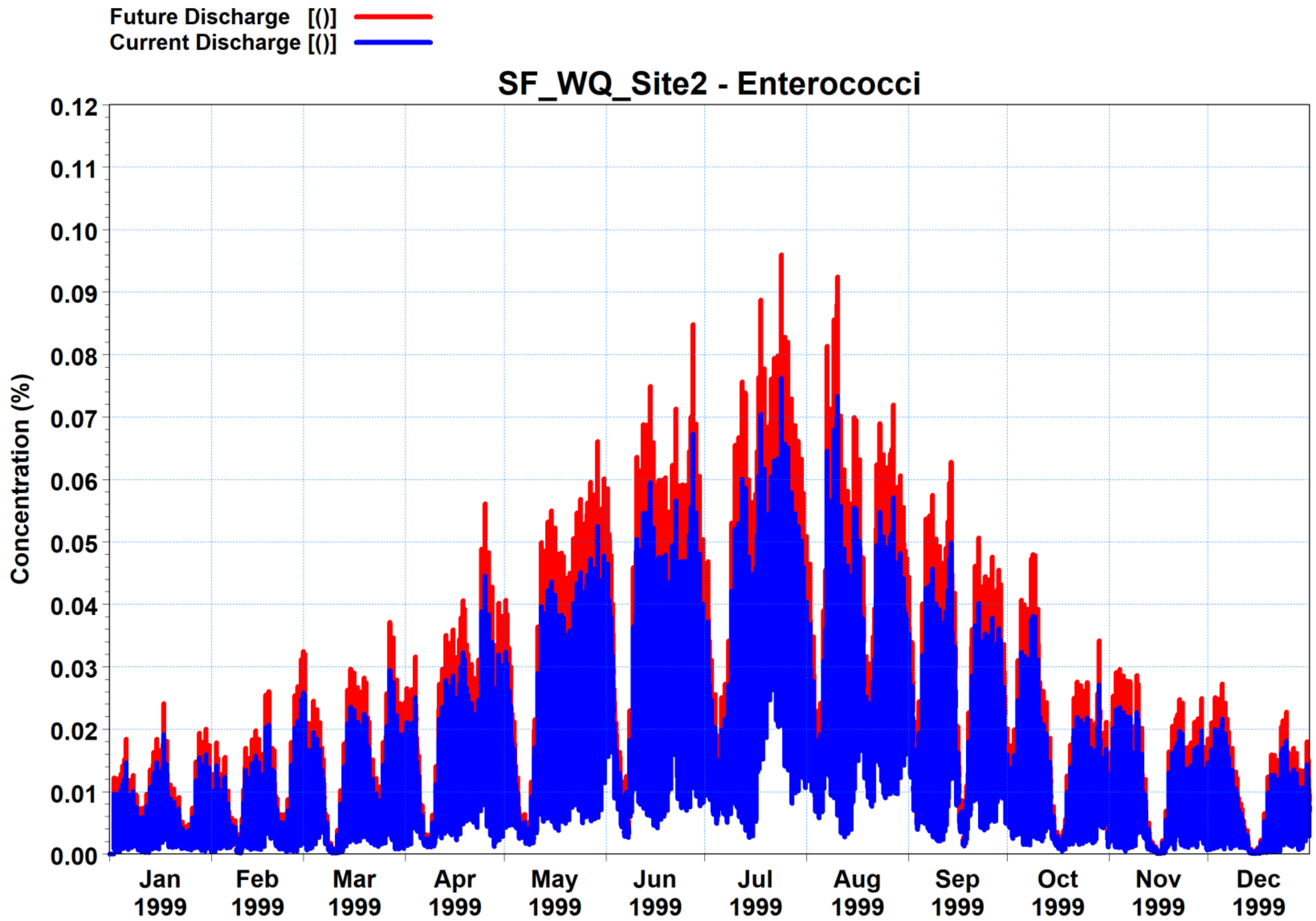


Figure B-1 Time-series of predicted Enterococci concentrations at SF WQ Site 2.

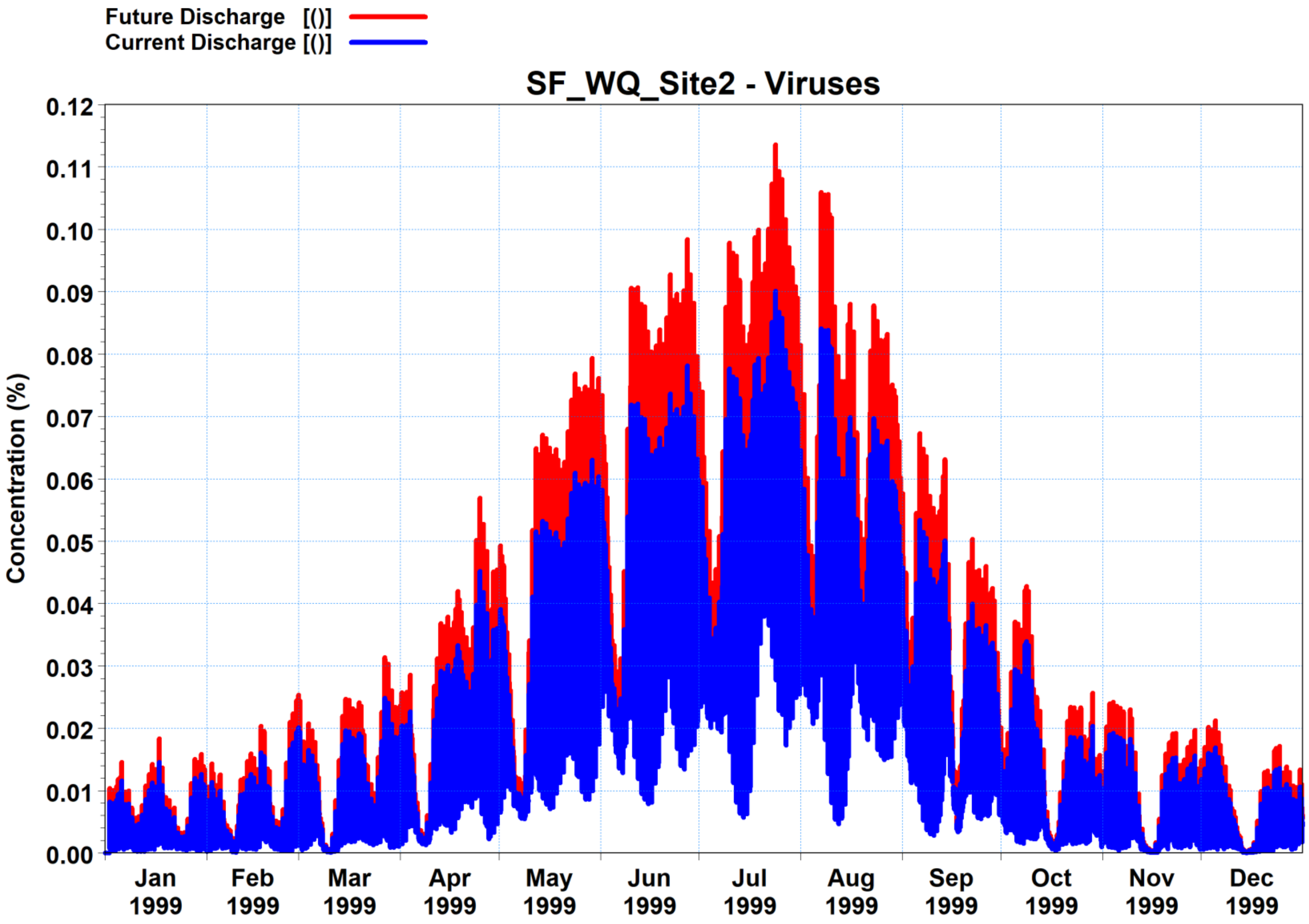


Figure B-2 Time-series of predicted virus concentrations at SF WQ Site 2.

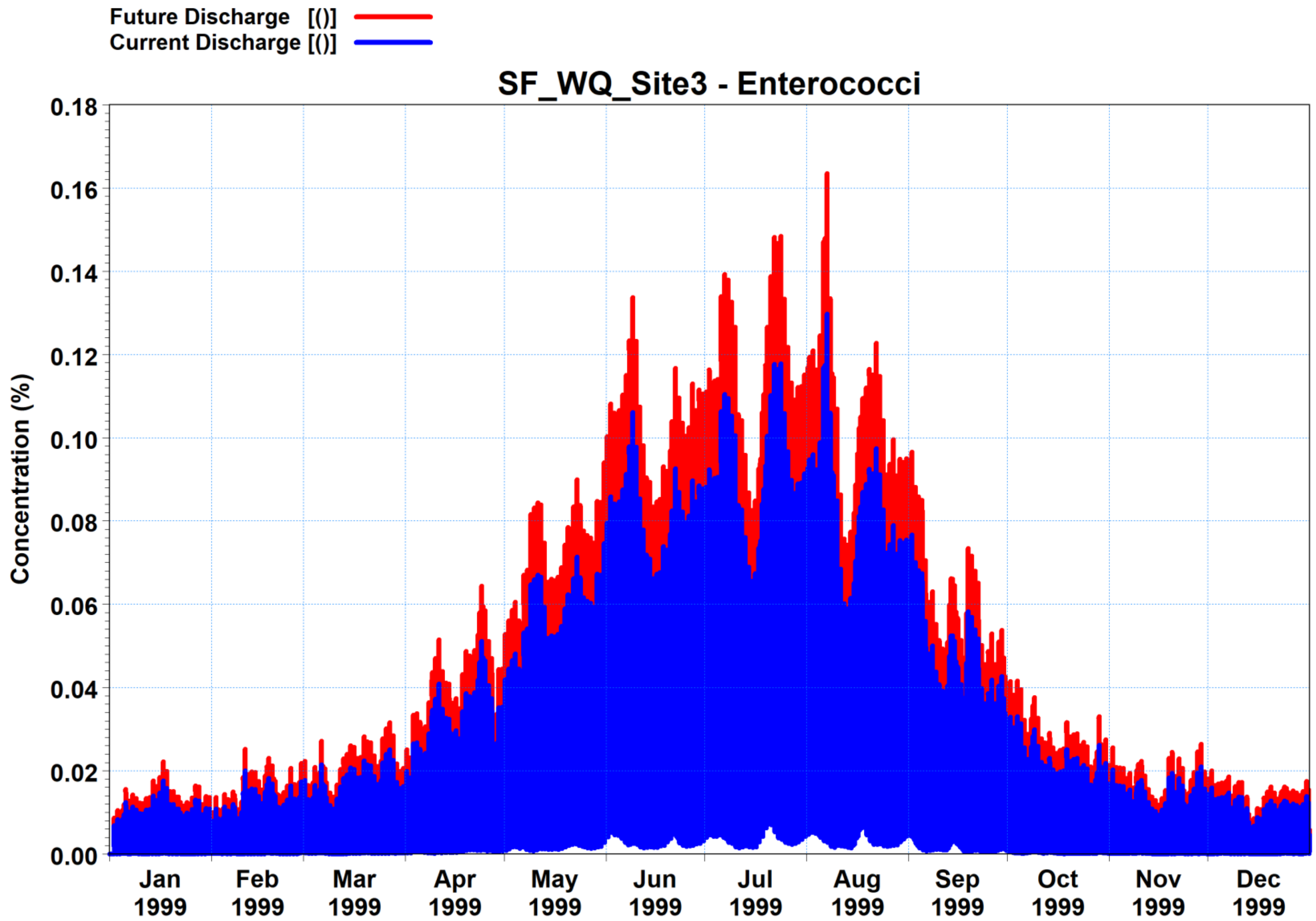


Figure B-3 Time-series of predicted Enterococci concentrations at SF WQ Site 3.

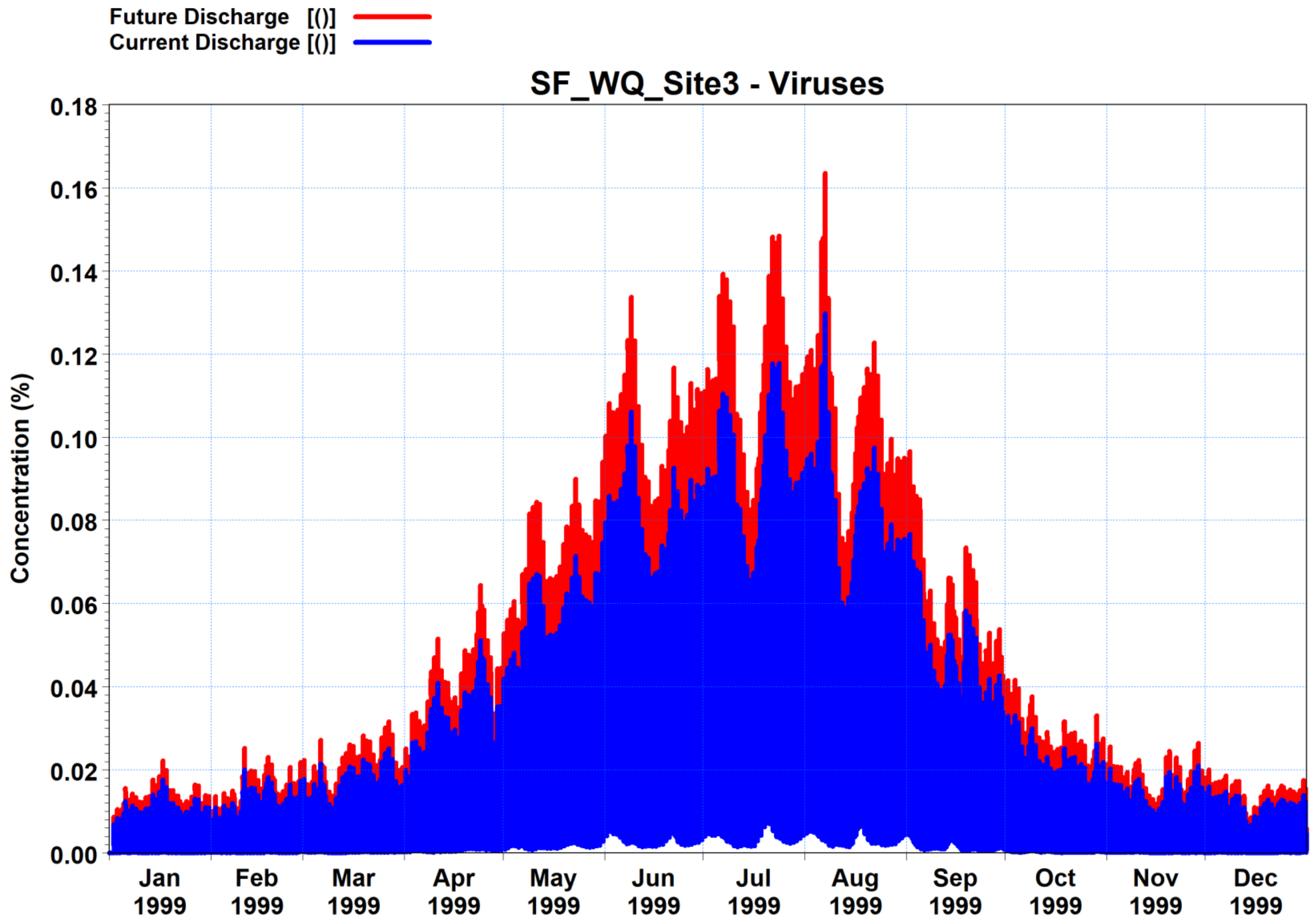


Figure B-4 Time-series of predicted virus concentrations at SF WQ Site 3.

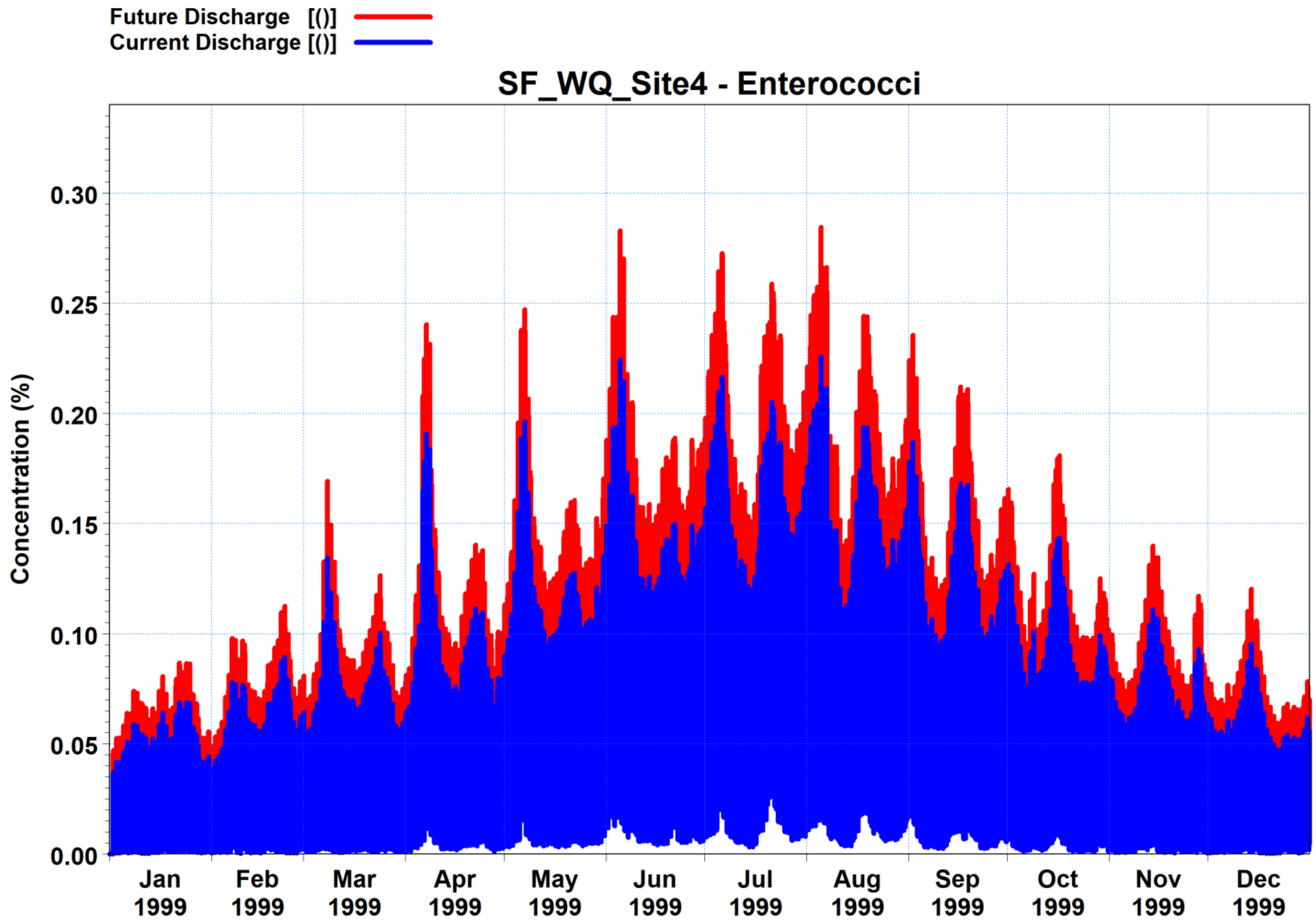


Figure B-5 Time-series of predicted Enterococci concentrations at SF WQ Site 4 (nearest the outfall).

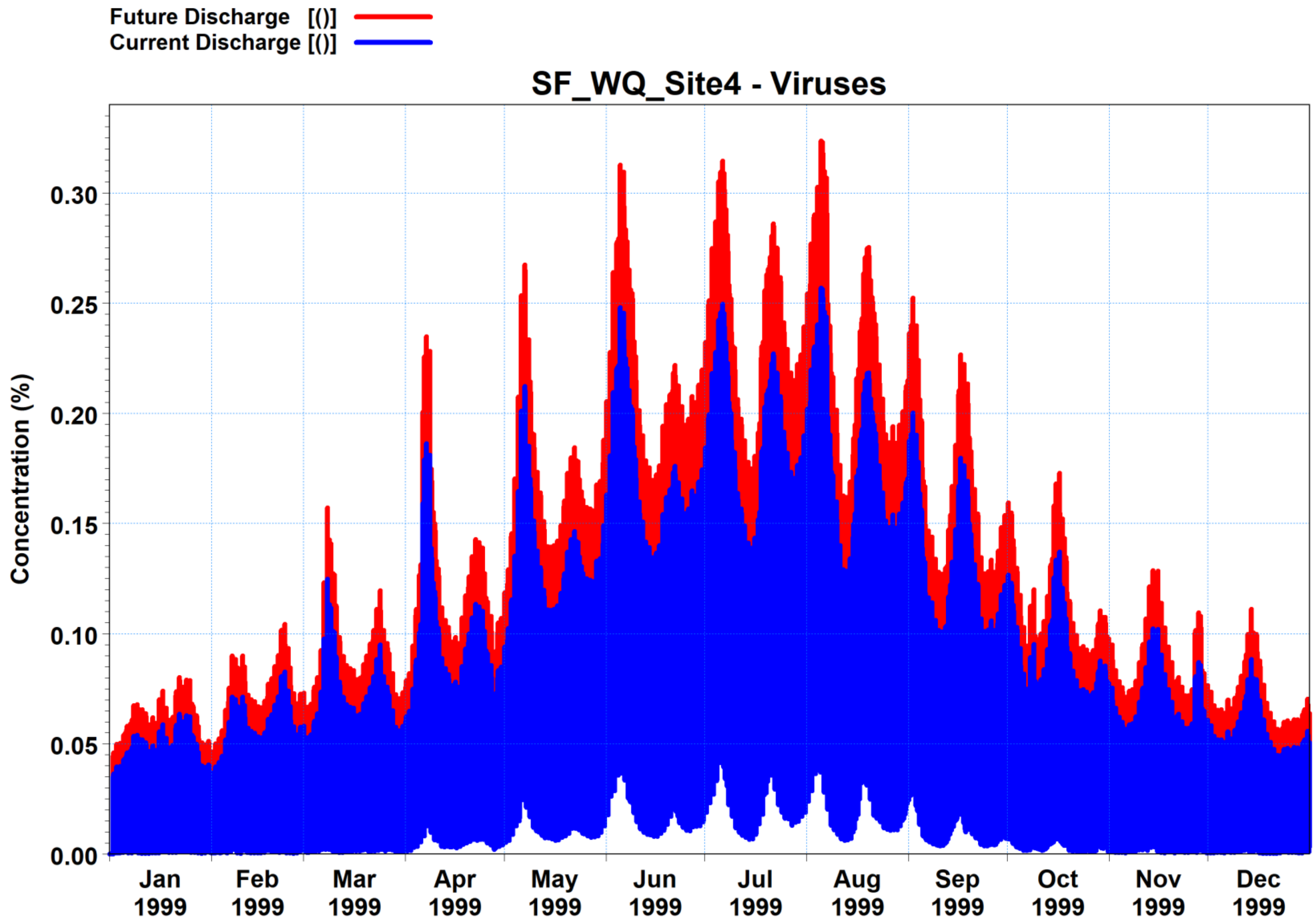


Figure B-6 Time-series of predicted virus concentrations at SF WQ Site 4.

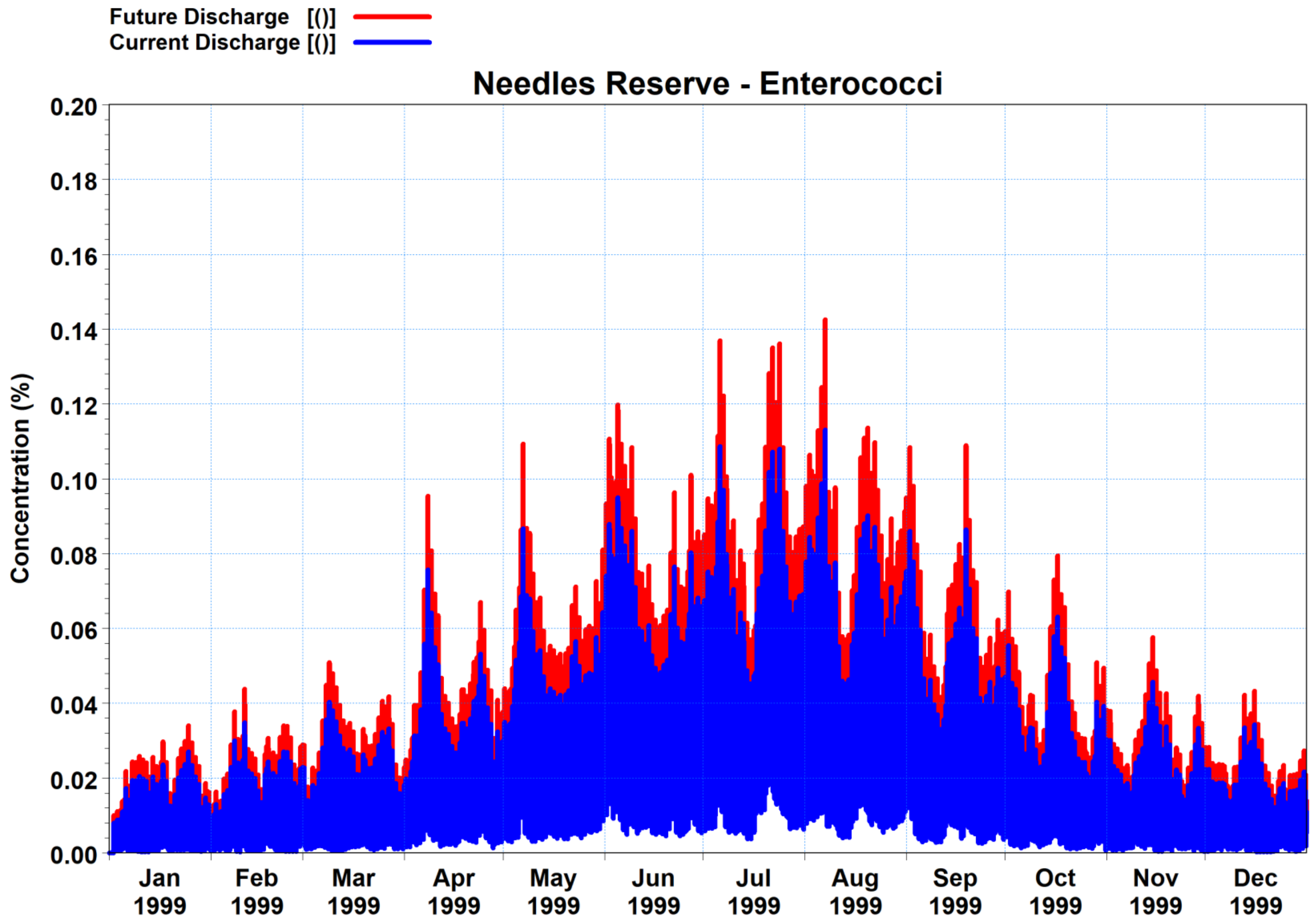


Figure B-7 Time-series of predicted Enterococci concentrations at Needles Reserve Site.

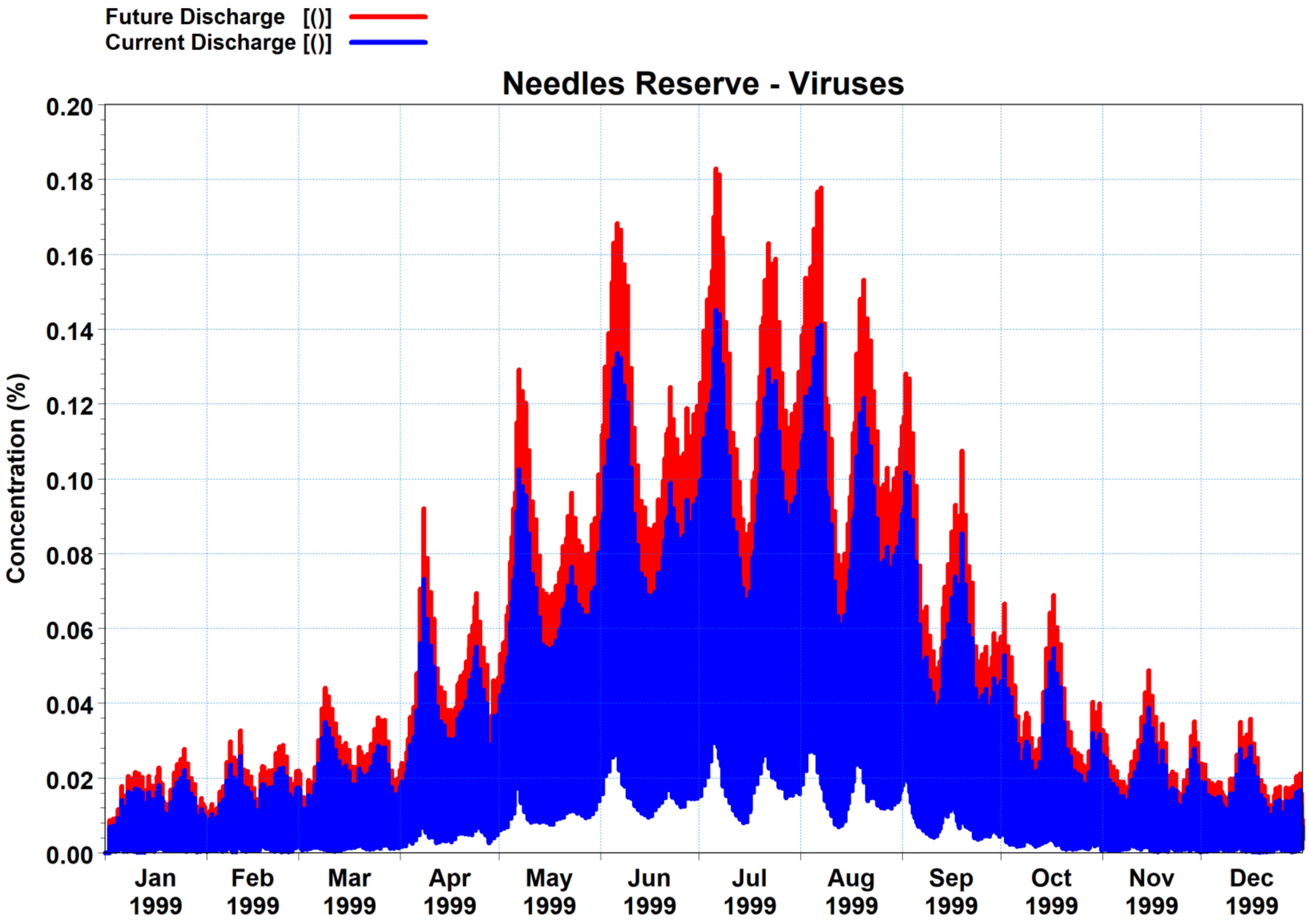


Figure B-8 Time-series of predicted virus concentrations at Needles Reserve Site.

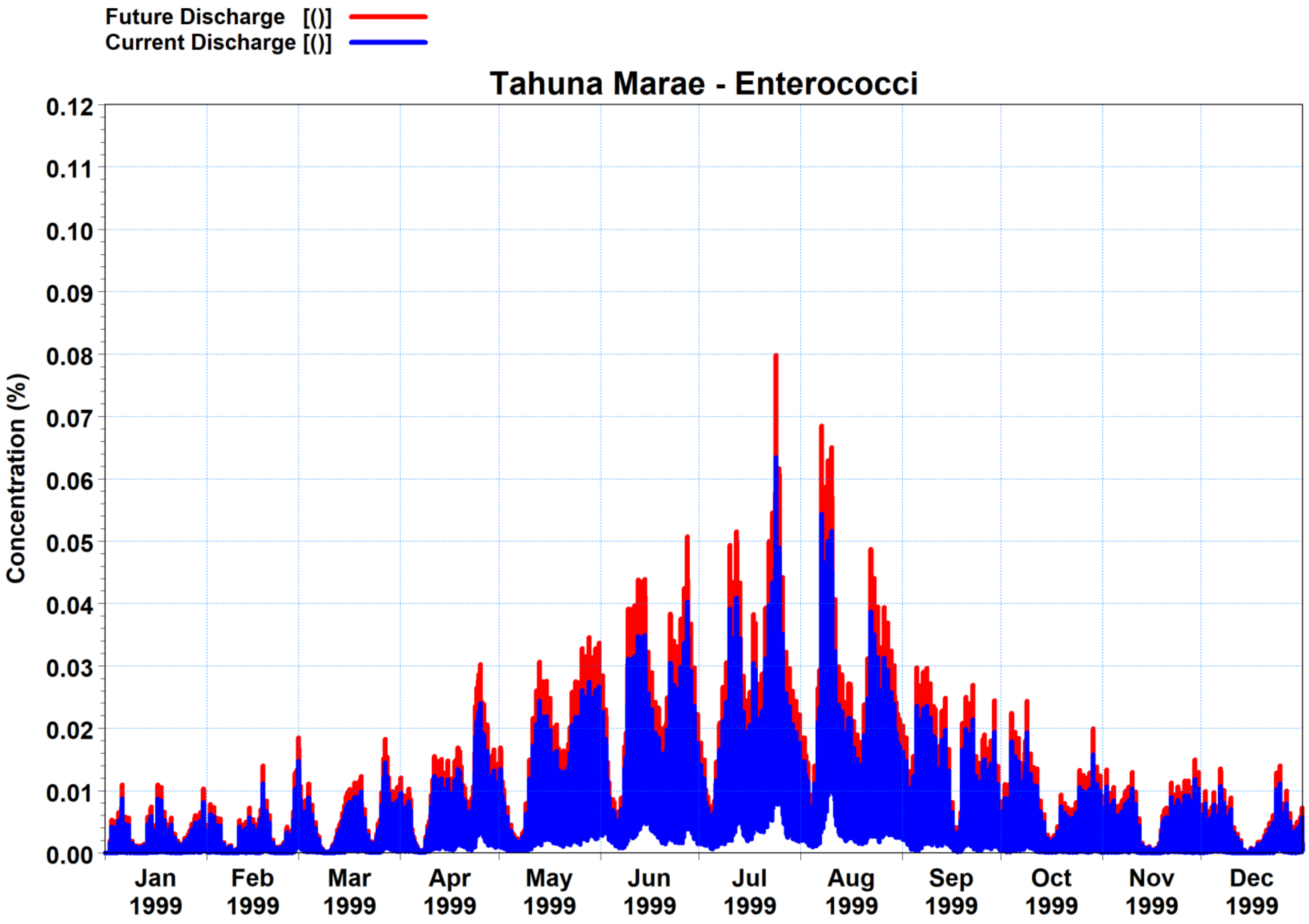


Figure B-9 Time-series of predicted Enterococci concentrations at Tahuna Marae Site.

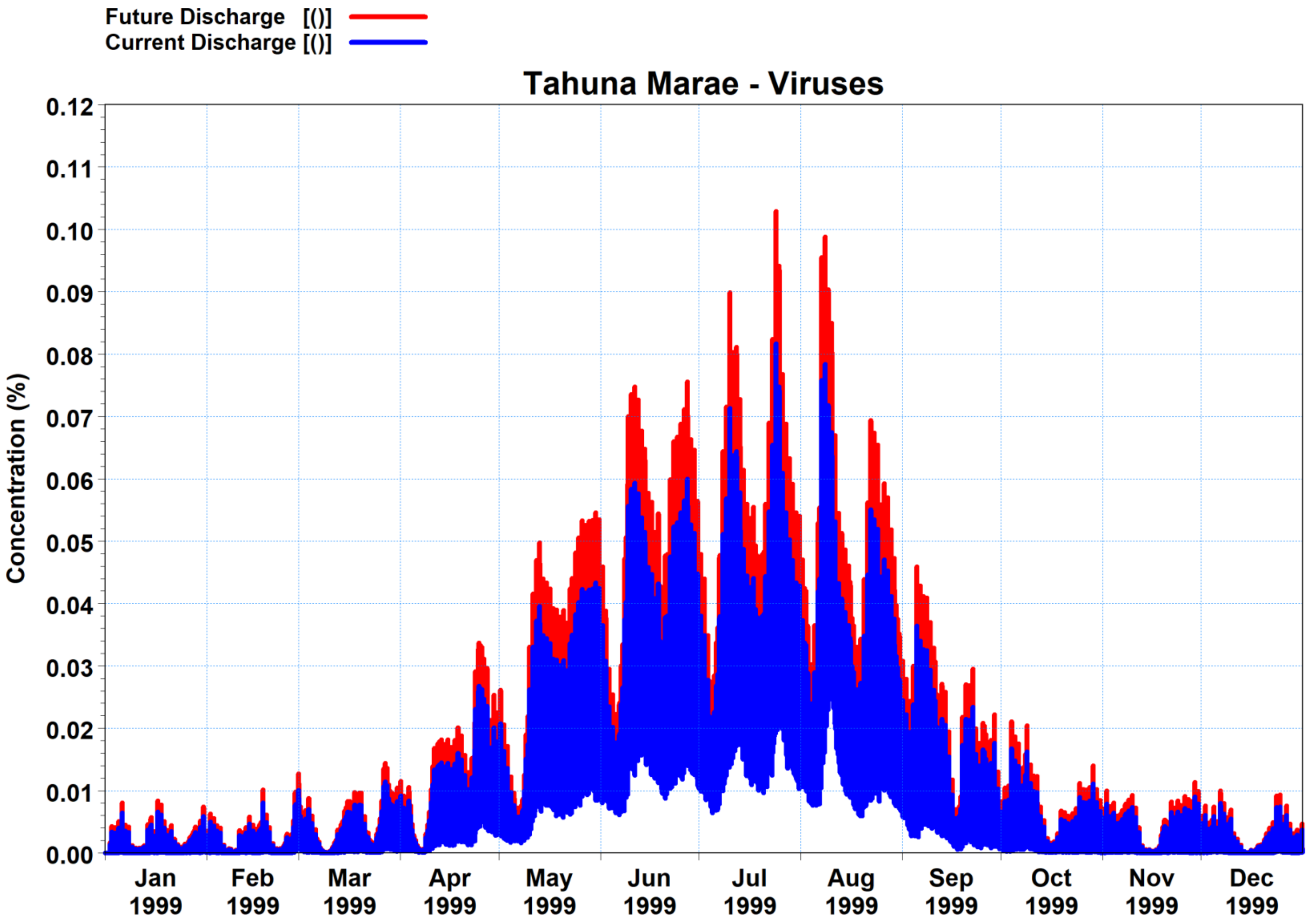


Figure B-10 Time-series of predicted virus concentrations at Tahuna Marae Site.

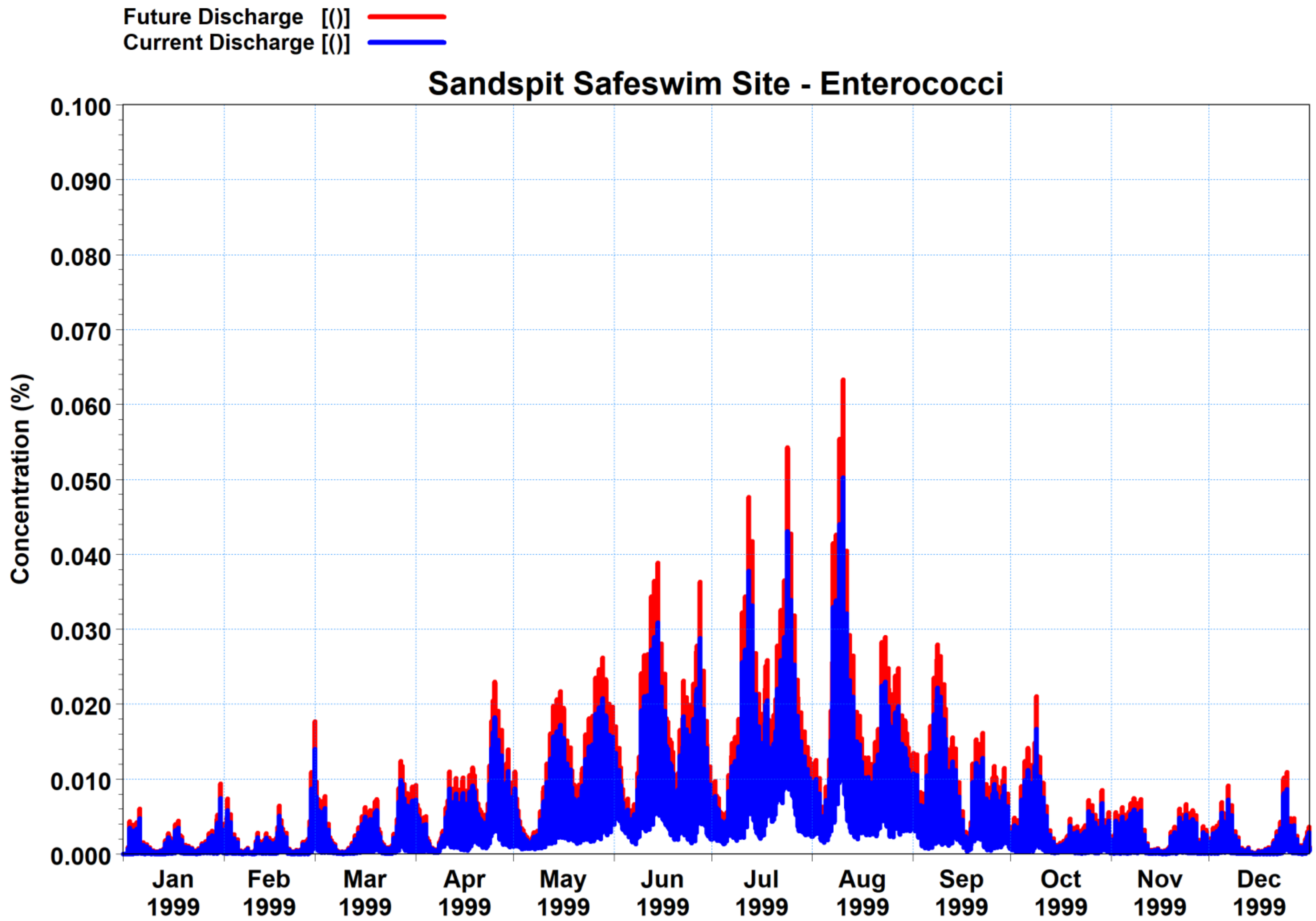


Figure B-11 Time-series of predicted Enterococci concentrations at Sandspit Safeswim Site (nearest the outfall).

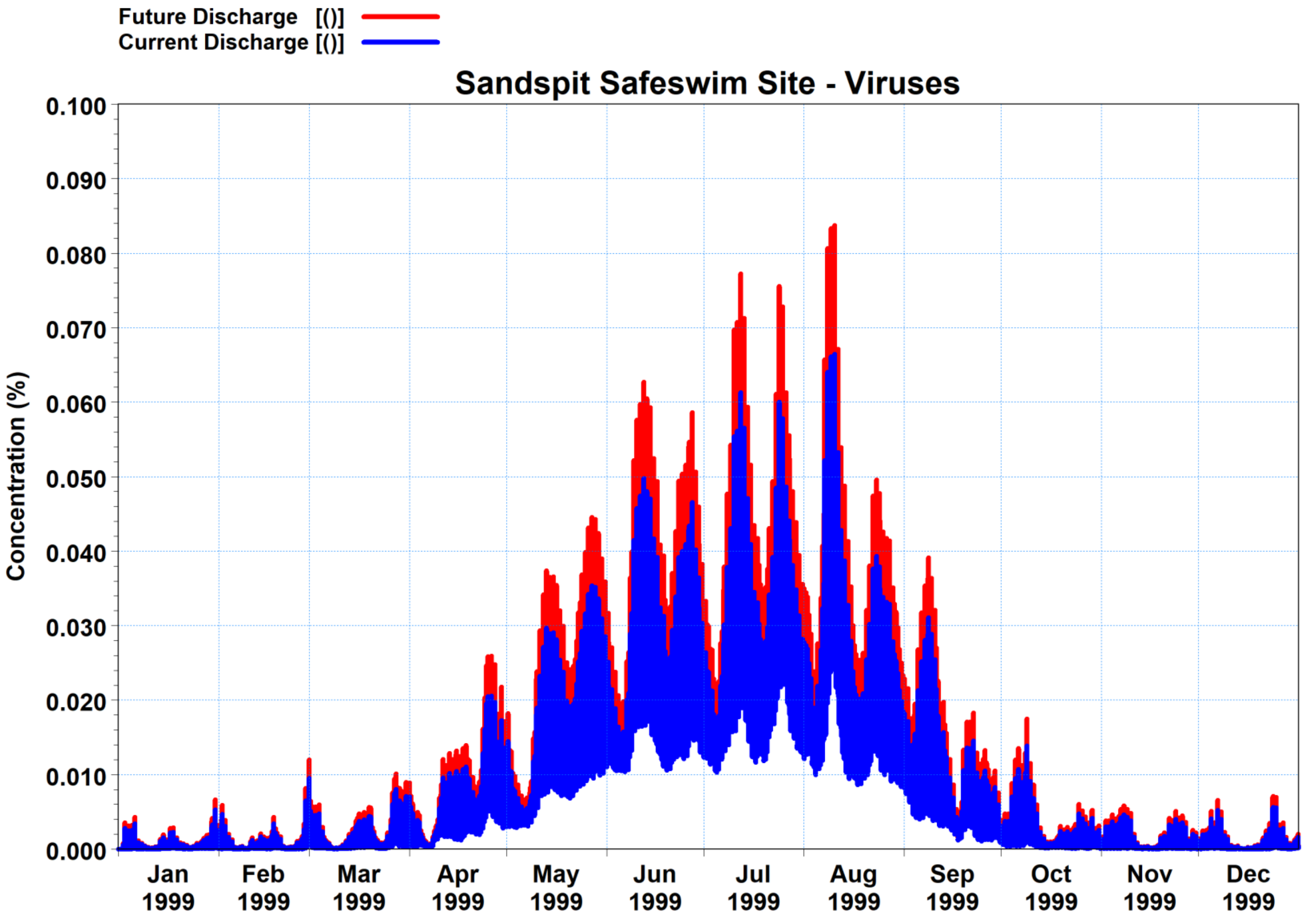


Figure B-12 Time-series of predicted virus concentrations at Sandspit Safeswim Site.